The Dissertation Committee for Jay Michael Truitt Certifies that this is the approved version of the following dissertation:

Role of the IKKβ/NF-κB Pathway in Alcoholism

Committee:

Adron Harris, Supervisor

Roy Dayne Mayfield, Co-Supervisor

Marie Monfils

Casey Wright

Harold Zakon

Role of the IKKβ/NF-κB Pathway in Alcoholism

by

Jay Michael Truitt, BS

Dissertation

Presented to the Faculty of the Graduate School of

The University of Texas at Austin

in Partial Fulfillment

of the Requirements

for the Degree of

Doctor of Philosophy

The University of Texas at Austin

August, 2015

Role of the IKKβ/NF-κB Pathway in Alcoholism

Jay Michael Truitt, PhD

The University of Texas at Austin, 2015

Supervisors: Adron Harris, Roy Dayne Mayfield

Pro-inflammatory neuroimmune signaling pathways are implicated in the acute and chronic effects of alcohol exposure. Genetic association studies in humans, gene expression microarray studies in postmortem brains of alcoholics, transcriptome meta-analysis in rodents, and drinking models in mice support the role of neuroimmune signaling in alcohol abuse disorder. Nuclear factor kappa-B (NF-κB) is a ubiquitously expressed transcription factor that controls the expression of genes important for innate- and adaptive-immune responses, cell proliferation/death, and inflammation. More specifically, the NF-κB canonical pathway is responsible for the expression of pro-inflammatory genes. The inhibitory kappa-B kinase (IKK) complex, composed of IKKα, IKKβ, and IKKγ represents a point of convergence for many extracellular signals and regulates the NF-κB canonical pathway by targeting the inhibitor of NF-κB (IκB) for degradation. NF-κB is disinhibited, translocates to the nucleus, and acts as a transcription factor for numerous pro-inflammatory chemokines and cytokines. However, IKKβ is the only member of the IKK complex that specifically mediates this pathway. As such, I hypothesized that inhibiting IKKβ/NF-κB pathway would limit/decrease voluntary ethanol consumption. This was studied by determining the brain region and cell type-specificity of all the IKK isoforms. It was observed

that all IKKs were primarily expressed in neurons and ubiquitously expressed throughout the brain regions studied [prefrontal cortex (PFC), nucleus accumbens (NAc), amygdala (AMY), and ventral tegmental area (VTA)]. Subsequently, the effects of inhibiting/knocking down IKKβ were investigated both systemically and centrally to determine the effects on voluntary ethanol drinking. It was observed that both antagonizing IKKβ peripherally and genetically knocking it down centrally in the NAc and central amygdala (CeA) reduced voluntary ethanol consumption and preference in two bottle choice (2BC) ethanol drinking paradigms. Lastly, ethanol-responsive microRNAs were explored in the PFC, NAc, and AMY. Several differentially expressed MicroRNAs were discovered that were either predicted/validated to target genes of the IKKβ/NF-κB pathway. One candidate, let-7g, was manipulated *in vivo* to determine its effect on voluntary ethanol drinking behaviors, however, no significant phenotypes were observed. These results demonstrate that blocking IKKβ decreases voluntary ethanol consumption and indicate its role as a potential therapeutic target for alcohol abuse.

Table of Contents

List of Tables

List of Figures

CHAPTER I: Background and Significance

The production and consumption of fermented beverages dates back to the seventh millennium B.C. in Neolithic villages in what is now China. Since then, fermented drinks have been used throughout history in nearly every society all around the world, and have played an important role in the development of human culture (McGovern *et al.* 2004). This widespread usage can be explained by alcohol's combined disinfectant, analgesic, and psychotropic effects (McGovern *et al.* 2004). For most people, the use of ethanol is enjoyable and produces no ill effects (Carr 2011). In fact, greater that 85% of adults in the United States reported that they drank alcohol at some time in their life, and 56.4% of these adults have consumed alcohol within the past month (Manit *et al.* 2009). Many studies have shown that moderate ethanol consumption as defined as 1 drink per day for women and 2 drinks per day for men is beneficial and reduces the risk of developing some diseases, such as coronary artery disease, ischemic strokes, and diabetes (Ahmed and Blumberg 2011).

However, alcohol's mind altering properties and its ability to produce dependence have made it arguably the oldest and most devastating drug of abuse (Carr 2011; World Health Organization 2014). The fifth edition of the Diagnostic and Statistical Manual (DSM–5), published by the American Psychiatric Association, defines Alcohol Use Disorder (AUD) as a problematic pattern of alcohol use that results in noticeable distress or impairment in daily life that continues despite negative consequences (American Psychiatric Association 2013). A person must also exhibit, within the same one year period, at least two additional criteria, such as craving, tolerance, withdraw, inability to control use, drinking more than intended, inability to fulfill obligations, and continued use despite problems with health or relationships, etc. (American Psychiatric Association 2013). The social, economic, and health burden associated with the harmful

use of alcohol is staggering (World Health Organization 2014). Approximately 10% of the United States population over the age of 12 (7% of adults and 2.8% of youth) have AUD, which amounts to over 17 million individuals suffering from this disease (Manit *et al.* 2009). This 10% of individuals is responsible for consuming about 75% of alcohol ingested in the United States (Dombrowski *et al.* 2001). In regards to economic damage, it was estimated that excessive alcohol consumption costs the United States $223.5 billion annually (Bouchery *et al.* 2011). Health wise, irresponsible use of alcohol plays a role in more than 200 different diseases and injury-related conditions such as cancers, liver cirrhosis, and suicides (World Health Organization 2014). It is estimated that alcohol contributes to 5.1% of the burden of disease and injury globally, and to 5.9% of all deaths worldwide, or roughly 3.3 million deaths/year (World Health Organization 2014).

It is not clear what distinguishes the person that can consume alcohol in moderate amounts with no ill effects compared to individuals who consume excessive amounts despite the negative consequences. Thus, a major goal of alcohol research is to better understand the neurobiology associated with AUD. Although the exact etiology of AUD is currently unknown, we do know that repeated exposure to alcohol induces changes in the neural circuits that control reward, stress, arousal, and decision making. These neuroadapative changes have been traditionally thought to be mediated by the signaling molecules, such as dopamine, serotonin, opioid peptides, glutamate, γ-aminobutyric acid, and systems that modulate the brain's stress response systems (Gilpin and Koob 2008). However, in recent years it has become increasing evident that pro-inflammatory neuroimmune signaling contribute to the cognitive dysfunction and behavioral alterations that are observed in AUD (Szabo and Lippai 2014). Thus, it is imperative to investigate key pro-inflammatory neuroimmune signaling pathways to gain

a better understanding of this devastating disease and to discover new therapeutic treatments that could help individuals suffering from this ailment.

IKKβ/NF-κB PATHWAY

NF-κB is an important contributor to neuroinflammation in numerous neuroimmune pathways. It is a ubiquitously expressed transcription factor family that controls the transcription of hundreds of genes that are involved in many physiological processes, including inflammation, immunity, cell proliferation, and cell death (Perkins and Gilmore 2006; Scheidereit 2006). More specifically, NF-κB transcription factors are homo- or heterodimers of the Rel family composed of the proteins NF-κB1 (p50/p105), NF-κB2 (p52/p100), RelA (p65), RelB, and c-Rel. All the Rel proteins possess a conserved N-terminal region, called the Rel Homology Domain (RHD). DNA-binding and dimerization domains are located in the N-terminal and C-terminal regions of the RHD, respectively. The Nuclear Localization Signal (NLS), which is essential for the transport of active NF-κB transcription factors into the nucleus, is located close to the C-terminal end of the RHD. NF-κB dimers are normally found in the cytosol of unstimulated cells due to the masked NLS (Perkins 2007; Schmid and Birbach 2008; Okvist *et al.* 2007).

Different signaling pathways stimulate each NF-κB dimer, and as a direct result, specific NF-κB dimers are responsible for transcribing unique sets of genes. However, it is the NF-κB canonical pathway that is most responsible for the expression of pro-inflammatory genes. The NF-κB dimer most commonly associated with this pathway is composed of the Rel proteins p65 and p50, which are normally sequestered in the cytosol of unstimulated cells by non-covalent interactions with the IκB that masks the NLS (Perkins 2007; Schmid and Birbach 2008; Okvist *et al.* 2007). NF-κB (p65/p50) activation requires degradation of IκB. Degradation is achieved when the inhibitory kappa-B kinase (IKK) complex, composed of IKKα, IKKβ, and two non-enzymatic IKKγ

accessory molecules, phosphorylates two adjacent serine residues in IκB which leads to ubiquitination and proteasomal degradation of the inhibitor. The NLS is then exposed and NF-κB is subsequently released where it translocates to the nucleus and acts as a transcription factor for numerous pro-inflammatory chemokines and cytokines, such as Tumor Necrosis Factor α (TNFα) and Interleukin-6 (IL-6) (Gamble *et al.* 2012; Schmid and Birbach 2008). The IKK complex represents a point of convergence for many pro-inflammatory extracellular signals, including endotoxins (LPS), pro-inflammatory cytokines (IL-6 and TNF-α), lymphokines, growth factors, double stranded RNA, certain bacterial antigens, and B or T-Cell activation, etc. (Fig.1.1). Thus, IKKs plays a key role in a number of diseases where inflammation is important (Gamble *et al.* 2012; Schmid and Birbach 2008). However, IKKβ is the only member of the IKK complex that specifically mediates the NF-κB canonical pathway, which is why the IKKβ/NF-κB pathway is the desired target of the proposed studies (Hayden and Ghosh 2004; Perkins 2007; Schmid and Birbach 2008).

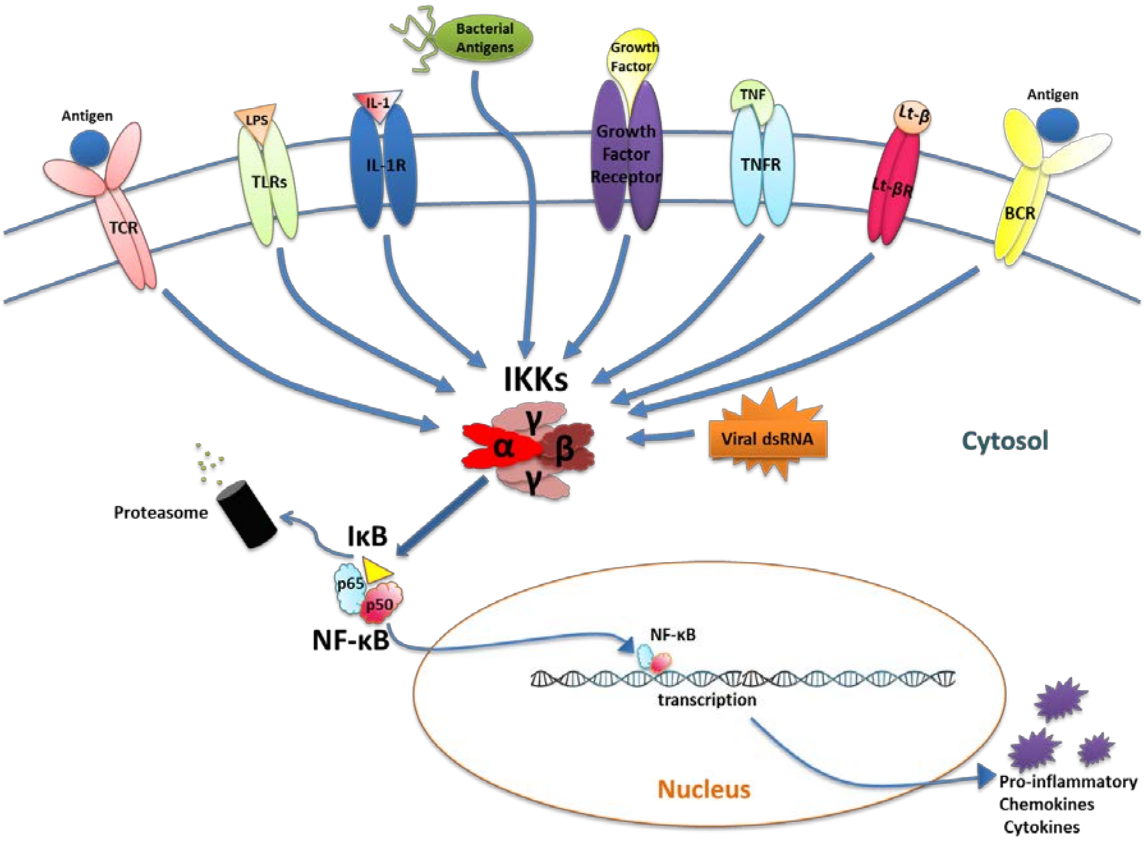

Figure 1.1. NF-κB Canonical Pathway (IKKβ/NF-κB Pathway). The IKK complex (IKKα, IKKβ, IKKγ) mediates numerous pro-inflammatory extracellular signaling pathways. When the IKK complex is activated, IKKα and IKKβ phosphorylate IκB to target it for proteasomal degradation, which in turn disinhibits the NF-κB dimer (p65/p50), which translocates to the nucleus and acts as transcription factor for pro-inflammatory chemokines and cytokines. TCR: T-cell Receptor; TLR: Toll-like Receptor; LPS: Lipopolysaccharide; IL-1(R): Interleukin-1 (Receptor); TNF(R): Tumor Necrosis Factor (Receptor); Lt-β(R): Leukotriene Beta (Receptor); BCR: B-cell Receptor; dsRNA: double stranded RNA; IKK: Inhibitory Kappa Kinase; NF-κB: Nuclear Factor Kappa B; IκB: Inhibitor of NF-κB.

BRAIN REGIONS IMPLICATED IN ALCOHOLISM

Many areas of the brain are thought to be involved in mediating ethanol drinking behaviors, but arguable the most import are the AMY, PFC, NAc, and VTA (Fig. 1.2) (Koob 2014; Koob and Volkow 2010). The AMY is linked to motivational behavior associated with drug abuse and alcoholism. For example, the CeA has been shown to mediate the behavioral effects of acute and chronic ethanol consumption in rodents (Lam *et al.* 2008; Roberto *et al.* 2004b; Roberto *et al.* 2004a; Roberto *et al.* 2005). Specifically, lesions of the central, but not basolateral, amygdala decrease voluntary alcohol consumption (Möller, Wiklund, Sommer, Thorsell, & Heilig, 1997). In addition, Koob and Volkow (2010) reviewed the neurocircuitry of drug addiction and concluded that plasticity in both frontal cortical and sub regions of the amygdala are important for craving, withdrawal, negative affect, and loss of control. The extended amygdala "circuit" emphasizes the CeA as well as the projections from the PFC (Peters *et al.* 2009).

The PFC is critical for executive function, which involves decision-making, planning, goal setting, motivation, and inhibiting impulses. It helps individuals predict the consequences of their choices. The lack of the PFC's control over impulsivity is one of the reasons alcoholics make high-risk, poorly conceived actions that often result in undesired consequences (Crews and Boettiger 2009; Zou and Crews 2010). Interesting, the PFC is the most severely damaged region of the brain in human alcoholics, and is closely related to the reward system (Liu *et al.* 2005).

The mesolimbic reward pathway includes the VTA and NAc, where dopaminergic neurons project from the VTA to the NAc. This "reward pathway" has been widely implicated in the development of AUD since it regulates behaviors associated with pleasurable outcomes (Engel and Jerlhag 2014). In rodents, ethanol increases dopamine release in the NAc (Engel and Jerlhag 2014; Blomqvist *et al.* 1997; Larsson

et al. 2003). Specifically, dopamine is released in the NAc in rats after voluntary ethanol consumption (Larsson *et al.* 2005). Likewise, ethanol administration increases firing rates of dopaminergic neurons in the VTA projecting to NAc (Gessa *et al.* 1985). In humans, intoxicating doses of ethanol increase dopamine release in the ventral striatum (Boileau *et al.* 2003). While knockdowns of metabotropic glutamate 7 and dopamine D1 receptors in the nucleus accumbens decrease alcohol drinking in mice (Bahi and Dreyer 2012; Bahi 2012).

In summary, four important brain regions involved in AUD include the AMY (involved in fear-motivated behaviors), the PFC (which controls decision making and the prediction of rewarding activities), and the NAc/VTA (mediates reward-related activities) (Jakobsson and Lundberg 2006). Investigation of these brain regions (homologous across multiple species) will allow us to better understand how the IKKβ/NF-κB pathways play a role in mediating the behavioral effects of alcohol.

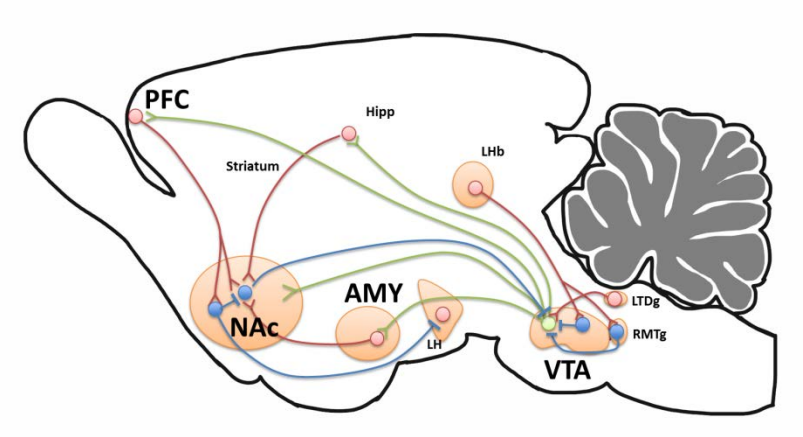

Figure 1.2. Brain Regions Important in the Development of Alcoholism. A simplified schematic of the mouse brain showing the regions associated with the neurobiology of alcoholism. Relevant dopaminergic (Green), glutamatergic (Red) and GABAergic (Blue) connections are shown between the areas of interest. PFC: Prefrontal Cortex; NAc: Nucleus Accumbens; AMY; Amygdala; VTA: Ventral Tegmental Area; Hipp: Hippocampus; LDTg: lateral dorsal tegmentum; LHb: Lateral Habenula; LH: Lateral Hypothalamus; RTMg: Rostromedial Tegmentum.

NEUROIMMUNE SIGNALING GENES AND ALCOHOLISM

Molecular and behavioral studies support the importance of neuroimmune signaling in the development of alcohol and drug abuse (Mayfield *et al.* 2013). For example, innate immune signaling has been implicated in paying a role in binge/intoxication, withdrawal/negative affect, and craving in alcohol abuse (Coller and Hutchinson 2012; Crews *et al.* 2011; Harris and Blednov 2012; Mayfield *et al.* 2013). The role of innate immunity genes in alcoholism is also supported by genetic association studies in humans (Edenberg *et al.* 2007; Pastor *et al.* 2005; Pastor *et al.* 2000; Saiz *et al.* 2009), transcriptome meta-analysis in rodents (Mulligan *et al.* 2006), and gene expression microarray studies in postmortem brains of alcoholics (Liu *et al.* 2006; Okvist *et al.* 2007). Behavioral studies in mice with null mutations of neuroimmune genes demonstrate reduced ethanol consumption (Blednov *et al.* 2005; Blednov *et al.* 2012; Blednov 2003). Many of the immune-related genes implicated in the above mentioned studies mediate their affect through NF-κB. Moreover, systemic injection of LPS, which conveys its signal through Toll-like receptor 4 (TLR4), and the IKKβ/NF-κB pathway, produces long-lasting elevations of brain pro-inflammatory cytokines and increases ethanol consumption in mice (Blednov *et al.* 2011; Qin *et al.* 2008; Qin *et al.* 2007). Likewise, knockdown of TLR4 in the CeA shows reduced operant self-administration of ethanol (Liu *et al.* 2011). Interestingly, NF-κB DNA binding in the brain has been shown to increase with ethanol treatments (Crews *et al.* 2006) and the human NF-κB1 gene, which codes for the precursor of the p50, is genetically linked to alcoholism (Edenberg *et al.* 2007). Ethanol increases transcription of NF-κB target genes, including pro-inflammatory chemokines (MCP-1) and cytokines (TNF-α, IL-6, and IL-1β) (Zou and Crews 2010). It is thought that the repeated alcohol exposures promote the activation of NF-κB in neurons and glia leading to autocrine and paracrine amplification of pro-inflammatory innate immune genes. This activation is thought to

spread through positive feedback loops that eventually lead to progressive and persistent changes associated with alcohol abuse (Crews *et al.* 2011). This evidence suggests that a neuroimmune signaling pathway mediated by IKKβ/NF-κB pathway is important in the neurobiology of alcoholism.

NEUROIMMUNE SIGNALING MICRORNAS AND ALCOHOLISM

However, genes do not solely regulate the neuroimmune response to alcohol. In recent years, microRNAs have emerged as important regulators of gene expression. MicroRNAs are small (18-22 nucleotides) non-coding RNA molecules. They post-transcriptionally regulate gene expression by binding to complementary sequences in the 3' untranslated regions (UTR) of mRNAs, which results in either translational repression or cleavage of the message (Miranda *et al.* 2010) (Fig 1.3). A single microRNA can target numerous mRNA transcripts, while a single mRNA transcript can be targeted by many microRNAs. There is considerable regulatory potential of microRNAs since over 1000 microRNAs have been identified in humans and are thought to target over 60% of protein-coding genes (Iliopoulos *et al.* 2009; Miranda *et al.* 2010). Since microRNAs are capable of silencing the expression of large collections of target genes, it is reasonable to expect that they are involved in regulating the neuroimmune system, such as the IKKβ/NF-κB pathway. Recent studies have revealed that microRNAs play important roles in immune signaling, neuronal differentiation, and neurogenesis (Miranda *et al.* 2010). For example, let-7 family members (let-7i, let-7e) directly targets expression of TLR4 and thus regulate responsiveness to LPS (Androulidaki *et al.* 2009; Chen *et al.* 2007; Virtue *et al.* 2012). MiR-146a fine tunes many pro-inflammatory genes that utilize the IKKβ/NF-κB pathway (TLR4, IRAK1, TRAF6 and cytokine signaling) (Sonkoly *et al.* 2007; Virtue *et al.* 2012). MiR-152 inhibits TLR-triggered major histocompatibility complex (MHC) II expression (Liu *et al.* 2010).

MiR-9 regulates NF-κB1, and mir-199 targets IKKβ (Bazzoni *et al.* 2009; Virtue *et al.* 2012). MicroRNAs also participate in positive pro-inflammatory feedback loops involving NF-κB, let-7, and IL-6 (Iliopoulos *et al.* 2009). Even with this supporting evidence, the role of neuroimmune signaling in the induction and maintenance of AUD remains elusive.

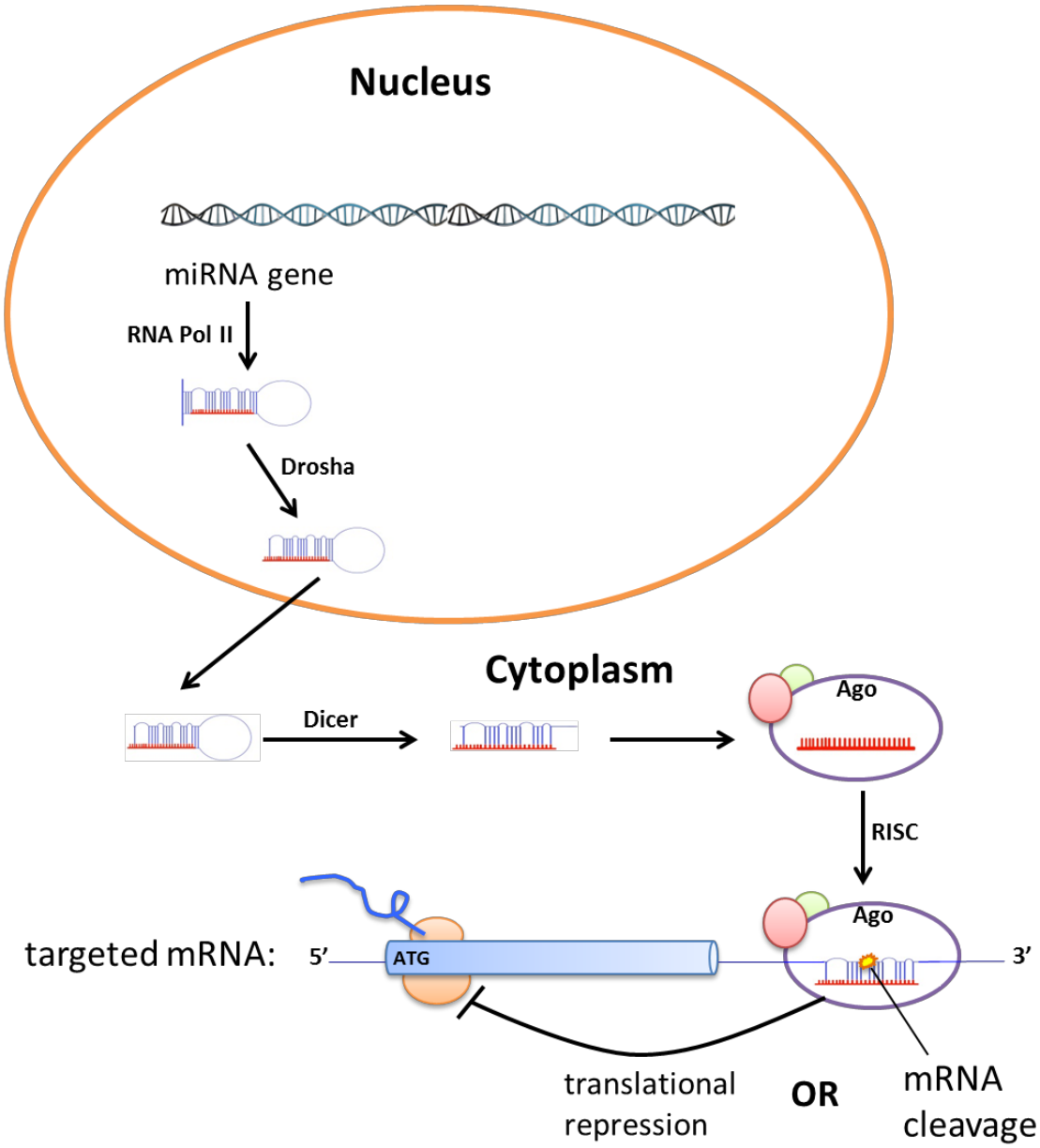

Figure 1.3. MicroRNA Post-Transcriptional Regulation of mRNAs. Primary microRNA hairpin transcripts are transcribed by RNA polymerase II. Cleaved by the RNAase Drosha into a shorter hairpin that is transported from the nucleus to the cytoplasm. Subsequently, another RNAase, called Dicer, removes the hairpin and the mature microRNA associates with the Argonaut protein (Ago) to form to the RNA-induced silencing complex (RISC). Ago directs the complex to the 3'UTR of mRNAs complementary to the mature microRNA where translation is disrupted or mRNA cleavage occurs.

GAPS IN OUR KNOWLEDGE

Our understanding of the neuroimmune system and its impact on ethanol-drinking behaviors has improved in recent years; however, little is known about the potential involvement of IKKβ/NF-κB pathways. There are no published studies to date that have directly manipulated IKKβ-specific pathways either *in vitro* or *in vivo* to investigate alcohol or other substance abuse disorders. Thus, we lack the appropriate evidence to discern whether the IKKβ/NF-κB pathway is important centrally in the brain, in the periphery, or in both. There is also limited information about the brain region and central nervous system (CNS) cell-type specificity of IKKβ, and even less in the brain regions commonly associated with alcoholism (PFC, NAc, AMY, VTA). In essence, we do not know which brain regions or what cell types IKKβ, or more generally, the IKKβ/NF-κB pathway is predominately expressed. Nor do we know which of the cell types or brain regions, if any, are most important in regulating voluntary ethanol drinking phenotypes. Moreover, there is a scarcity of knowledge on potential upstream pro-inflammatory signaling pathways that may activate the IKKβ/NF-κB pathway in the response to alcohol intake. Lastly, even though the field of investigating ethanol-responsive microRNAs is increasing, we still lack knowledge about which microRNAs change and where they change in the brain in response to ethanol exposure. More specifically, there are only a few studies that have looked at which microRNAs are important for regulating the IKKβ/NF-κB pathway in the brain, but none have investigated how modulating these specific microRNAs would affect ethanol-drinking behaviors. This dissertation contains two specific aims that will address many of these areas and will contribute to a more thorough understanding of IKKβ/NF-κB pathway's role in alcoholism.

SPECIFIC AIMS

1. Assess how neuroimmune signaling genes in the IKKβ/NF-κB pathway modulate voluntary ethanol drinking.
    a. Investigate brain region and cell type-specific expression of signaling genes associated with the IKKβ/NF-κB pathway.
    b. Modulate signaling genes associated with the IKKβ/NF-κB pathway in brain-specific regions.
2. Assess how ethanol-responsive microRNAs associated with the IKKβ/NF-κB pathway modulate voluntary ETOH drinking in the brain.
    a. Determine differentially expressed microRNAs in brain-specific regions associated with the IKKβ/NF-κB pathway.
    b. Manipulate microRNAs associated with the IKKβ/NF-κB pathway in brain-specific regions.

CHAPTER II: IKK Isoform Expression in Brain Regions Associated with Alcohol Use Disorder

INTRODUCTION

Over 17 million individuals in the United States, or approximately 10% of the total population over 12 years old abuse alcohol (Manit *et al.* 2009). Excessive alcohol consumption is the third leading cause of preventable mortality in the United States trailing only behind tobacco use and obesity/poor diet (Mokdad 2004). The economic burden in the United States due to loss of productivity, societal damage, and healthcare costs amounts to a staggering $223.5 billion annually (Bouchery *et al.* 2011). Alcohol use disorder (AUD) is a chronic, relapsing condition with few treatment options. In fact, there are only 3 drugs currently approved by the FDA for use in AUD (disulfiram, naltrexone, and acamprosate) (Jonas *et al.* 2014).

Although the etiology of AUD is unknown, cortical executive dysfunction, cognitive inflexibility, and increased limbic anxiety and impulsivity may be involved (Vetreno and Crews 2014). Brain areas that are important in the development of AUD include the AMY, PFC, NAc, and VTA (Fig. 1.2) (Vetreno and Crews 2014; Koob 2014; Koob and Volkow 2010; Crews and Vetreno 2014). The AMY is linked to motivational behavior associated with drug and alcohol abuse. Koob and Volkow reviewed the neurocircuitry of drug addiction and concluded that plasticity in both PFC and AMY is important for craving, withdrawal, negative affect, and loss of control (Koob and Volkow 2010). More specifically, the PFC is critical for executive function, which involves decision making, planning, goal setting, motivation, and inhibiting impulses (Crews and Boettiger 2009; Crews *et al.* 2011). Interestingly, the PFC is the most severely damaged region of the brain in human alcoholics, and is closely related to the reward system (Liu *et al.* 2006). The mesolimbic dopamine reward system, consisting of the NAc and VTA,

is a well-documented pathway in alcohol and other substance abuse disorders. The NAc receives dopaminergic input from neurons in the VTA and has been shown to positively reinforce addictive behaviors (Bahi and Dreyer 2012; Koob and Volkow 2010; Ross and Peselow 2009).

The neurobiological changes in brain regions associated with the addictive process may be partly mediated by increased pro-inflammatory immune signaling. The IKK isoforms (IKKα, IKKβ, IKKγ) and the IKK-related kinase (IKKε) are critical for innate/adaptive immunity activation through either NF-κB or interferon regulatory factors (IRFs), respectively (Chau *et al.* 2008). IKKε is also known to activate NF-κB through an poorly understood mechanism (Chau *et al.* 2008; Sankar *et al.* 2006; Takeda and Akira 2004). NF-κB is a ubiquitously expressed transcription factor that plays an essential role in transcribing genes related to inflammation, immunity, cell proliferation, and cell death (Perkins and Gilmore 2006; Scheidereit 2006).

NF-κB exerts most of its effects through the IKK-dependent canonical and non-canonical pathways (Fig 2.1) (Oeckinghaus and Ghosh 2009). However, the majority of the physiologically diverse signaling pathways activate NF-κB through the canonical pathway, which is mediated by the IKK complex (composed of IKKα, IKKβ, and two non-enzymatic IKKγ accessory molecules). This particular pathway is activated by numerous pro-inflammatory stimuli such as endotoxins (LPS), inflammatory cytokines (IL-1), TNF-α, lymphokines, growth factors, double stranded RNA, certain bacterial antigens, and B or T-Cell activation, etc. (Gamble *et al.* 2012; Perkins 2007; Schmid and Birbach 2008). The IKK complex activates this pathway when IKKβ phosphorylates two adjacent serine residues in the inhibitor IκB, which leads to ubiquitination and proteasomal degradation of the inhibitor. This unmasks NLS and NF-κB is subsequently released where it translocates to the nucleus and acts as a transcription factor for

numerous pro-inflammatory chemokines and cytokines (Gamble *et al.* 2012; Perkins 2007; Schmid and Birbach 2008). Thus, the IKK isoforms represent an important mediatory step for numerous pro-inflammatory signaling cascades (Fig 1.1) (Gamble *et al.* 2012; Oeckinghaus and Ghosh 2009). Although IKKα and IKKγ are required, IKKβ is the only member of the IKK complex that specifically mediates the NF-κB canonical pathway (Hayden and Ghosh 2004; Perkins 2007; Perkins and Gilmore 2006; Schmid and Birbach 2008).

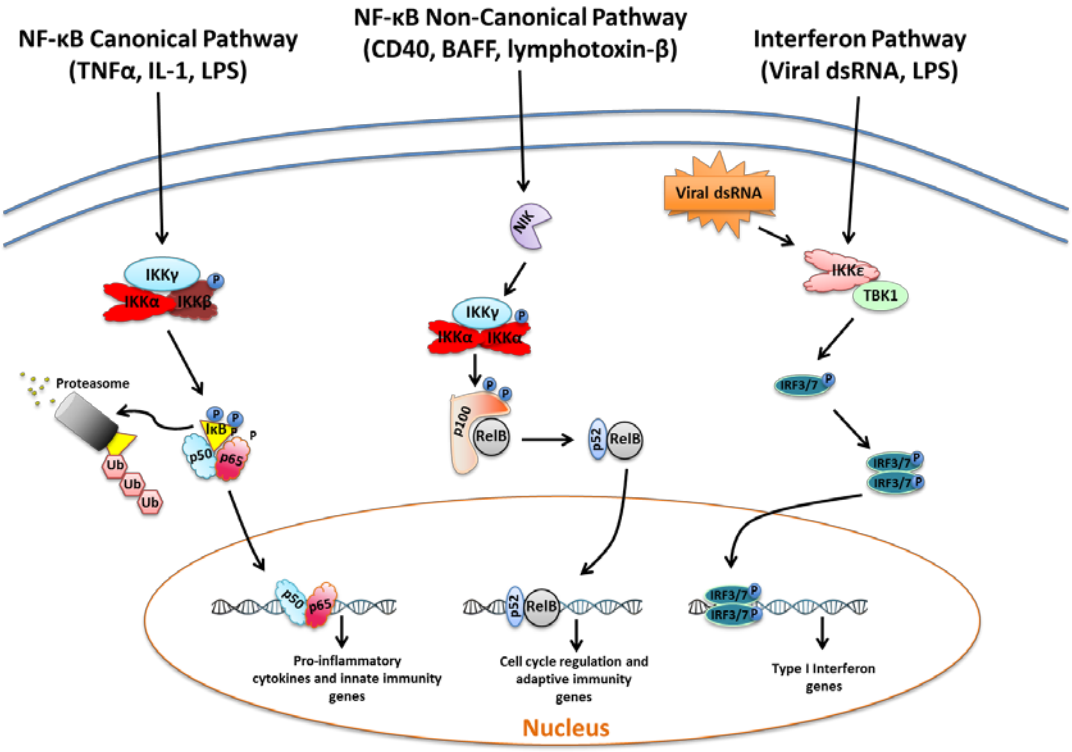

Figure 2.1 IKK-Dependent Signaling Pathways. IKKs play a critical role in numerous signaling pathways involving innate/adaptive immunity. The IKK complex consisting of IKKα, IKKβ, and IKKγ mediates the NF-κB canonical pathway (IKKβ/NF-κB pathway). The canonical pathway is activated by numerous pro-inflammatory stimuli, such as TNF-α, IL-1, and LPS. IKKβ phosphorylates IκB targeting it for proteasomal degradation and releases NF-κB (p50/p65) that translocates to the nucleus and transcribes numerous pro-inflammatory cytokines and other innate immunity genes. In contrast, IKKα dimers and IKKγ modulate the NF-κB non-canonical pathway, which is activated by stimuli such as CD40, BAFF, and lymphotoxin-β. The IKKα dimers are activated by way of NIK, which in turn phosphorylates NF-κB (p100/RelB), and proteolytically process it to NF-κB (p52/RelB) that translocates to the nucleus and transcribes genes important for cycle regulation and the adaptive immune system. IKKε mediates the interferon response and is activated by stimuli such as LPS or viral dsRNA and phosphorylates IRF3 or IRF7, which translocates to the nucleus to transcribe Type I interferon genes.

In contrast, the non-canonical pathway proceeds via activation of NF-kB-inducing kinase (NIK), which in turn activates a complex consisting of an IKKα dimer and IKKγ, ultimately resulting in the transcription of genes important for cell cycle regulation and the adaptive immune system (Oeckinghaus and Ghosh 2009; Perkins 2007; Perkins and Gilmore 2006).

IKKε is preferentially expressed in T cells and peripheral blood cells. The IKK-related kinase IKKε (also called IKKi) has a similar sequence to IKKα and IKKβ, and is also implicated in activating NF-κB. However, IKKε's primary function is to mediate the expression of type I interferon genes from stimuli that activate the TLR4- and TLR3-dependent signaling cascades, such as LPS (component of gram negative bacteria) and double-stranded RNA (product of replicating viruses), respectively. Once IKKε is activated, it phosphorylates either IRF3 or IRF7 transcription factors, which translocate to the nucleus and transcribe type I interferon genes (Chau *et al.* 2008; Hacker and Karin 2006).

Considering the role of IKKα, IKKβ, IKKγ, and IKKε in mediating pro-inflammatory cytokine expression in NF-κB pathways together with the evidence for a neuroimmune component of AUD, we studied the expression patterns of individual IKK isoforms in brain regions that are important in addiction. The brain region, cell type specificity, and subcellular expression patterns for the IKK isoforms were previously unexamined. Thus, determining the expression patterns of these isoforms would provide us with the necessary information to selectively manipulate specific isoforms *in vivo* in order to study their potential role in ethanol drinking behaviors.

MATERIALS AND METHODS

Animals

IKK isoform expression studies were conducted in adult male C57BL/6J mice purchased from Jackson Laboratories (Jackson Laboratories, Bar Harbor, ME). The C57BL/6J strain was chosen because of its propensity for voluntary ethanol

consumption (Belknap *et al.* 1997). Mice were group-housed 4 or 5 per cage in the Animal Resources Center at The University of Texas at Austin on a 12 h light/12 h dark cycle (lights on at 7:00 a.m.) with ad libitum access to water and rodent chow (Prolab RMH 180 5LL2 chow, TestDiet, Richmond, IN). The temperature and humidity of the room were kept constant. All experiments were approved by the university's Institute for Animal Care and Use Committee and conducted in accordance with NIH guidelines with regard to the use of animals in research.

Tissue harvest

Animals were sacrificed and transcardially perfused with Phosphate Buffer Saline (PBS) and 4% paraformaldehyde (PFA). Brains were harvested, postfixed for 24 h in 4% PFA at 4°C, and cyroprotected for 24 h in 20% sucrose in PBS at 4°C. Brains were placed in molds containing OCT compound (VWR, Radnor, PA) and frozen in isopentane on dry ice. The brains were equilibrated in a -12 to -14°C cryostat (Thermo Fischer Scientific) for at least 1 h and coronal 30-µm sections between +3.20 and -4.00 mm relative to bregma were collected. Sections of sequential triplicate samples were placed in sterile PBS and stored at 4°C.

Immunohistochemistry

Brains sections were categorized using low magnification light microscopy relative to bregma with a mouse stereotaxic brain atlas in order to identify the PFC (+3.20 mm to +2.00 mm), NAc (+1.80 mm to +0.90 mm), AMY (-0.60 mm to -2.00 mm), and VTA (-2.80 mm to -3.40 mm). Sections from each region were selected and stained. Sections were permeabilized with 0.1% Triton-X 100 (2 x 10 min at 25°C), washed in PBS (3 x 5 min at 25°C), blocked with 10% goat or donkey serum (30 min at 25°C), and treated with 1:50 anti-IKKα (Novus, Littleton, CO), 1:250 anti-IKKβ (Millipore, Billerica, MA), 1:250 anti-IKKγ (Abcam, Cambridge, MA), 1:100 anti-IKKε (Santa Cruz,

Santa Cruz, CA), 1:500 anti-NeuN (Santa Cruz), 1:300 anti-GFAP (Santa Cruz), 1:1000 anti-Iba1 (Dako, Dako, Denmark), and 1:1000 anti-GFP (Santa Cruz) antibodies (at 4°C overnight). Sections were washed in PBS (3 x 10 min at 25°C), subjected to reaction with fluorescence-conjugated secondary antibodies of 1:1000 Alexa 488 and 1:1000 Alexa 568 (Invitrogen, Waltham, MA) (2 hr at 25°C), and rinsed with PBS (3 x 10 min at 25°C). The sections were mounted on slides using sterile 0.2% gelatin and DAPI mounting media (Vector Laboratories, Burlingame, CA) and cover slipped. Two sets of control experiments were performed to test antibody specificity: 1) replacement of the primary antibody with only the serum of the appropriate species and 2) omission of secondary antibodies. No immunostaining was detected under either of these conditions.

Imaging/Analysis

Epi-fluorescent images were acquired using a Zeiss Axiovert 200M Fluorescent Microscope (Zeiss, Oberkocheen, Germany) equipped with a 20x objective and an automated stage. Images of the PFC, NAc, AMY and VTA were captured (nine 20x images per brain half for anti-IKKs co-stained with anti-NeuN or anti-Iba1; entire half of brain for anti-IKKs co-stained with anti-GFAP and for examination of overall cell type composition, which equaled twenty-four 20x images/side) in red, green, and blue channels then stitched together creating a composite view for further analysis. Images were taken without saturating the signal and digitized at 8-bits using the full intensity range of 0–256 and imported into the ImageJ software package (http://imagej.nih.gov/ij/). Composite images were split into the individual channels and overlaid with grids that contained 100 cells per square (for anti-IKKs co-stained with anti-NeuN and anti-Iba1) or entire halves of the brain (for anti-IKKs co-stained with anti-GFAP). Cells were co-localized with the aid of a cell counter to quantify cell-type specificity. For determining overall cell type composition in each brain area, entire

halves of the brain were analyzed using an automatic cell counting plugin (ICTN) in ImageJ. A Zeiss LSM 710 Confocal Microscope (Zeiss) equipped with a 63x objective was used to take representative images for IKK cell-type specificity and to investigate subcellular localization patterns using a z-stack of images throughout the width of the cell.

Statistical Analysis

Numerical data are given as mean ± SEM, and n represents the number of animals tested.

RESULTS

Cell Type-Specificity of IKK Isoforms in the Brain

High magnification confocal microscopy was used to qualitatively investigate the cell type-specificity of each of the IKK isoforms (IKKα, IKKβ, IKKγ, and IKKε) in the PFC, NAc, AMY, and VTA. All of the IKK isoforms were ubiquitously expressed throughout all brain regions studied and were present in neurons, microglia, and astrocytes (Fig. 2.2, 2.3, 2.4, 2.5). However, each isoform demonstrated some unique brain regional and subcellular distributions. For example, IKKγ was co-localized in almost every neuron in each brain region. In general, IKKε was not seen in astrocytes in the VTA. Interestingly, each isoform had unique subcellular expression characteristics. IKKα was observed throughout the nucleus and cytoplasm, including the soma and processes, in both neurons (Fig. 2.2 A-C) and astrocytes (Fig 2.2 D-E), but was localized to very distinct regions in the microglia near the major processes (Fig 2.2 G-H). IKKβ and IKKε demonstrated almost exactly the same pattern as IKKα, except that IKKβ and IKKε were not found in the processes of neurons (Fig 2.3, 2.5). In contrast, IKKγ's expression was different than IKKα and IKKβ. IKKγ appeared to be localized in the nucleus but not the cytoplasm of neurons and astrocytes, and exhibited the same localization in microglia as seen with the other IKK isoforms.

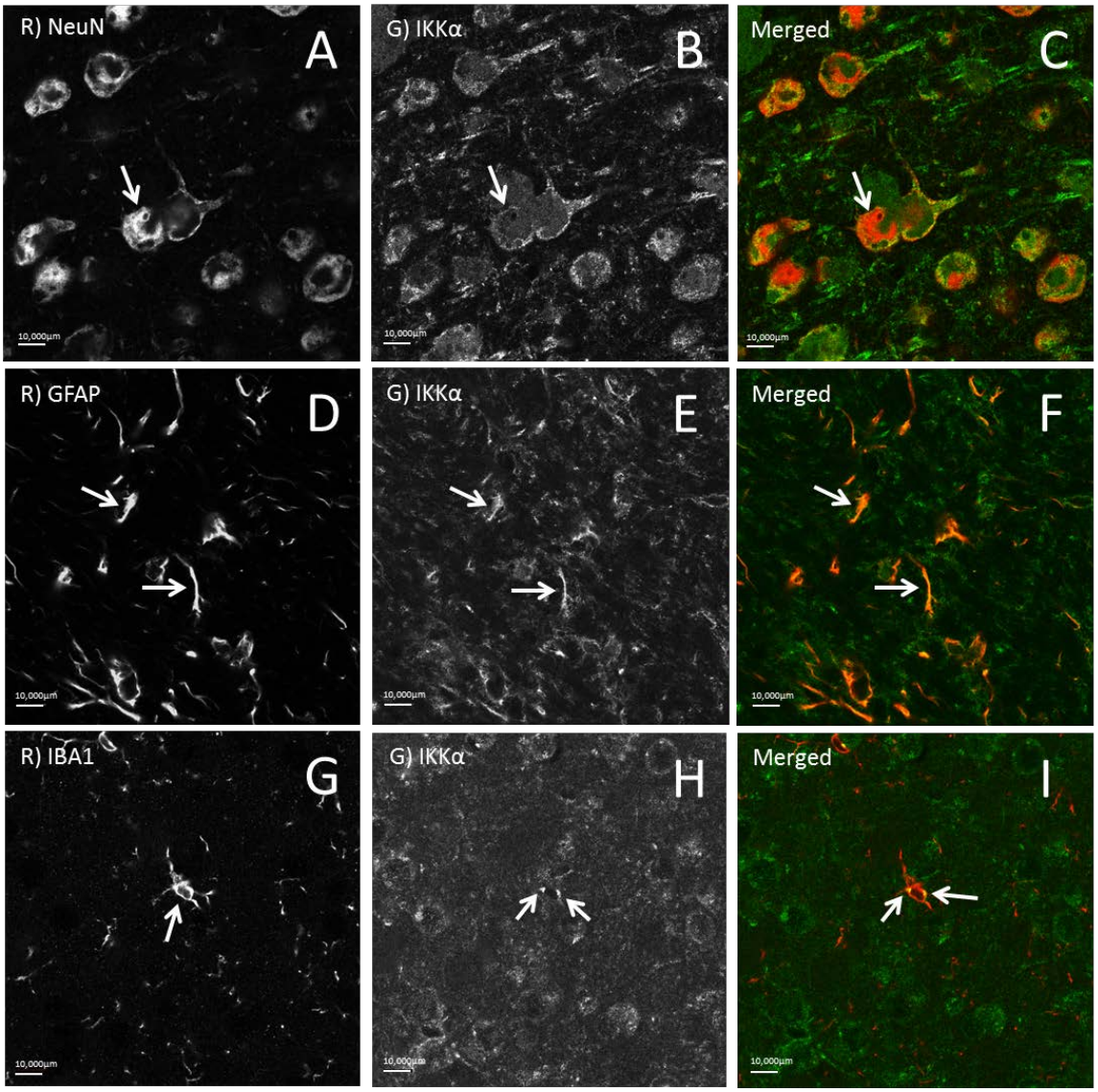

Figure 2.2. Cell Type-Specificity of IKKα in the Brain. Representative fluorescent light microscope images illustrating cell-type specific antibodies in the first column (A: anti-NeuN for neurons; D: anti-GFAP for astrocytes; G: anti-Iba1 for microglia), anti-IKKα stains in the second column (B, E, H), and overlay of the first two in the third column (C, F, I). Arrows illustrate co-localization of cells using anti-IKKα and cell type-specific stains.

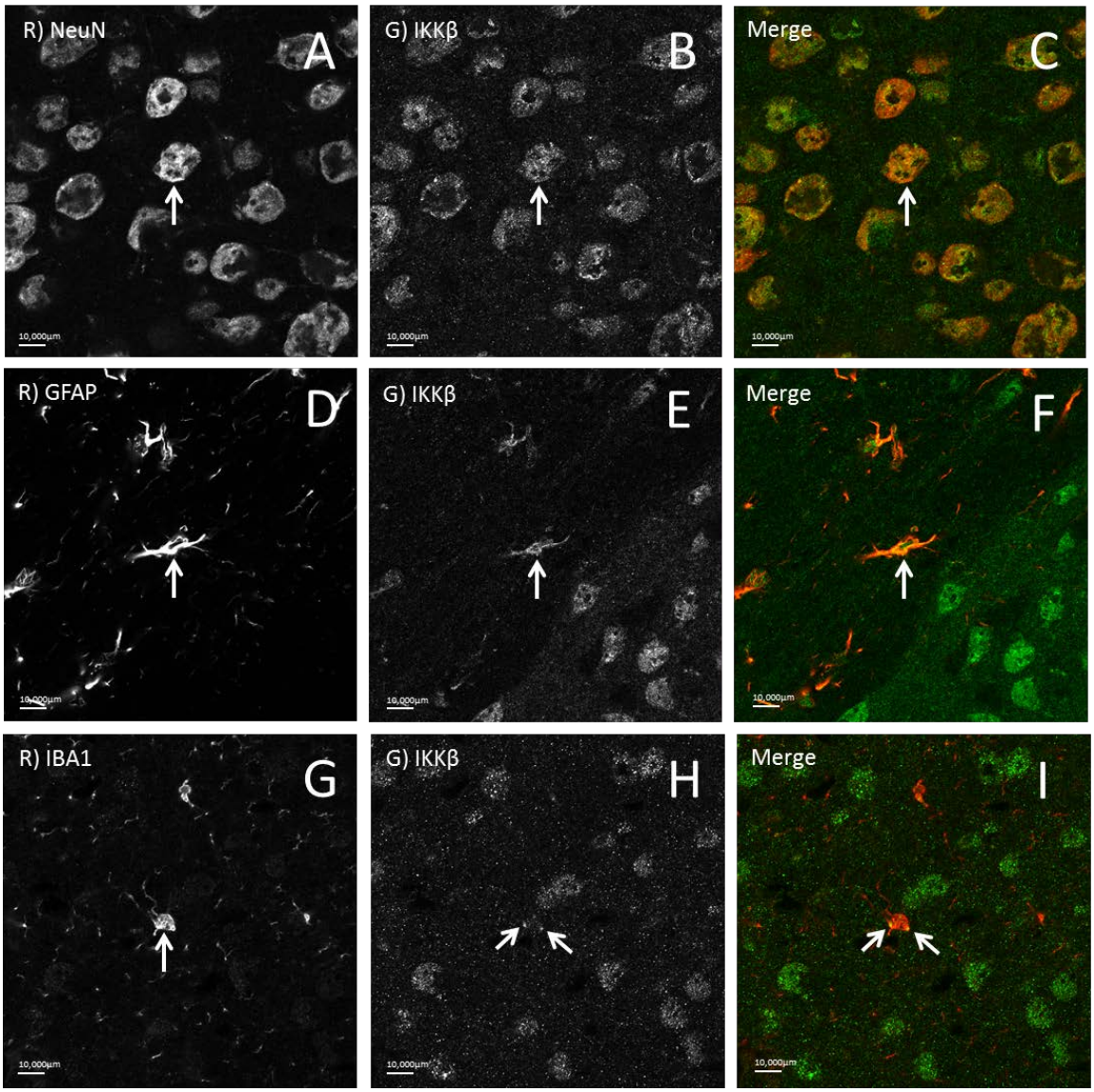

Figure 2.3. Cell Type-Specificity of IKKβ in the Brain. Representative fluorescent light microscope images illustrating cell-type specific antibodies in the first column (A: anti-NeuN for neurons; D: anti-GFAP for astrocytes; G: anti-Iba1 for microglia), anti-IKKβ stains in the second column (B, E, H), and overlay of the first two in the third column (C, F, I). Arrows illustrate co-localization of cells using anti-IKKβ and cell type-specific stains.

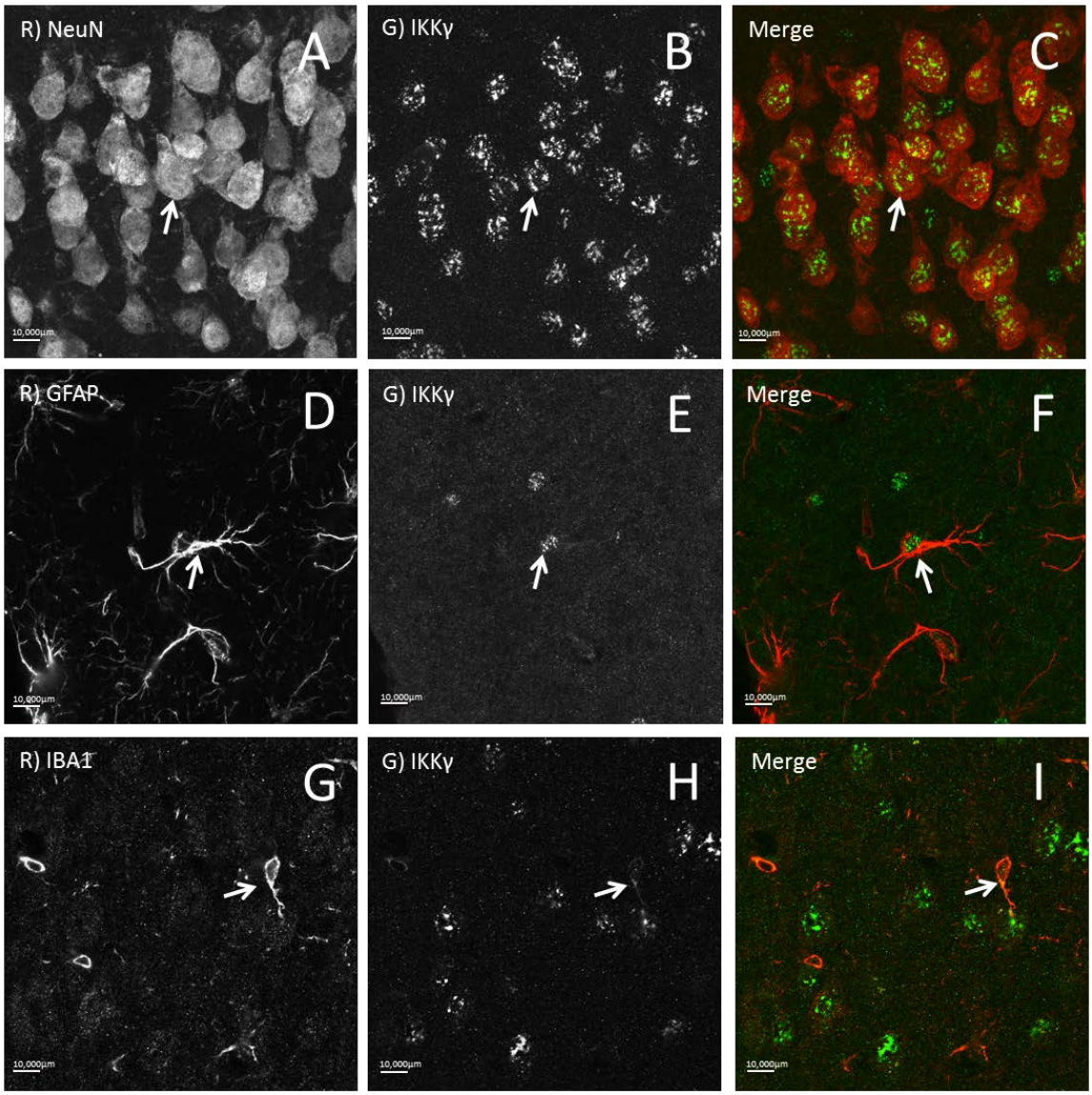

Figure 2.4. Cell Type-Specificity of IKKγ in the Brain. Representative fluorescent light microscope images illustrating cell-type specific antibodies in the first column (A: anti-NeuN for neurons; D: anti-GFAP for astrocytes; G: anti-Iba1 for microglia), anti-IKKγ stains in the second column (B, E, H), and overlay of the first two in the third column (C, F, I). Arrows illustrate co-localization of cells using anti-IKKγ and cell type-specific stains.

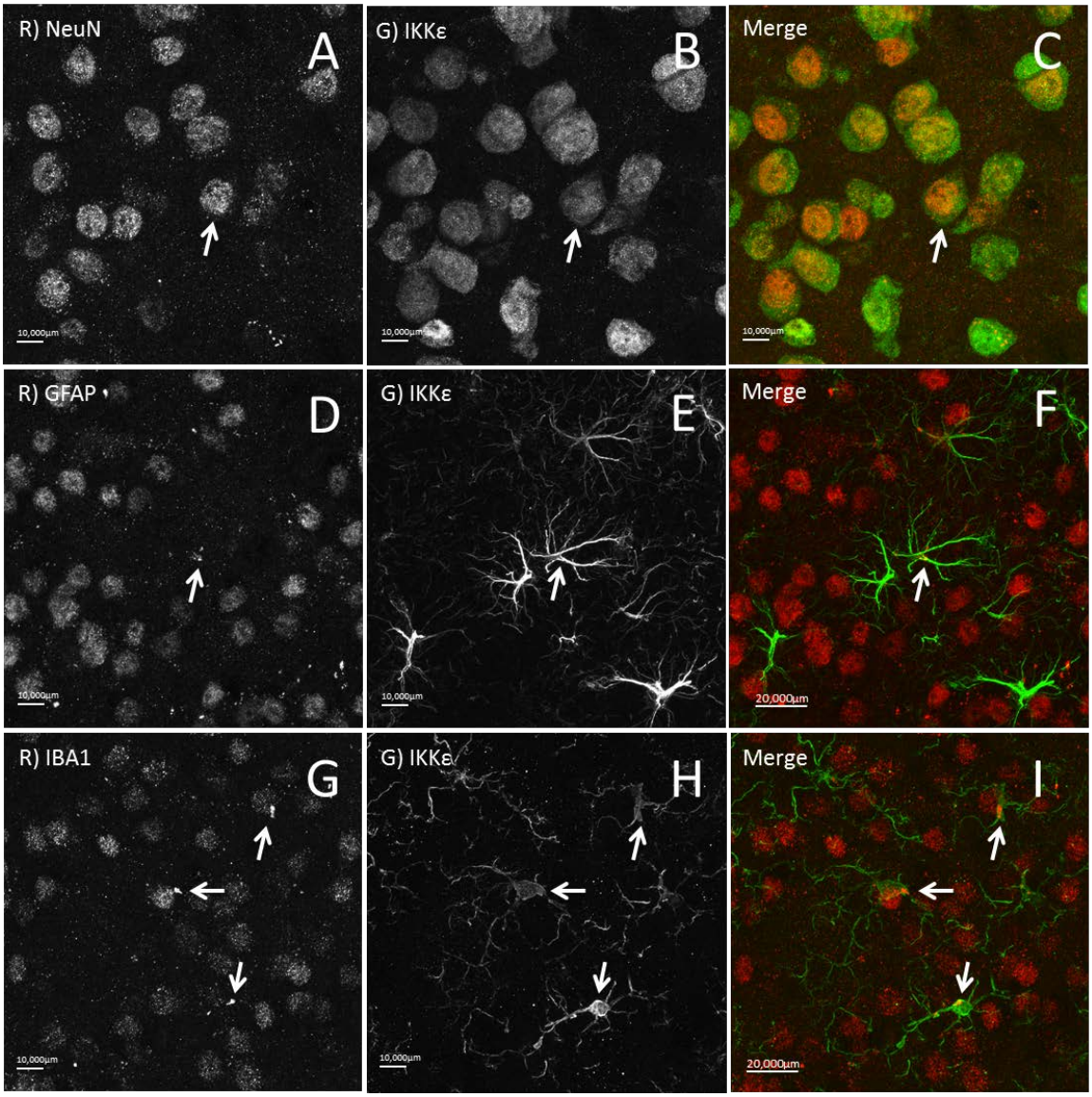

Figure 2.5. Cell Type-Specificity of IKKε in the Brain. Representative fluorescent light microscope images illustrating cell-type specific antibodies in the first column (A: anti-NeuN for neurons; D: anti-GFAP for astrocytes; G: anti-Iba1 for microglia), anti-IKKε stains in the second column (B, E, H), and overlay of the first two in the third column (C, F, I). Arrows illustrate co-localization of cells using anti-IKKε and cell type-specific stains.

Brain Region-Specific Protein Expression of IKK Isoforms

Expression levels of the IKK isoforms (IKKα, IKKβ, IKKγ, and IKKε) were quantified by immunostaining sections from the PFC, NAc, AMY, and VTA with antibodies against each IKK isoform and using the nuclear DNA stain, DAPI. The total IKK expression was determined by calculating the percentage of DAPI-positive cells co-localized with the IKK antibodies out of the total DAPI-positive cells (n=5/group for IKKα, IKKβ, IKKγ and n=3 for IKKε). All the IKK isoforms, except IKKε, appeared to have a similar overall expression pattern. For example, the highest levels of IKKα, IKKβ, and IKKγ were in the NAc followed by roughly equal levels in the PFC and AMY, while the VTA contained markedly lesser amounts. In contrast, IKKε levels were almost constant throughout the brain (PFC: 63.5% ± 4.4%; NAc: 66.0% ± 2.0%; AMY: 72.7% ± 2.9%; VTA: 63.3% ± 2.7%). Interestingly, all the IKK isoforms were expressed in > 60% of the cells in the PFC, NAc, and AMY. IKK expression in the VTA was more varied, ranging from approximately 30% of the cells containing IKKα and IKKβ, to over 60% of cells containing IKKε. IKKγ was the most abundant in the PFC and NAc, while IKKε was the most abundant in the AMY and VTA. However, IKKγ was the most abundant in all brain regions when compared to the IKKα and IKKβ (Fig. 2.2).

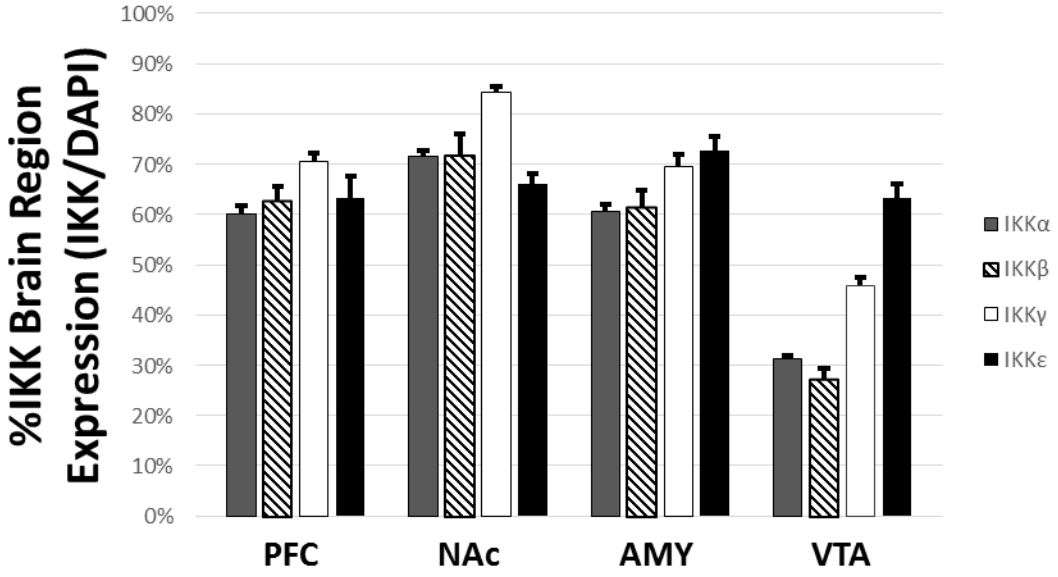

Figure 2.6. Brain Region-Specific Protein Expression of IKK Isoforms. Expression levels of the IKK isoforms (IKKα, IKKβ, IKKγ, and IKKε) were quantified by determining the percentage of DAPI-positive cells co-localized with the IKK antibodies out of the total DAPI-positive cells in the sampling area in the PFC, NAC, AMY, and VTA. (n=6/group for IKKα, IKKβ, IKKγ and n=3 for IKKε). Mean ± SEM.

Cell Type-Specific Protein Expression of IKK Isoforms

Cell-specific expression levels of the IKK isoforms (IKKα, IKKβ, IKKγ, and IKKε) were quantified by immunostaining sections from the PFC, NAc, AMY, and VTA with antibodies against each IKK isoform, co-stained with the nuclear DNA stain (DAPI), and antibodies against cell-specific markers for neurons (NeuN), microglia (Iba1), and astrocytes (GFAP). Cell-specific IKK isoform expression was determined using only DAPI-positive cells and by calculating the percentage of cells co-localized with the IKK antibodies and cell-specific markers out of cells with only the cell-specific marker (n=3-5/group for IKKα, IKKβ, IKKγ, IKKε). All IKK isoforms, except IKKε, appeared to have a similar overall expression pattern. For example, IKKα, IKKβ, and IKKγ were most abundant in neurons, with lower expression in microglia, and lowest expression in astrocytes in the PFC, NAc, AMY, and VTA. In contrast, IKKε was expressed in approximately equal amounts in neurons and microglia, but significantly less in astrocytes. Interestingly, over 80% of the neurons in all brain regions expressed IKKs regardless of the isoform, and IKKγ was expressed in at least 95% of neurons. Microglia expression was more variable ranging from 35 to 84%, depending on the brain region and IKK isoform (Fig. 2.3). More specifically, IKKα, IKKβ, IKKγ were expressed in approximately half of microglia cells (IKKα: 48.8% ± 2.8%; IKKβ 55.5% ± 4.2%; IKKγ: 61.9% ± 5.1%), while IKKε was expressed in over three fourths of microglial cells (IKKε: 78.4% ± 3.1%) (Fig.2.4). The only notable exception was IKKγ microglia expression in the VTA, where IKKγ (75.9% ±9.8%) and IKKε (73.4% ±.0.5%) were about the same (Fig. 2.3). In contrast to microglia, IKKα, IKKβ, IKKγ were expressed in greater amounts than IKKε (Fig 2.3). However, the IKK isoforms were not well expressed in astrocytes in any brain region. IKKα, IKKβ, IKKγ were found in approximately one third of astrocytes throughout the brain (IKKα: 30.6.8% ± 4.6%; IKKβ 30.2% ± 7.5%; IKKγ: 39.8% ± 6.1%), while IKKε was present in only 15.9% ± 6.4 of astrocytes (Fig 2.4). One notable

difference is that astrocytic expression of IKKα and IKKβ was much lower in VTA than the other brain regions (IKKα: 18.2% ± 6.3%; IKKβ 16.1% ± 5.9%) (Fig 2.3).

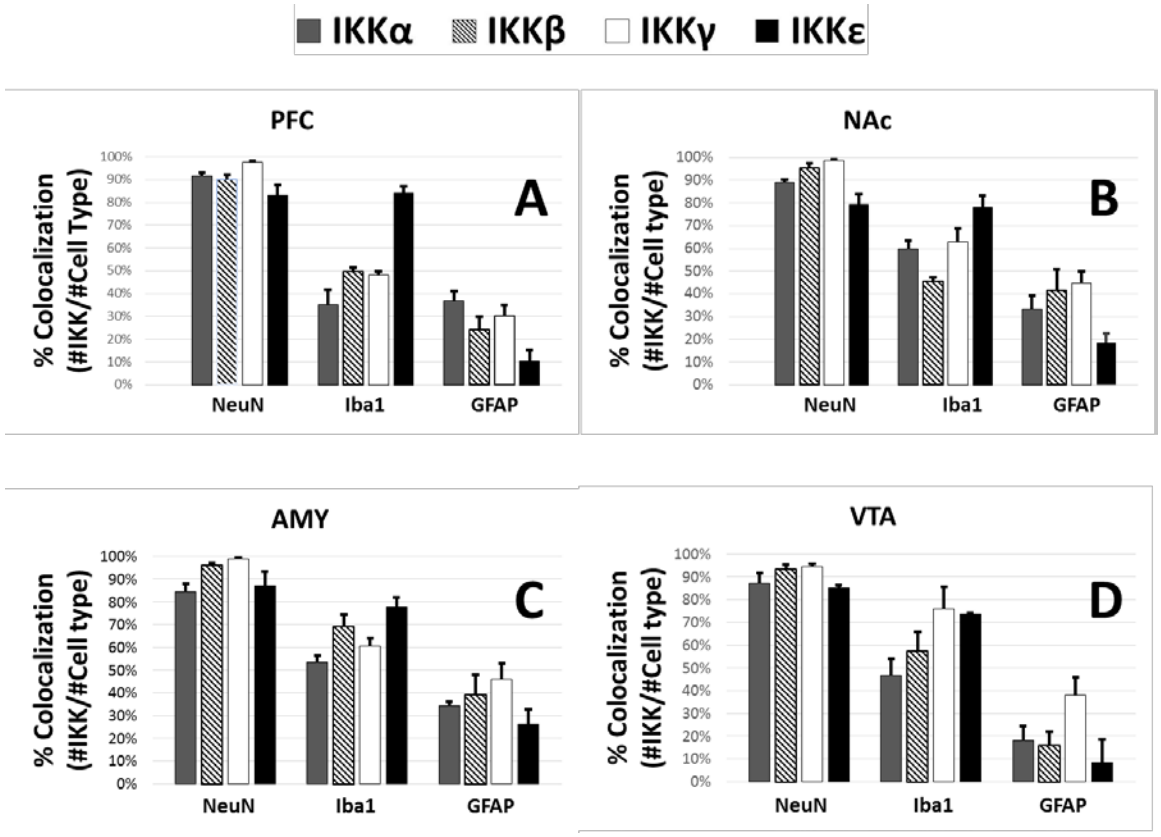

Figure 2.7. Cell-Specific Protein Expression of IKK Isoforms. Expression levels of the IKK isoforms (IKKα, IKKβ, IKKγ, and IKKε) were quantified in DAPI-positive cells by calculating the percentage of cells co-localized with the IKK antibodies and cell-specific markers out of the total cells expressing the cell-specific marker (neurons: NeuN; microglia: Iba1; astrocytes: GFAP) in the A: PFC, B: NAC, C: AMY, and D: VTA. (n=5/group for IKKα, IKKβ, IKKγ, IKKε, except n=3 for IKKε/NeuN). Mean ± SEM.

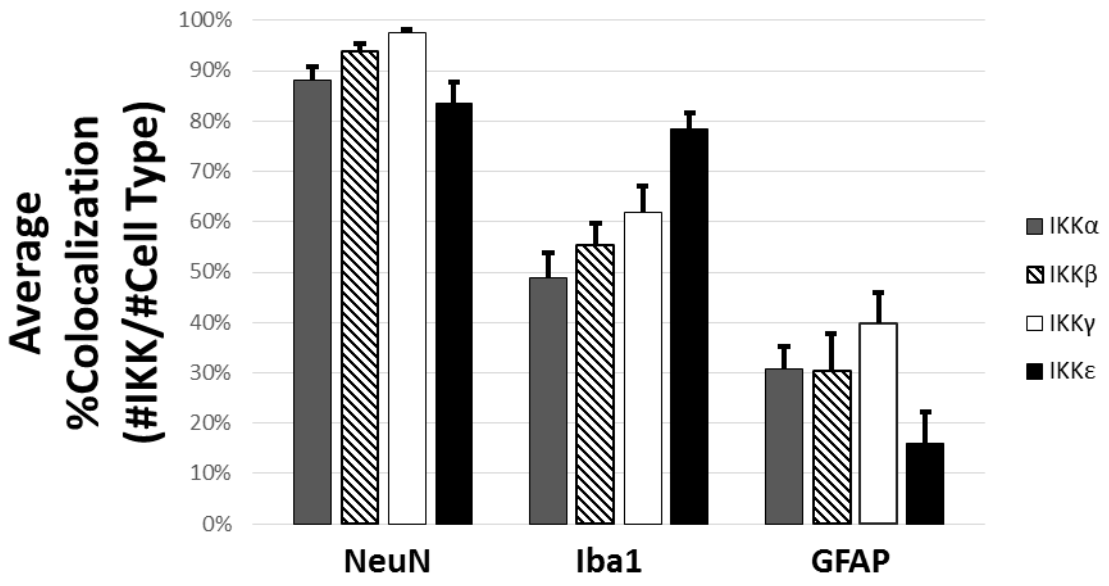

Figure 2.8. Average Cell-Specific Protein Expression of IKK Isoforms in the PFC, NAc, AMY, and VTA. Average expression levels across the PFC, NAc, AMY, and VTA of the IKK isoforms (IKKα, IKKβ, IKKγ, and IKKε) were quantified in DAPI-positive cells by calculating the percentage of cells co-localized with the IKK antibodies and cell-specific markers out of the total cells expressing the cell-specific marker (neurons: NeuN; microglia: Iba1; astrocytes: GFAP). (n=5/group for IKKα, IKKβ, IKKε, except n=3 for IKKε/NeuN). Mean ± SEM.

Cell Type Composition in the PFC, AMY, NAc, and VTA

The brain region and cell type-specificity for the IKK isoforms were explored both qualitatively and quantitatively. Understanding cell type composition for each of these brain regions would provide an additional quantitative metric of where IKK isoforms are predominately expressed. Percentages of the different cell types were measured by immunostaining sections from the PFC, NAc, AMY, and VTA with DAPI and antibodies against cell-specific markers for neurons (NeuN), microglia (Iba1), and astrocytes (GFAP). The total IKK expression was determined by calculating the percentage of DAPI-positive cells co-localized with the cell type-specific antibodies out of the total DAPI-positive cells (n=6/group per brain region/cell type combination). Neurons were the predominant cell type in all the brain regions studied, present in over 80% of the total cells in the PFC, NAc, and AMY. Although the VTA had a significantly lower amount of neurons (68%), they were still the most prevalent cell type in that region. The second most abundant cell type was microglia, which accounted for 9 to 15% of all cells, followed by astrocytes, which made up only 1 to 3% of the total cell population. Cells that did not co-localize with cell type-specific markers were classified as “Unknown” and ranged anywhere from 3% to upwards of 19% of all cells. This group was probably composed of glial cells that did not express IBA1 or GFAP, such as oligodendrocytes or populations of neurons, microglia, and astrocytes deficient in the cell type-specific markers used in the immunostaining process. Nevertheless, if the “Unknown” group is assumed to be predominately glial cells, then the glia to neuron ratio would be approximately 0.25 in the PFC, NAc, and AMY, and 0.5 in the VTA.

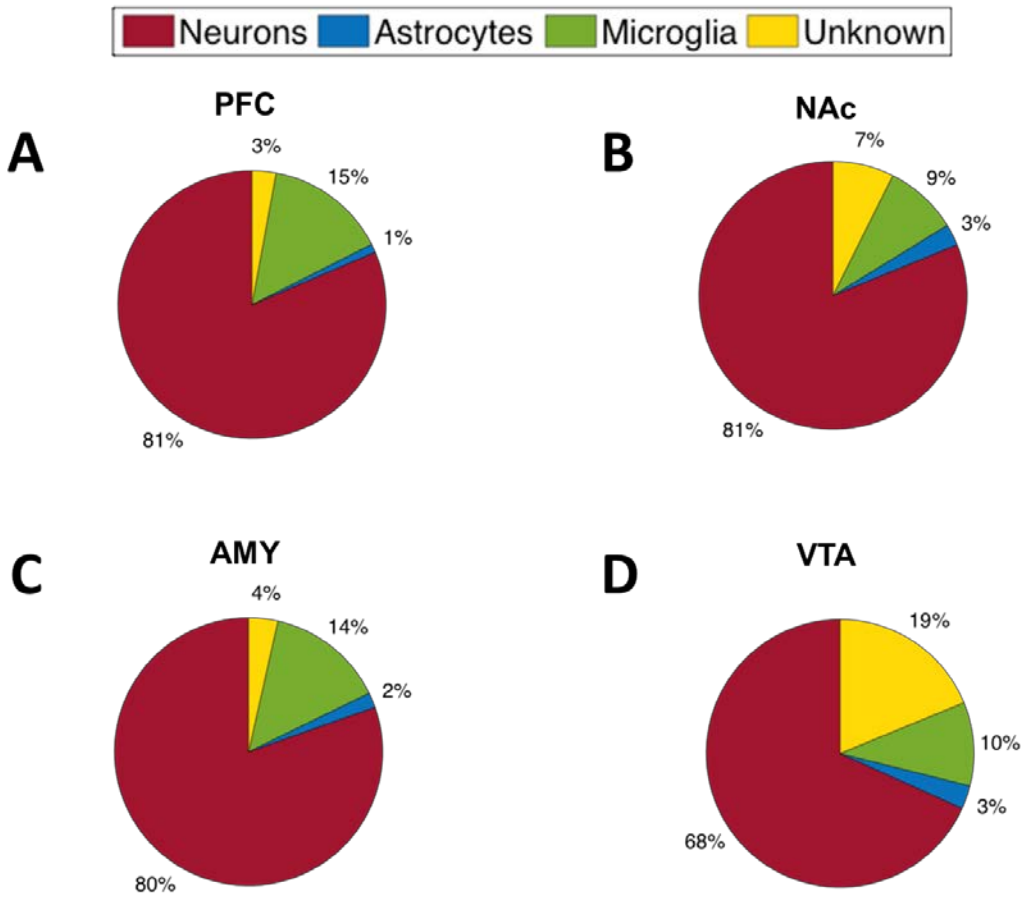

Figure 2.9. Cell-Type Composition per Brain Region. The percentages of NeuN+ neurons, Iba1+ microglia, and GFAP+ astrocytes in the A) PFC, B) NAc, C) AMY, and D) VTA represented relative to the total number of cells stained with the DAPI nuclear stain. The “Unknown” designation refers to the percentage of DAPI+ cells that did not co-localize with any of the cell type-specific stains (n=6/group per brain region/cell type combination).

DISCUSSION

The neurobiological changes associated with AUD may be mediated by increased pro-inflammatory neuroimmune signaling in the brain. It is thought that pro-inflammatory cytokines promote excessive alcohol consumption (Blednov *et al.* 2011; Crews and Vetreno 2015; Vetreno and Crews 2014), which subsequently induces a positive feedback loop that promotes further inflammatory responses. NF-κB represents a point of convergence for many inflammatory cascades and a potential target for regulating alcohol consumption. The IKK isoforms (IKKα, IKKβ, IKKγ, and IKKε) all mediate NF-κB activation in some capacity and with a certain degree of specificity (Hacker and Karin 2006). Because the expression of these isoforms in brain had not been previously determined, we studied their brain region and cell type-specificity in brain regions known to be important in addictive behaviors. Ultimately, this information was used to facilitate *in vivo* manipulations of IKK isoforms in specific brain regions to study their discrete effects on ethanol drinking behaviors.

IKKα, IKKβ, IKKγ, and IKKε were ubiquitously expressed in all the brain regions (PFC, NAc, AMY, and VTA) and cell types (neurons, microglia, and astrocytes) that were examined. This observation is likely due to the essential involvement of the IKK isoforms in many critical physiological pathways, such as immunity, inflammation, and cell-cycle regulation (Chau *et al.* 2008; Hacker and Karin 2006). One key observation was that the PFC, NAc, AMY, and VTA were composed primarily of neurons, and all IKK isoforms were primarily found in neurons. These results suggest that neurons play an integral role in IKK-mediated pathways. The neuroimmune system is generally understood to be regulated by microglia and astrocytes (Bailey *et al.* 2006; Tian *et al.* 2012; Tian *et al.* 2009), and neurons are thought to serve a more passive role of receiving input from the glial cells rather than actively regulating the neuroimmune system (Tian *et al.* 2012; Tian *et al.* 2009). Nevertheless, neurons have been shown to

produce numerous neuropeptides and neurotransmitters that are immunoregulatory (Tian *et al.* 2012; Tian *et al.* 2009). In our study, the glia to neuron ratios ranged from approximately 0.25 (PFC, NAc , AMY) to 0.5 in the VTA. However, it is generally accepted that glial cells out number neurons at least 10 to 1 (Allen and Barres 2009; Bear *et al.* 2007; Kandel *et al.* 2000), which would mean that the expected percentage of neurons should have been closer to 10% instead of the observed 68% to 80%. Other studies have demonstrated glia to neuron ratios of 0.5 or 1 (Dombrowski *et al.* 2001; Azevedo *et al.* 2009; Lidow and Song 2001). Although there is limited published data of the cell type composition in the areas examined in this study, one report found a glia to neuron ratio of 1 in the PFC of rhesus monkeys (Dombrowski *et al.* 2001).

Interestingly, all the IKK isoforms (IKKα, IKKβ, IKKγ) primarily associated with regulating the NF-κB canonical pathway had similar expression profiles (Oeckinghaus and Ghosh 2009). For example, IKKα, IKKβ, and IKKγ were highly expressed in the NAc, with lower expression in the PFC and AMY, followed by weak expression in the VTA. The low VTA expression was probably due the overall lower number of neurons in that region. Cell-type specificity was comparable between the isoforms, with each being found in almost all the neurons, about half of the microglia, and one third of astrocytes across brain regions. The expression of IKKγ was slightly greater in every brain region and cell type. This could be due to the fact that IKKγ acts as an important non-catalytic accessory protein in both the IKKβ- and IKKα-containing complexes of the NF-κB canonical and non-canonical pathways, respectively (Gamble *et al.* 2012; Perkins 2007). IKKγ also mediates an additional pathway that responds to genotoxic stress such as DNA double stranded breaks (Hacker and Karin 2006; Perkins 2007) and is thus a key cellular mediator. Moreover, while IKKα and IKKβ were found in both the nucleus and cytoplasm of neurons and astrocytes, IKKγ was found only in the nucleus. NF-κB

dimers are normally sequestered in the cytoplasm of unstimulated cells by non-covalent interactions with IκB (Gamble *et al.* 2012; Perkins 2007). This physical separation of IKKγ from the other isoforms offers a possible explanation for the abundant expression of IKKα, IKKβ, and IKKγ in the absence of a major pro-inflammatory response in naive mice. Perhaps IKKγ resides in the nucleus under normal conditions and translocates to the cytoplasm in response to pro-inflammatory stimuli and disinhibits the NF-κB dimers. Alternatively, IKKα, IKKβ, and IKKγ shared the same unique localization pattern in microglia, which appeared to be at beginning of the major processes. Microglia are known to play a critical role in neuroimmune signaling (Bailey *et al.* 2006), and the NF-κB canonical pathway may first be activated in microglia since it is the only cell type where IKKα, IKKβ, and IKKγ have a similar localization.

IKKε demonstrated a different expression profile when compared to the other IKK isoforms. IKKα, IKKβ, and IKKγ expression varied depending on the brain region, but IKKε was uniformly expressed throughout the PFC, AMY, NAc, and VTA in approximately two thirds of the total cells. Another distinction between IKKε and the other isoforms was in cell type distribution. For example, IKKε was expressed in roughly the same percentage of neurons and microglia, and relatively scarce in astrocytes (neurons = microglia >> astrocytes), while the other IKK isoforms were expressed in nearly all neurons and sequentially decreased in the other cell types (neurons > microglia > astrocytes). The markedly higher expression of IKKε in microglia compared to astrocytes is supported by evidence that demonstrates IKKε mediates signals primarily from TLR3 and TLR4 (Chau *et al.* 2008), and astrocytes only express these receptors in an activated state, while microglia express them in both resting and active states (Suzumura 2013). There is, however, no clear explanation of why IKKε is

expressed in significantly more microglia than the rest of the IKK isoforms, other than it known that IKKε is preferentially expressed in peripheral leukocytes (Shimada 1999).

In summary, we showed that all the IKK isoforms were primarily neuronal and ubiquitously expressed throughout areas of the brain that had a predominantly neuronal composition (PFC, NAc, AMY, and VTA). Thus, modulating IKK isoforms specifically in neurons in these areas would offer important insight into the neuronal role of IKKs. Ultimately, this information could be used for developing targeted strategies for manipulating IKKs within the brain in order to determine their effects on alcohol drinking behaviors. Knowledge of such IKK characterizations will possibly aid the development of new therapeutic treatments for AUD.

CHAPTER III: Inhibition of IKKβ Reduces Ethanol Consumption in C57BL/6J Mice

INTRODUCTION

The World Health Organization estimates that approximately 3.3 million deaths/year worldwide are related to the harmful use of alcohol (World Health Organization 2014) and the Centers for Disease Control and Prevention determined the economic costs related to excessive alcohol consumption to be greater than $223.5 billion/year in the US alone (Bouchery *et al.* 2011). These statistics, become even more concerning given the limited number of FDA-approved medications to treat alcohol use disorder (AUD) and their limited efficacy. (Jonas *et al.* 2014).

There is an increasing body of evidence linking pro-inflammatory neuroimmune signaling to alcohol intake (Crews 2012), suggesting that these pathways may be targets for medication development. A role of neuroimmune signaling in alcohol abuse is supported by genetic association studies in humans (Edenberg *et al.* 2007; Pastor *et al.* 2000; Pastor *et al.* 2005; Saiz *et al.* 2009), gene expression microarray studies in postmortem brains of alcoholics (Liu *et al.* 2005; Okvist *et al.* 2007), transcriptome meta-analysis in rodents (Mulligan *et al.* 2006), and drinking models in mice (Gorini *et al.* 2013a; Gorini *et al.* 2013b; Nunez *et al.* 2013; Osterndorff 2013). Mice with null mutations of immune-related genes showed reduced ethanol drinking (Ponomarev *et al.* 2012), while stimulation of the immune system using lipopolysaccharide (LPS) produced prolonged increases in ethanol intake (Blednov *et al.* 2011). Many of the immune-related genes implicated in the above mentioned studies mediate their affect through NF-κB.

NF-κB transcription family members are ubiquitously expressed throughout the body and play important roles in innate and adaptive immune responses, cell death, and

inflammation (Perkins 2007; Scheidereit 2006). However, it is the NF-κB canonical pathway that is most responsible for the expression of pro-inflammatory genes. The NF-κB dimer most commonly associated with this pathway is composed of the Rel proteins p65 and p50, and is normally sequestered in the cytosol of unstimulated cells by non-covalent interactions with IκB (Perkins 2007; Schmid and Birbach 2008; Okvist *et al.* 2007). NF-κB activation requires degradation of IκB. This is achieved when the inhibitory kappa-B kinase (IKK) complex (composed of IKKα, IKKβ, and two non-enzymatic IKKγ accessory molecules) phosphorylates two adjacent serine residues in IκB, which leads to ubiquitination and proteasomal degradation of the inhibitor. NF-κB is subsequently released where it translocates to the nucleus and acts as a transcription factor for numerous pro-inflammatory chemokines and cytokines such as TNFα and IL-6 (Gamble *et al.* 2012; Schmid and Birbach 2008). The IKK complex represents a point of convergence for many pro-inflammatory extracellular signals (Fig. 1.1) and plays a key role in inflammation and a number of diseases (Gamble *et al.* 2012; Schmid and Birbach 2008). IKKβ is the only member of the IKK complex that specifically mediates the NF-κB canonical pathway (Hayden and Ghosh 2004; Perkins 2007; Perkins and Gilmore 2006; Schmid and Birbach 2008).

IKKβ has a clearly established role as an intermediate in NF-κB-mediated cellular inflammation and is involved in many inflammatory disease conditions such as asthma, atherosclerosis, hepatitis, pancreatitis, neurodegeneration, inflammatory bowel disease, and arthritis (Grivennikov *et al.* 2010; Sunami *et al.* 2012). Specific modulation of IKKβ has been successfully shown to improve outcomes in many *in vivo* animal models of the above-mentioned diseases (Ethridge *et al.* 2002; Ziegelbauer *et al.* 2005; Jimi *et al.* 2004; Long *et al.* 2009), and IKKβ antagonists have even been through phase II clinical trials in humans for the treatment of osteoarthritis (Manit *et al.* 2009). Only a few studies

have examined the relationship between IKKβ and ethanol exposure, and these focused on the peripheral effects of chronic ethanol exposure, such as exacerbation of pancreatic and hepatic inflammation (Huang *et al.* 2014; Sunami *et al.* 2012). Furthermore, only a few studies examined the central actions of IKKβ, and these focused on its role neurodegeneration and metabolic disorders and none involved ethanol exposure (Maqbool *et al.* 2013; Zhang *et al.* 2008). To date, no studies have explored the peripheral or central role of IKKβ on ethanol drinking behavior or any other substance abuse disorders.

In this study, we examined the effect of IKKβ on voluntary alcohol drinking in mice peripheral administration of pharmacological inhibition and brain region-specific knockdown of IKKβ. Two different inhibitors were used (TPCA-1 and sulfasalazine), both of which act peripherally and do not cross the blood brain barrier (BBB) (Liu *et al.* 2012a). TPCA-1 is a selective small molecule inhibitor of IKKβ (Podolin *et al.* 2005). Sulfasalazine possess strong IKKβ inhibitory activity and is commonly used for treating patients with inflammatory bowel disease, ulcerative colitis, and Crohn's disease (Lappas *et al.* 2005). Centrally, we used a virally mediated Cre/Lox system to selectively knockdown IKKβ in the nucleus accumbens (NAc) and central amygdala (CeA). Based on our previous work (Blednov *et al.* 2011; Blednov *et al.* 2012), we hypothesized that inhibition of IKKβ would limit/decrease alcohol drinking.

MATERIALS AND METHODS

Animals

Pharmacological antagonist studies were conducted in adult male C57BL/6J mice taken from a colony maintained at The University of Texas at Austin (original breeders were purchased from Jackson Laboratories, Bar Harbor, ME). Genetic knockdown studies used adult male mice with a floxed *Ikkβ* gene on a C57BL/6J

background (i.e., C57BL/6J mice with *Ikkβ* flanked by LoxP sites or more commonly denoted as $Ikk\beta^{F/F}$). Original breeders were acquired from Casey W. Wright, College of Pharmacy, The University of Texas at Austin. The C57BL/6J strain was chosen because of its propensity for voluntary ethanol consumption (Belknap *et al*. 1997). Mice were group-housed 4 or 5 per cage on a 12-hour light/dark cycle (lights on at 7:00 a.m.) with ad libitum access to water and rodent chow (Prolab RMH 180 5LL2 chow, TestDiet, Richmond, IN). The temperature and humidity of the room were kept constant. Behavioral testing began when the mice were at least 2 months of age. Experiments were conducted in isolated behavioral testing rooms in the Animal Resources Center at The University of Texas at Austin. All experiments were approved by the university's Institute for Animal Care and Use Committee and conducted in accordance with NIH guidelines with regard to the use of animals in research.

Pharmacological Inhibitors of IKKβ

Sulfasalazine (Sigma-Aldrich, St. Louis, MO) was injected i.p., and TPCA-1 (Tocris Bioscience, Minneapolis, MN) was administered p.o. Both drugs were freshly prepared as suspensions in saline with 4-5 drops of Tween-80 and injected in a volume of 0.1ml/10 g of body weight for i.p. administration and 0.05 ml/10 g of body weight for oral administration. Drugs were administered 30 min prior to ethanol presentation times (see below). Doses of drugs and routes of administration were based on published data that showed anti-inflammatory activity *in vivo*.

Brain Region-Specific Lentiviral-Mediated Knockdown of IKKβ

$Ikk\beta^{F/F}$ mice were injected bilaterally into the NAc or CeA with either a vesicular stomatitis virus (VSV-G) pseudotyped lentivirus expressing Cre recombinase fused to enhanced green fluorescent protein (EGFP) under the control of a CMV promoter (LV-

Cre-EGFP) or an “empty” VSV-G pseudotyped lentiviral vector expressing only the EGFP transgene under a CMV promoter. Mice were anesthetized by isoflurane inhalation, placed in a model 1900 stereotaxic apparatus (David Kopf, Tujunga, CA), and administered preoperative analgesic (Rimadyl, 5 mg/kg). The skull was exposed, and bregma and lambda visualized with a dissecting microscope. A digitizer attached to the micromanipulator of the stereotaxic apparatus was used to locate coordinates relative to bregma. Burr holes were drilled bilaterally above the injection sites in the skull using a drill equipped with a #75 carbide bit (David Kopf, Tujunga, CA). The injection sites targeted either the NAc using the following coordinates relative to bregma: anteroposterior (AP) +1.49 mm, mediolateral (ML) ±0.9 mm, dorsoventral (DV) -4.8 mm or the CeA using the following coordinates: AP -1.14 mm, ML ±2.84 mm, DV -4.8 mm. Injections were performed using a Hamilton 10-µL microsyringe (model #1701) and a 30-gauge needle. The syringe was lowered to the DV coordinate and retracted 0.2 mm. Viral solution (1.0 µL with titer of 1.8×10^8 vp/mL in PBS) was injected into each site at a rate of 200 nL/min. After each injection, the syringe was left in place for 5 min before being retracted over a period of 3 minutes. Incisions were closed with tissue adhesive (Vetbond, 3 M; St. Paul, MN). Mice were individually housed after surgery and given a 4-week recovery before starting the ethanol drinking tests.

Behavioral Testing

Three different ethanol drinking models were used in this study: 1) continuous 24-hr 2BC with access to water or ethanol using a constant high ethanol concentration, 2) two-bottle choice with limited 3-hr access to ethanol (2BC-DID), and 3) 2BC using ascending concentrations of ethanol solutions.

Pharmacological inhibitors of IKKβ. The effects IKKβ antagonists on ethanol intake were measured in adult male C57BL/6J mice in two different drinking paradigms:

2BC with 15% ethanol and 2BC-DID per protocols previously described (Blednov 2003; Blednov *et al.* 2014). For both tests, mice were pre-trained to consume 15% ethanol for at least 3 weeks to provide stable consumption. Ethanol intake was measured after saline injection (i.p. or p.o.) for 2 days and mice were grouped to provide similar levels of ethanol intake and preference. In the 2BC test, measurements of ethanol intake were made 6 and 24 hr after beginning the drinking test, which began immediately after lights off. In the 2BC-DID test, drinking began 3 hr after lights off and lasted for 3 hr. Ethanol intake was measured once at the end of the 3-hr drinking period. Position of administration tubes was changed daily to control for side preferences. Mice were weighed every 4 days. For both experiments, ethanol consumption (g/kg/time), preference (ratio of alcohol consumption to total fluid consumption), and total fluid intake were measured at the appropriate time points.

Brain region-specific lentiviral-mediated knockdown of IKKβ. The effects IKKβ knockdown in NAc and CeA were measured in adult male *Ikkβ*$^{F/F}$ mice using the 2BC test. This 2BC test consisted of giving mice treated with either LV-Cre-EGFP or LV-EGFP-Empty 24-hr continuous access to water and ascending concentrations of ethanol solutions (3%, 6%, 8%, 10%, 12%, 14%, 16% v/v) at 2-day intervals (Blednov *et al.* 2014). The position of administration tubes was changed daily to control for position preferences. Mice were weighed every 4 days. Ethanol consumption (g/kg/day), preference, and total fluid intake were measured.

Preference for non-ethanol tastants in the two-bottle choice test. Upon completion of the 2BC test described above, the *Ikkβ*$^{F/F}$ mice were also tested for saccharin to evaluate sweet taste preferences. The mice were offered saccharin in increasing concentration (0.008%, 0.016%, and 0.033%) and 24-hr ethanol intake was calculated. Each concentration was offered for 2 days with bottle positions changed

daily. The low concentration was always presented first, followed by the higher concentrations.

RNA Isolation

Upon completion of behavioral experiments, mice were sacrificed by cervical dislocation and decapitated. The brains were quickly removed, flash frozen in liquid nitrogen, and later embedded in Optimal Cutting Temperature (OCT) media in isopentane on dry ice. Brains were then stored at −80° C for future processing. Brains were transferred to a cryostat set at −6° C for at least 1 hr before sectioning. Sections (300 µm) were collected from +1.80 to +0.60 mm, and -0.60 to -1.80 mm (AP) relative to bregma for NAc and CeA, respectively, and transferred to pre-cooled glass slides on dry ice. Micropunch sampling was performed on a frozen stage (−25° C) using Dual Fluorescent Protein Flashlight (Nightsea, Bedford, MA), and a mouse stereotaxic atlas to identify the EGFP expression and anatomical location of the injection site. Microdissection punches (Stoelting Co., Wood Dale, IL) with an inner diameter of 0.75 mm and 0.50 mm were used to obtain samples of NAc and CeA, respectively. This inner diameter fit within the viral spread around the injection site and minimized contamination from other tissue. Punches were taken bilaterally from 4-300 µm sections and stored at −80° C until RNA extraction. Micropunches were washed with 100% ETOH and RNasZap (Life Technologies) between each animal. All equipment used to obtain tissue was treated with RNAseZap (Life Technologies) to prevent RNA degradation. Total RNA was extracted using the MagMAX™-96 for Microarrays Total RNA Isolation Kit (Life Technologies, Carlsbad, CA) according to the manufacturer's instructions. RNA yields and purity were assessed using a NanoDrop 8000 (Thermo Fisher Scientific, Waltham, MA) with both the 260/230 and 260/280 ratios >2.00. RNA

quality was determined using the Agilent 2200 TapeStation (Agilent, Santa Clara, CA) with RNA integrity numbers (RIN) averaging above 8.0.

Quantitative PCR

To verify *Ikkβ* mRNA knockdown, single-stranded cDNA was synthesized from total RNA using the TaqMan® High Capacity RNA-to-cNA kit (Life Technologies). Following reverse transcription, quantitative real-time PCR (qPCR) was performed in triplicate using TaqMan® Gene Expression Assays together with the TaqMan® Gene Expression Master Mix (Life Technologies), per manufacturer's instructions. TaqMan® Gene Expression assays used were *Ikbkb* (ID: Mm01222247_m1), *Tnf-α* (ID: Mm00443258_m1), *Il-6* (ID: Mm00446190_m1), and Enhanced GFP (ID: Mr04097229_mr). *Gapdh* (Mm99999915_g1) (glyceraldehyde-3-phosphate dehydrogenase) gene was used as a reference gene, and relative mRNA levels were determined using the $2^{-\Delta\Delta CT}$ method (Schmittgen and Livak 2008). *Gapdh* was used as the endogenous control because it's low variability between samples. Reactions were carried out in a CFX384™ Real-Time PCR Detection System (Bio-Rad) and data collected using Bio-Rad CFX Manger. All genes were normalized to the endogenous housekeeping gene, *Gapdh*, and expressed relative to their respective LV-EGFP-Empty control treatment.

Immunohistochemistry

Tissue harvesting. Animals were sacrificed, transcardially perfused with Phosphate Buffer Saline (PBS) and 4% paraformaldehyde (PFA), harvested, postfixed for 24 hr in 4% PFA at 4°C, and cyroprotected for 24 hr in 20% sucrose in PBS at 4°C. Brains were placed in molds containing OCT compound (VWR, Radnor, PA) and frozen in isopentane on dry ice. The brains were equilibrated in a -12 to -14°C cryostat

(Thermo Fischer Scientific) for at least 1 hr and coronal sections of 30µm were taken of the NAc and CeA and placed in sterile PBS.

Immunostaining. Sections were penetrated with 0.1% Triton-X 100 (2 x 10 min at 25°C), washed in PBS (3 x 5 min at 25°C), blocked with 10% serum of either goat or donkey (30 min at 25°C), and treated with 1:250 anti-IKKβ (Millipore, Billerica, MA), 1:500 anti-NeuN (Santa Cruz, Santa Cruz, CA), 1:300 anti-GFAP (Santa Cruz), 1:1000 anti-Iba1 (Dako, Dako, Denmark), 1:1000 anti-GFP (Santa Cruz) antibodies (4°C overnight), washed in PBS (3 x 10 min at 25°C), and then subjected to reaction with fluorescence-conjugated secondary antibodies of 1:1000 Alexa 488 and 1:1000 Alexa 568 (Invitrogen, Waltham, MA) (2 hr at 25°C), and rinsed with PBS (3 x 10 min at 25°C). The sections were mounted on slides using sterile 0.2% gelatin and DAPI mounting media (Vector Laboratories, Burlingame, CA) and cover slipped. Images were taken using either a Zeiss Axiovert 200M Fluorescent Microscope (Zeiss, Oberkocheen, Germany) equipped with a 20x objective or a Zeiss LSM 710 Confocal Microscope (Zeiss) equipped with a 63x objective. For the immunohistochemistry, two sets of control experiments were performed to test specificity: 1) replacement of the primary antibody with only the serum of the appropriate species and 2) omission of secondary antibodies. No immunostaining was detected under either of these conditions.

Target verification. Serial sections (30 µm) of NAc (AP +2.00 to 0.00 mm) and CeA (AP 0.00 to -2.00 mm) were mounted on slides with DAPI mounting media (Vector Laboratories) and visualized using a Zeiss Axiovert 200M Fluorescent Microscope (Zeiss) equipped with a 10x objective to assess the location of the injection site. The quality of injection was quantitatively scored based of the strength of EGFP viral expression, injection location relative to target, and the spread of the virus. The injection was considered on target if the needle placement was within 0.3 mm of the desired

stereotaxic coordinates and the virus EGFP expression covered at least 1/3 of the brain region of interest (i.e., NAc, CeA) on at least one side of the brain. If the animals failed the target verification analysis, they were included in the statistical analysis of the data.

Image analysis. Brain sections were prepared as described in the Immunohistochemistry methods. Epi-fluorescent images were acquired using a Zeiss Axiovert 200M Fluorescent Microscope (Zeiss) equipped with a 20x objective and an automated stage. Images of the brain region of interest were captured (multiple 20X images in red, green, and blue channels) then stitched together creating a composite view for further analysis. Images were taken without saturating the signal and digitized at 8-bits using the full intensity range of 0–256 and imported into the ImageJ software package (http://imagej.nih.gov/ij/). Composite images were split into the individual channels, overlaid with a grid. A Zeiss LSM 710 Confocal Microscope (Zeiss) equipped with a 63x objective was used to take representative images for IKKβ cell-type specificity viral-trophism.

Statistical Analysis

Numerical data were given as mean ± SEM, and n represents the number of animals tested. Data were analyzed using either analysis of variance (ANOVA) with repeated measures followed by Bonferroni post hoc tests or Student's t-test as appropriate (GraphPad Software, Inc., La Jolla, CA). Calculated p-values of less than 0.05 were considered statistically significant.

RESULTS

Pharmacological Inhibitors of IKKβ in a Continuous 24h Two-Bottle Choice (2BC) Test

We first investigated how global IKKβ inhibition affected voluntary ethanol drinking behavior. A pharmacological approach was selected because it has previously been shown that IKKβ-deficient mice demonstrate embryonic lethality due to liver degeneration and apoptosis (Tanaka *et al.* 1999). A low and high dose of either TPCA-1 or sulfasalazine paired was administered to adult male C57BL/6J mice on a daily basis. Voluntary ethanol drinking was evaluated using a continuous 24-hr 2BC bottle-drinking test in which the mice could drink either water or 15% ethanol. The lower dose of TPCA-1 (30 mg/kg) showed no significant differences, but the higher dose (50 mg/kg) reduced ethanol intake [$F(1,18) = 6.9$, $p<0.05$] and preference [$F(1,18) = 8.3$, $p<0.01$] 6 hrs after administration (Fig. 3.1 A and B). Both doses of sulfasalazine reduced ethanol intake [50 mg/kg: $p<0.05$; 100 mg/kg: $F(1,10) = 24.1$, $p<0.001$] and preference [50 mg/kg: $p<0.05$; 100 mg/kg: $F(1,10) = 12.4$, $p<0.01$] (Fig.3.1 D and E). No changes in total fluid intake after administration of either drug were observed (Fig. 3.1 C and F). There were also no differences in ethanol intake or preference between drug- and saline-treated groups of mice 18 hrs post treatment for either drug (data not shown; see Table 3.1 for complete statistical analyses).

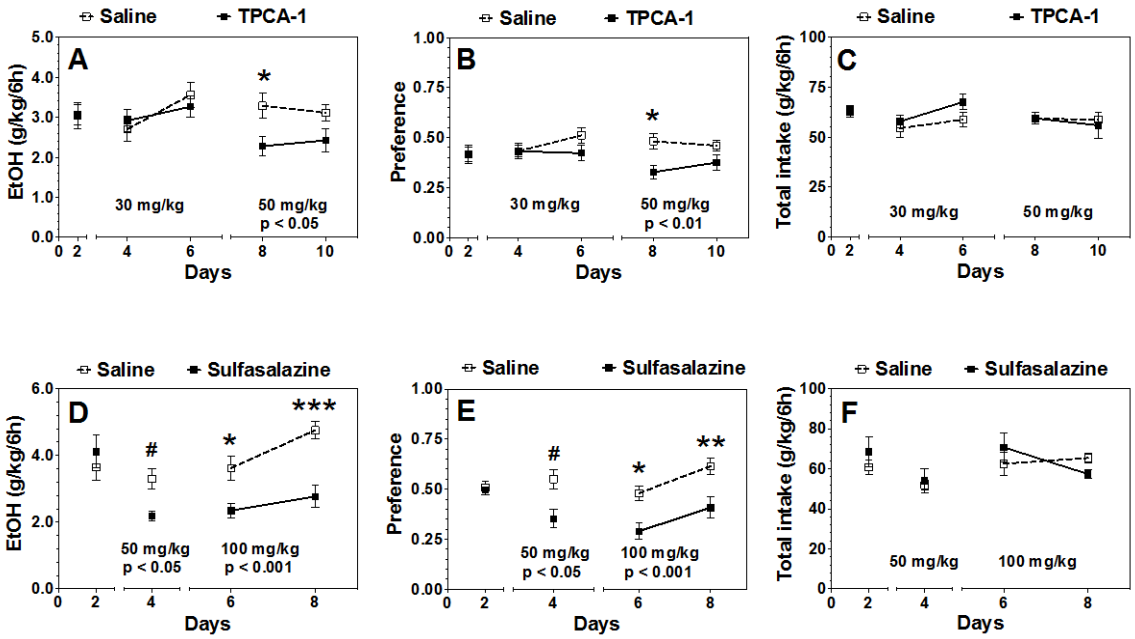

Figure 3.1. Effect of IKKβ Inhibitors on Ethanol Intake after the First 6h of a Continuous 24h 2BC Test in C57BL/6J Mice. A-C: TPCA-1-treated (n=13 per group). D-F: Sulfasalazine-treated (n=6 per group). A and D. 15% ethanol consumption (g/kg/6h). B and E: Preference for ethanol. C and F: Total fluid intake (g/kg/6h). Day 2 in each panel shows the averages of 2 days of saline injections for each group ± SEM. Additional time points are the averages of 2 days of drinking ± SEM. Significant main effect of treatment is shown by the p-value beneath the treatment dose (two-way ANOVA with repeated measures). Statistical significance of drug compared with the corresponding saline group is indicated by symbols above each time point (Bonferroni post-hoc test for multiple comparisons *p<0.05, **p<0.01, ***p<0.001, or a Student's t-test $^{\#}$p<0.05).

Drug	Dose	Factors	15% Ethanol		
			Amount of ethanol consumed (g/kg/6h)	Preference	Total fluid intake (g/kg/6h)
TPCA-1	30 mg/kg	treatment	F(1,21) = 0.01 p>0.05	F(1,21) = 1.1 p>0.05	F(1,21) = 3,5 p>0.05
		time	**F(1,21) = 10.1 p<0.01**	F(1,21) = 1.6 p>0.05	F(1,21) = 2.5 p>0.05
		interaction	F(1,21) = 1.8 p>0.05	F(1,21) = 2.7 p>0.05	F(1,21) = 0.4 p>0.05
	50 mg/kg	treatment	**F(1,18) = 6.9 p<0.05**	**F(1,18) = 8.3 p<0.01**	F(1,18) = 0,1 p>0.05
		time	F(1,18) = 0.1 p>0.05	F(1,18) = 0.2 p>0.05	F(1,18) = 0.8 p>0.05
		interaction	F(1,18) = 0.5 p>0.05	F(1,18) = 1.2 p>0.05	F(1,168) = 0.4 p>0.05
Sulfasalazine	50 mg/kg	Student's t-test	**p<0.05**	**p<0.05**	p>0.05
	100 mg/kg	treatment	**F(1,10) = 24.1 p<0.001**	**F(1,10) = 12.4 p<0.01**	F(1,10) = 0.1 p>0.05
		time	**F(1,10) = 9.1 p<0.05**	**F(1,10) = 25.5 p<0.001**	F(1,10) = 1.0 p>0.05
		interaction	F(1,10) = 1.9 p>0.05	F(1,10) = 0.1 p>0.05	F(1,10) = 2.5 p>0.05

Table 3.1. Statistical Analyses of the Effects of TPCA-1 and Sulfasalazine on Ethanol Intake in the 2BC Test (two-way ANOVA with repeated measures or Student's t-test). Statistically significant results are shown in bold font.

Pharmacological Inhibitors of IKKβ in a Limited Access Two-Bottle Choice Drinking Test

We administered TPCA-1 (50 mg/kg) or sulfasalazine (100 mg/kg) daily to a different cohort of adult male C57BL/6J mice and performed a two-bottle choice with limited access to 15% ethanol, also known as the Drinking in the Dark (2BC-DID) test. Compared to the previous continuous 2BC drinking test, the 2BC-DID drinking paradigm more closely replicates binge drinking because mice typically consume higher levels of ethanol and exhibit behavioral evidence of intoxication (Thiele and Navarro 2014). In this model, TPCA-1 reduced ethanol consumption ($F(1,10) = 14.0$, $p<0.01$) and preference ($F(1,10) = 21.6$, $p<0.01$) without affecting total fluid intake (Fig. 3.2 A-C). Sulfasalazine, however, did not significantly alter ethanol or total fluid intake, but did reduce ethanol preference ($F(1,14) = 31.7$, $p<0.001$) (Fig. 3.2 D-F). There was a significant interaction between treatment and time of ethanol consumption with a gradual time-dependent decrease in the effect of sulfasalazine (Fig. 3.2 D; see Table 3.2 for complete statistical analyses).

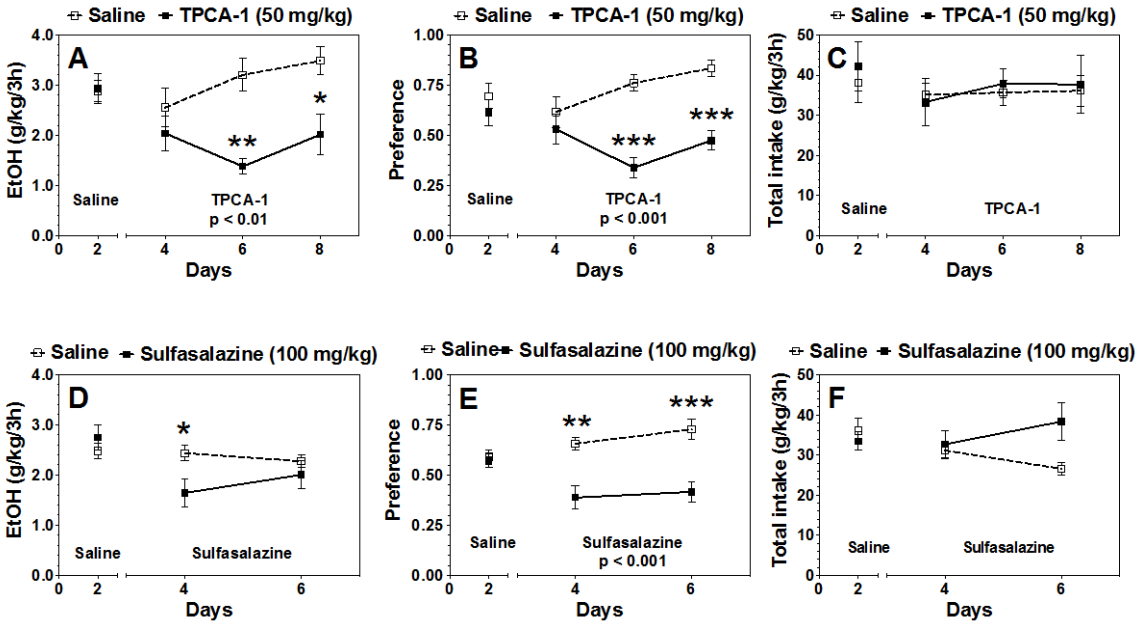

Figure 3.2. Effect of IKKβ Inhibitors on Ethanol Intake after the First 3h in a Limited Access 2BC-DID Test in C57BL/6J Mice. A-C: 50 mg/kg TPCA-1-treated (n=6 per group). D-F: 100 mg/kg sulfasalazine-treated (n=8 per group). A and D: 15% ethanol consumption (g/kg/3h). B and E: Preference for ethanol. C and F: Total fluid intake (g/kg/3h). Day 2 in each panel shows the averages of 2 days of saline injections for each group ± SEM. Additional time points are the averages of 2 days of drinking ± SEM. Significant main effect of treatment is shown by the p-value beneath the treatment dose (two-way ANOVA with repeated measures). Statistical significance of drug compared with corresponding saline group is indicated by symbols above each time point. (Bonferroni post-hoc test for multiple comparisons *p<0.05, **p<0.01, ***p<0.001).

Drug	Dose	Factors	15% Ethanol		
			Amount of ethanol consumed (g/kg/3h)	Preference	Total fluid intake (g/kg/3h)
TPCA-1	50 mg/kg	treatment	**F(1,10) = 14.0 p<0.01**	**F(1,10) = 21.6 p<0.001**	F(1,10) = 0,1 p>0.05
		time	F(2,20) = 1.9 p>0.05	F(2,20) = 2.8 p>0.05	F(2,20) = 0.4 p>0.05
		interaction	F(2,20) = 3.0 p>0.05	**F(2,20) = 7.5 p<0.01**	F(2,20) = 0.2 p>0.05
Sulfasalazine	100 mg/kg	treatment	F(1,14) = 3.2 p>0.05	**F(1,14) = 31.7 p<0.001**	F(1,14) = 3.2 p>0.05
		time	F(1,14) = 0.9 p>0.05	F(1,14) = 1.1 p>0.05	F(1,14) = 0.1 p>0.05
		interaction	**F(1,14) = 5.8 p<0.05**	F(1,14) = 0.2 p>0.05	F(1,14) = 3.8 p>0.05

Table 3.2. Statistical Analyses of the Effects of TPCA-1 and Sulfasalazine on Ethanol Intake in the 2BC-DID Test (two-way ANOVA with repeated measures). Statistically significant results are shown in bold font.

Brain Region-Specific Knockdown of IKKβ in the NAc and CeA in a Continuous 24h 2BC Test

We next examined the role IKKβ in areas of the brain implicated in the pathogenesis of AUD. The NAc was chosen because it is part of the mesolimbic dopamine reward system which positively reinforces addictive behavior (Koob 2014; Koob and Volkow 2010). The CeA was selected because it is in involved in activating brain stress systems through the release of corticotropin-releasing factor (CRF) and negatively reinforces addictive behaviors (Koob 2014; Koob and Le Moal 2008; Koob and Volkow 2010). To accomplish the brain region-specific knockdown, mice genetically engineered with a conditional *Ikkβ* deletion (*Ikkβ*$^{F/F}$) were injected bilaterally in the brain region of interest with a lentivirus expressing either *Cre* fused to EGFP (LV-EGFP-Cre) or only EGFP (LV-EGFP-Empty). The transgenes of both viral vectors were under the control of a cytomegalovirus (CMV) promoter and were pseudotyped with vesicular stomatitis virus glycoprotein (VSV-G). Expression of *Cre* results in the excision of *Ikkβ*. This method of local IKKβ deletion was validated by injecting LV-EGFP-Cre (n=8) and LV-EGFP-Empty (n=8) in the NAc of adult male *Ikkβ*$^{F/F}$ mice followed by a 3- or 8- week incubation period. The time points were selected based on a similar protocol used in mouse neurons that showed maximal change in expression 2 to 4 weeks post injection (Ahmed *et al.* 2004). We selected 3- and 8- post injection time points to assess the level of IKKβ knockdown near the beginning (4 weeks post injection) and end (8 weeks post injection) of the drinking studies. At the appropriate time points, brains were perfused, harvested, sectioned, and immunostained with anti-IKKβ and anti-EGFP. The number of cells with the viral EGFP that colocalized with IKKβ were measured and compared between the LV-EGFP-Cre and LV-EGFP-Empty treatments at each time point. The relative expression of IKKβ in Cre-treated animals vs. controls was 0.596 ± 0.012 ($p <$

0.01) at 3 weeks and 0.099 ± 0.023 ($p < 0.001$) at 8 weeks (Fig. 3.3). This equates to a 40% and a 90% decrease in IKKβ after 3 and 8 weeks, respectively.

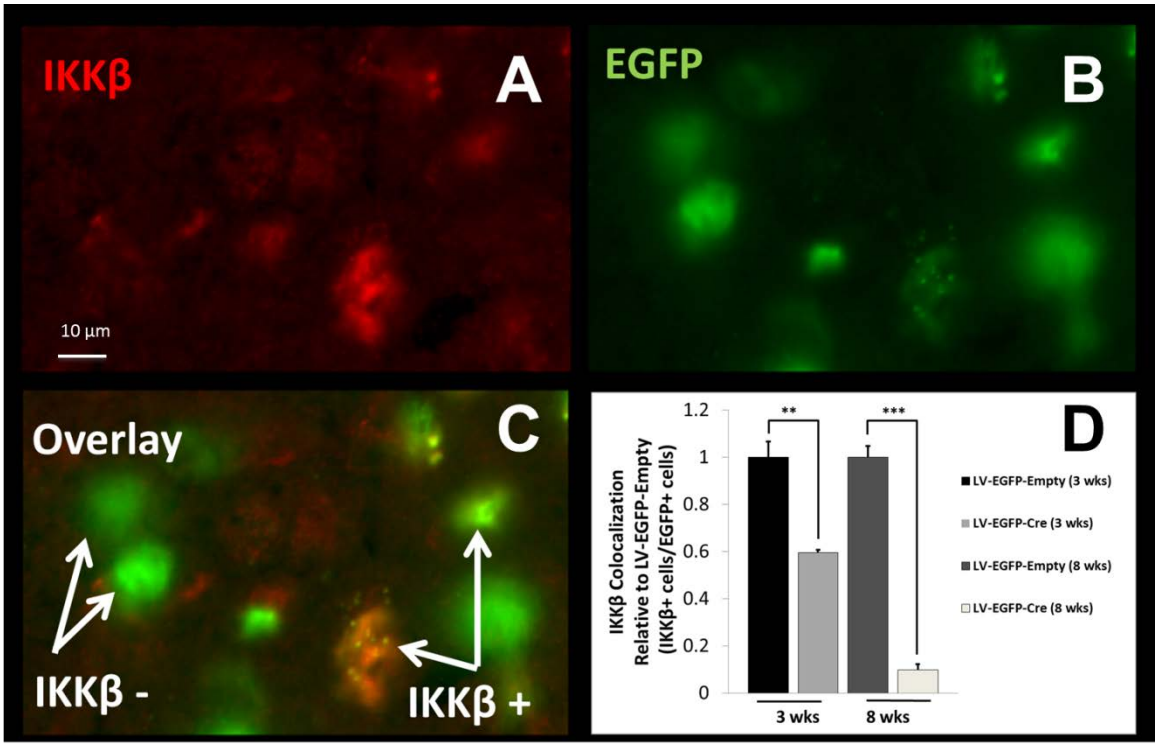

Figure 3.3. IKKβ Protein Knockdown (3 and 8 Weeks Post Injection) in NAc of *Ikkβ*$^{F/F}$ Mice. A fluorescent light microscope image is shown of a representative stain from the 3 week post-injection time point in NAc. A: anti-IKKβ fluorescently-labeled antibody. B: anti-EGFP fluorescently-labeled antibody. C: Overlay of A and B ("IKKβ –" represents transduced cells with no IKKβ and "IKKβ +" represents transduced cells with IKKβ) D: Knockdown of IKKβ (LV-EGFP-Cre) measured by IKKβ -positive cells colocalized with EGFP-positive cells relative to their time matched control (LV-EGFP-Empty). Each point is the average of eight fields of view (20x) per mouse for 4 mice (mean ± SEM) (n=4 for each group: 3wk LV-EGFP-Cre, 3wk LV-EGFP-Empty, 8wk LV-EGFP-Cre, 8 wk LV-EGFP-Empty). (Student's t-test **p<0.01, ***p<0.001).

Subsequently, *Ikkβ*$^{F/F}$ mice were injected bilaterally with LV-EGFP-Cre or LV-EGFP-Empty into either the NAc or CeA. After 4 weeks, the 2BC drinking test was administered in which the mice could drink either water or a series of increasing ethanol concentrations ranging from 0 to 16%. Similar to the results after global inhibition of IKKβ, local deletion of IKKβ in NAc also reduced ethanol consumption [$F(1, 50) = 10.0$, $p<0.005$] and preference [$F(1, 50) = 8.3$, $p<0.01$] without affecting total fluid intake (Fig. 3.4 A-C). Likewise, local deletion of IKKβ in the CeA reduced ethanol consumption [$F(1,196) = 19.1$, $p <0.0001$] and preference [$F(1,196) = 23.9$, $p <0.0001$] with no change in total fluid intake (Fig. 3.5 A-C). At the higher ethanol concentrations, consumption and preference were reduced by greater than 40% and 25% for each brain region (see Table 3.3 for complete statistical analyses).

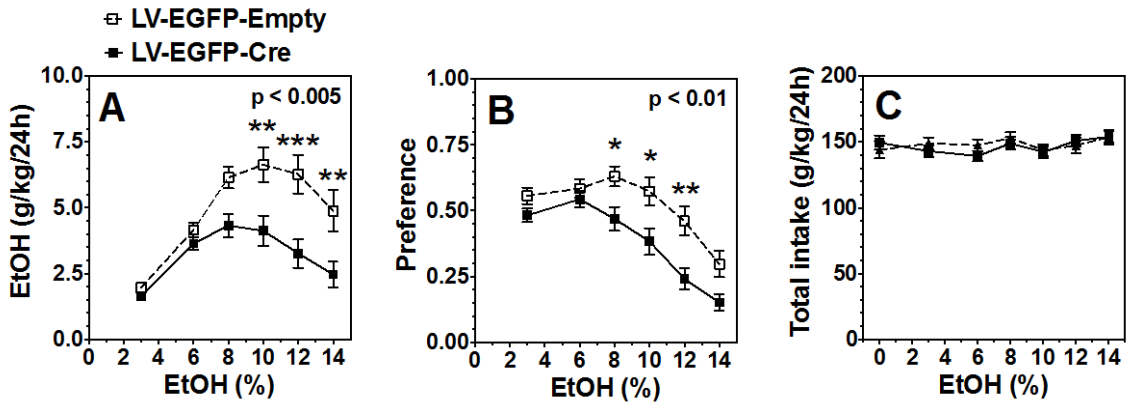

Figure 3.4. Effect of IKKβ Knockdown in NAc on Ethanol Intake During the 24h 2BC Test in *Ikkβ*$^{F/F}$ Mice. A-C: n = 32 animals injected with LV-Cre-EGFP and n = 20 injected with LV-Cre-Empty. A: Ethanol consumption (g/kg/24h). B: Preference for ethanol. C: Total fluid intake (g/kg/24). Each point is the average of 2 days of drinking ± SEM. Significant main effect of treatment is shown by the p-value in upper left hand corner (two-way ANOVA with repeated measures). Statistical significance of LV-EGFP-Cre treatment compared with corresponding LV-EGFP-Empty treatment is indicated by symbols above each time point (Bonferroni post-hoc test for multiple comparisons *p<0.05, **p<0.01, ***p<0.001).

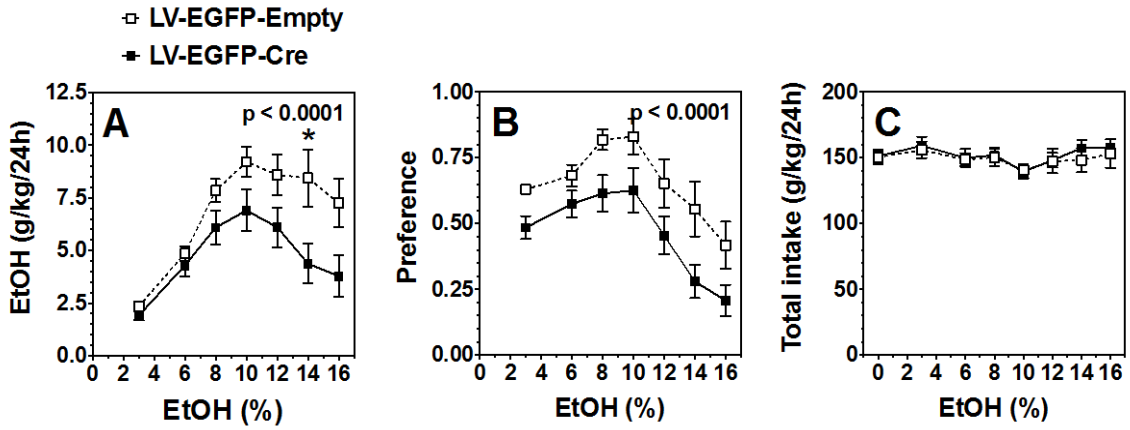

Figure 3.5. Effect of IKKβ Knockdown in CeA on Ethanol Intake during a Continuous 24 h 2BC Test in *Ikkβ*$^{F/F}$ Mice. A-C: n = 20 injected with LV-EGFP-Cre and n = 10 injected with LV-EGFP-Empty. A: Ethanol consumption (g/kg/24h). B: Preference for ethanol. C: Total fluid intake (g/kg/24h). Significant main effect of treatment is shown by the p-value in upper left hand corner (two-way ANOVA with repeated measures). Statistical significance of LV-EGFP-Cre treatment compared with corresponding LV-EGFP-Empty treatment is indicated by symbols above each time point (Bonferroni post-hoc test for multiple comparisons *p<0.05, **p<0.01, ***p<0.001).

Brain region	Factors	Ethanol concentrations		
		Amount of ethanol consumed (g/kg/24h)	Preference	Total fluid intake (g/kg/24h)
NAc	treatment	**F(1,50) = 10.0 p<0.005**	**F(1,50) = 8.3 p<0.01**	F(1,50) = 0.05 p>0.05
	concentration	**F(5,250) = 32.8 p<0.0001**	**F(5,250) = 45.3 p<0.0001**	**F(6,300) = 5.0 p<0.0001**
	interaction	**F(5,250) = 5.8 p<0.0001**	**F(5,250) = 3.0 p<0.05**	F(6,300) = 2.0 p>0.05
CeA	treatment	**F(1,196) = 19.1 p<0.0001**	**F(1,196) = 23.9 p<0.0001**	F(1,224) = 0.5 p>0.05
	concentration	**F(6,196) = 9.5 p<0.0001**	**F(6,196) = 8.6 p<0.0001**	F(7,224) = 1.2 p>0.05
	interaction	F(6,196) = 1.1 P>0.05	F(6,196) = 0.3 p>0.05	F(7,224) = 1.0 p>0.05

Table 3.3. Statistical Analyses of the Effects of IKKβ Knockdown in the NAc or CeA on Ethanol Intake in the 2BC Test (two-way ANOVA with repeated measures). Statistically significant results are shown in bold font.

Ethanol drinking behavior in the 2BC drinking tests depend partly on taste (Bachmanov *et al.* 2003). We investigated the effect of the lentiviral-mediated genetic knockdown of IKKβ in the NAc and CeA on preference for sweet/noncaloric (saccharin) solutions. After the ethanol drinking experiments, we administered a 2BC test using three different concentrations of saccharin versus water. Analysis of preference for saccharin indicated a significant main effect of concentration in both the NAc [$F(2,56) = 69.97$, $p < 0.0001$] and CeA [$F2,56 = 53.43$, $p < 0.0001$], but no effect of treatment (LV-EGFP-Cre, LV-EGFP-Empty) or treatment × concentration interaction (Fig. 3.6A and 3.6C, respectively). Analysis of total fluid intake revealed no significant differences between the LV-EGFP-Cre and LV-EGFP treatment groups (Fig. 3.6B and 3.6D, respectively). Knockdown of IKKβ in either the NAc or CeA did not change preference for saccharin.

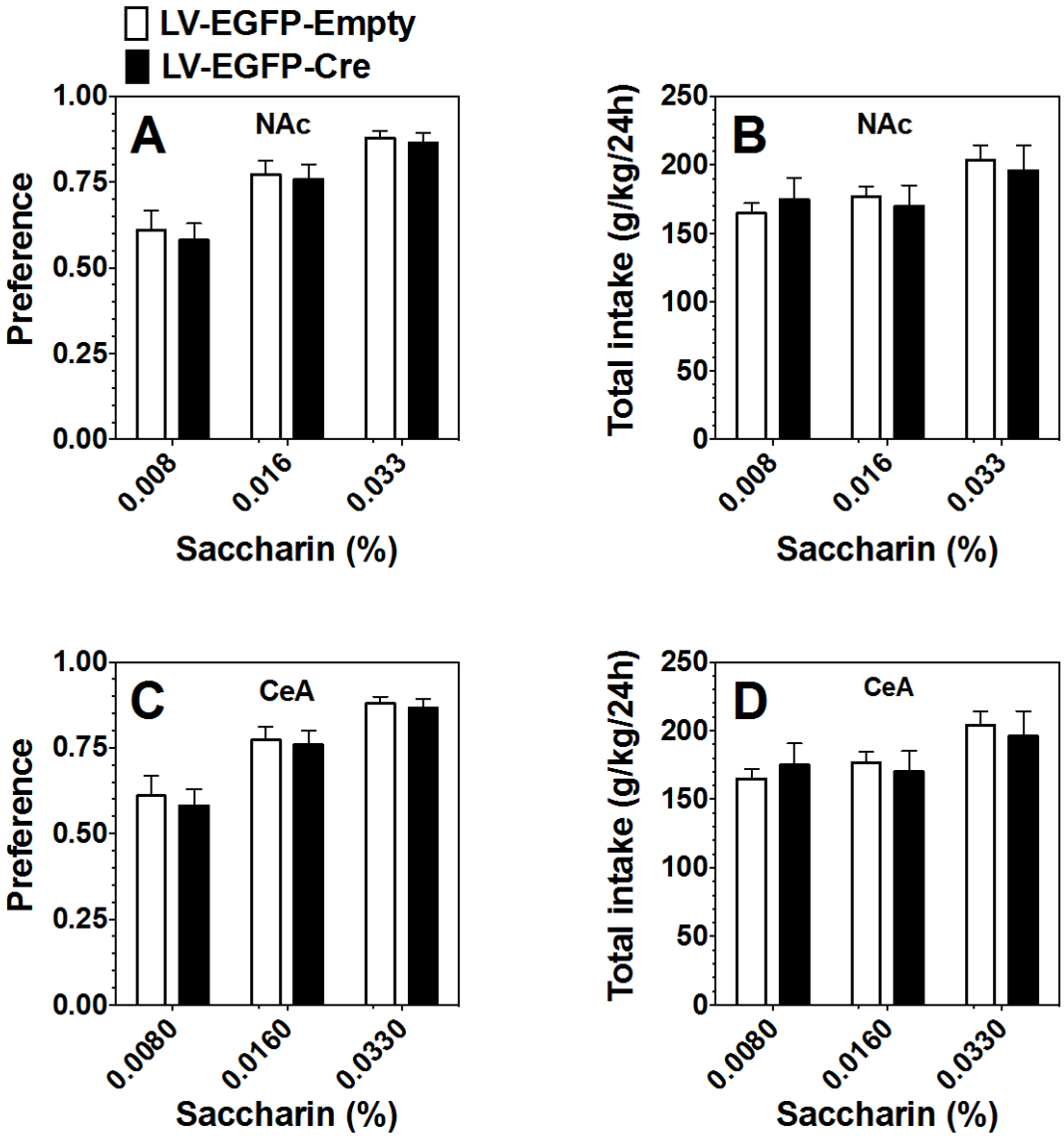

Figure 3.6. Preference for Non-Ethanol Tastants in the Two-Bottle Choice Test. Lentiviral-mediate knockdown of IKKβ in the NAc and CeA on saccharin preference using a continuous 24h 2BC test in *Ikkβ*$^{F/F}$ mice. Effect of knockdown of IKKβ in NAc (n = 32 LV-EGFP-Cre, n = 20 LV-EGFP-Empty) is shown in panels A and B. A: Preference for saccharin. B: Total fluid intake (g/kg/24h). The effect of knockdown of IKKβ in CeA (n = 20 LV-EGFP-Cre, n = 10 LV-EGFP-Empty) is shown in panels C and D. C: Preference for saccharin. D: Total fluid intake (g/kg/24h). Each point is the average of 2 days of drinking ± SEM. Main effects were determined using a two-way ANOVA with repeated measures. Statistical significance of LV-EGFP-Cre treatment compared with corresponding LV-EGFP-Empty was determined using a Bonferroni post-hoc test for multiple comparisons.

Upon completion of the behavior experiments (~8 weeks post injection), knockdown of IKKβ in the NAc and CeA was verified by 1) anatomical assessment of needle placement and viral spread, 2) confirmation of IKKβ protein knockdown, and 3) exploration of changes in mRNA levels of *Ikkβ* and downstream pro-inflammatory cytokines in the NF-κB canonical pathway. To assess needle placement and viral spread, animals were perfused and brains harvested from a subset of the lentiviral-treated $Ikk\beta^{F/F}$ mice used in the brain region-specific IKKβ knockdown experiments (NAc: n= 22 LV-EGFP-Cre, n= 14 LV-EGFP-Empty; CeA: n= 15 LV-EGFP-Cre, n= 5 LV-EGFP-Empty). Injection coordinates and coverage of the NAc and CeA were verified using immunofluorescence to detect EGFP. Figures 3.7A and 3.7C are representative images of coronal sections in the NAc [Anterior Posterior (AP) +1.49 mm] and CeA (AP -1.14 mm), respectively, of the $Ikk\beta^{F/F}$ mice treated with either LV-EGFP-Cre or LV-EGFP-Empty. The left side of the fluorescent image shows the EGFP signal (surrogate marker for lentiviral transduction) in green and DAPI (a stain that visualizes the nuclei of all cells) in blue. The right side of the image is a brightfield image used to better visualize the neuroanatomical landmarks. Figures 3.7C and 3.7D are coronal sections from a mouse brain atlas in the area of the desired target coordinates with the blue circles showing the NAc and CeA, and the green ovals demonstrating the typical area where the LV-EGFP-Cre and LV-EGFP-Empty treatments transduced. After completion of the drinking tests, analysis of brain sections from knockdowns in NAc and CeA revealed that 100% of the samples met the criteria of 1) needle placements in at least one side within ± 0.3 mm of the desired stereotaxic coordinates, and 2) viral expression coverage that was greater than 1/3 of the area in the brain region of interest. The average viral coverage per injection site as indicated by EGFP signal was 37.8% ± 4.8% in the NAc and 50.9% ± 5.7% in the CeA (mean ± SEM).

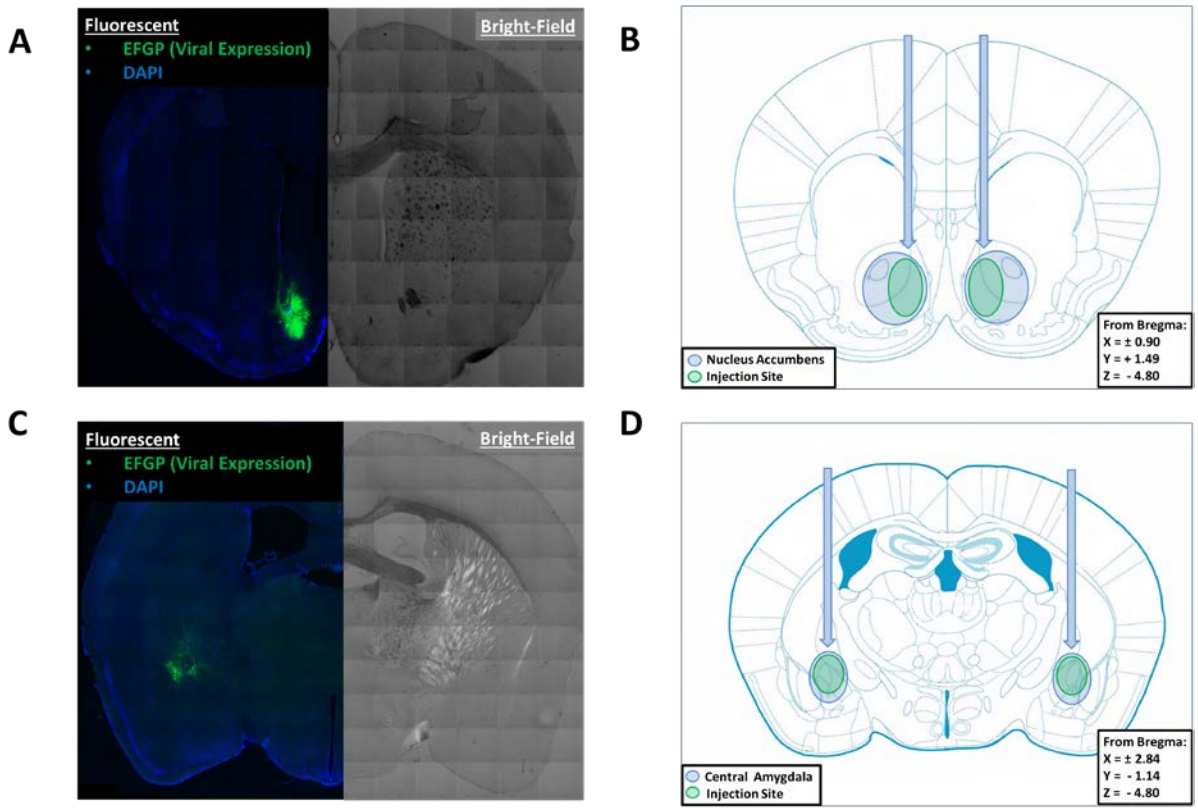

Figure 3.7: **Injection Target Verification for the Studies Involving Lentiviral-Mediated IKKβ Knockdown in the NAc and CeA.** A and C: Composite microscope images of a coronal section in the (A) NAc or (C) CeA of a representative lentiviral injection using fluorescent microscopy (on left) to show EGFP marker signal (green), and bright-field (on right) to demonstrate neuroanatomy. B and D: Coronal brain atlas figure at the injection site with blue circles indicating the (B) NAc or (D) CeA, and the green ovals illustrating the typical lentiviral injection location and spread.

After the 2BC drinking tests, we confirmed IKKβ protein knockdown in a subset of mice from the NAc and CeA experiments using immunohistochemistry (n=5 LV-EGFP-Cre and n=5 LV-EGFP-Empty for each experiment). Brains were prepared, immunostained, and analyzed in the same manner as the IKKβ knockdown experiment (3 weeks/8 weeks) previously described. The relative expression of IKKβ in Cre-treated animals vs. the control was 0.122 ± 0.026 ($p < 0.001$) in the NAc and 0.141 ± 0.028 ($p < 0.001$) in the CeA (mean ± SEM) (Fig. 3.8A). This represents an 88% and 86% decrease in the NAc and CeA, respectively. These results were consistent with those obtained in trial IKKβ knockdown experiment 8 weeks post injection.

To determine changes in mRNA levels of *Ikkβ* and downstream cytokines in the NF-κB canonical pathway, we performed quantitative PCR on micropunches from the NAc and CeA. A subset of brains from NAc (n= 10 LV-EGFP-Cre, n= 6 LV-EGFP-Empty) and CeA (n=5 LV-EGFP-Cre, n= 5 LV-EGFP-Empty) experiments were harvested, flash frozen, sectioned, and micropunches were collected at the injection site. The relative expression of *Ikkβ* was 0.321 ± 0.049 ($p < 0.001$) in the NAc and 0.360 ± 0.056 ($p < 0.001$) in the CeA; *Tnf-α* was 0.568 ± 0.059 ($p < 0.01$) in the NAc and 0.488 ± 0.084 ($p < 0.01$) in the CeA; and *Il-6* was 0.595 ± 0.055 ($p < 0.01$) in the NAc and 0.641 ± 0.060 ($p < 0.01$) in the CeA (mean ± SEM). This equates to an approximately 68% and 64% decrease in IKKβ mRNA in the NAc and CeA, respectively, and at least a 35% knockdown for TNF-α and IL-6 mRNA in both brain regions (Fig. 3.8).

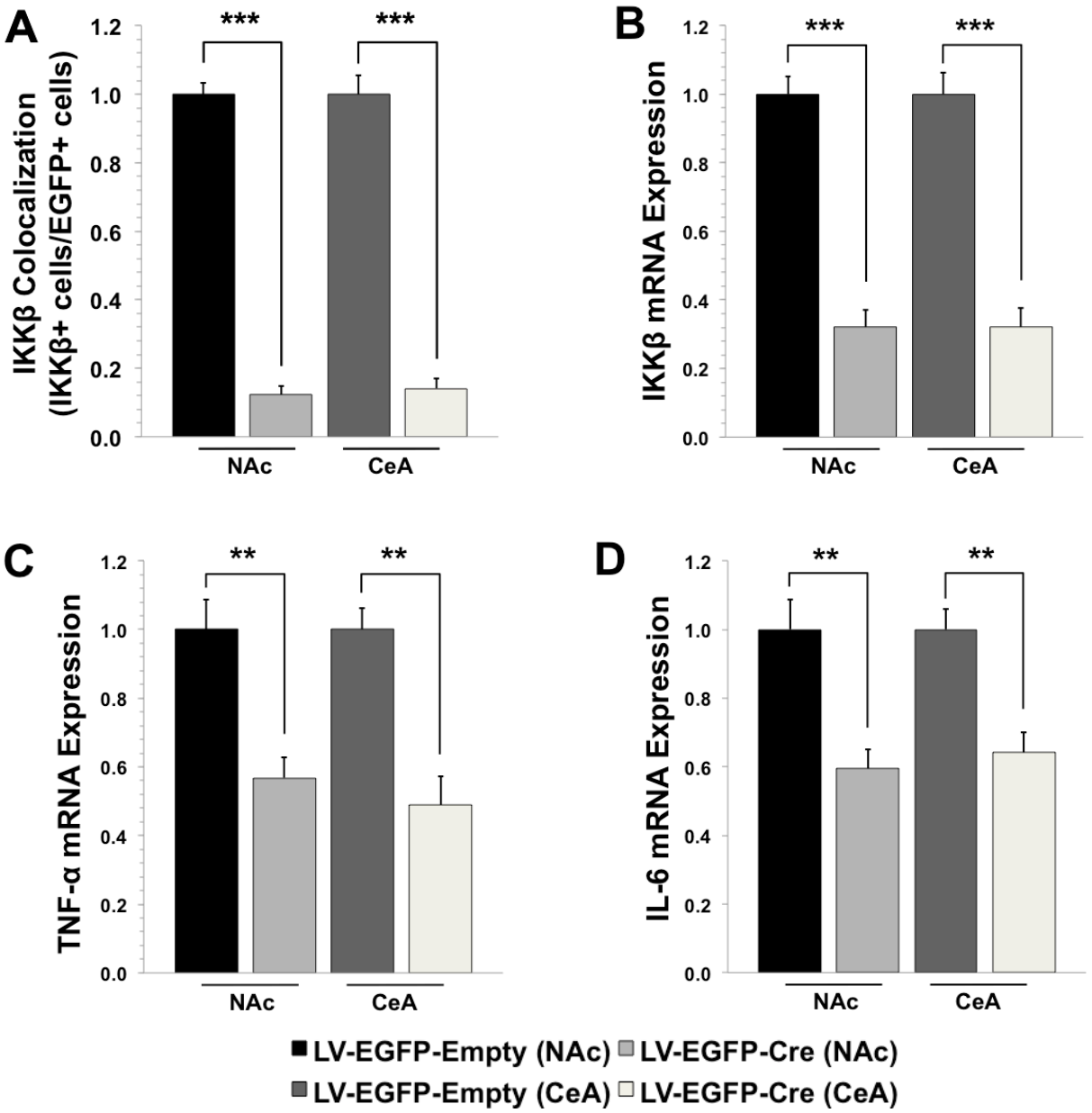

Figure 3.8. Determination of IKKβ Protein Levels and mRNA Expression of IKKβ, TNF-α, and IL-6 at Injection Site Upon Completion of Behavioral Studies. A: IKKβ protein levels in NAc and CeA (n=5 per group: NAc LV-EGFP-Cre, NAc LV-EGFP-Empty, CeA LV-EGFP-Cre, and CeA LV-EGFP-Empty). B-D: mRNA levels of IKKβ, TNF-α, and IL-6 in the NAc (n = 10 LV-EGFP-Cre, n = 5 LV-EGFP-Empty) and CeA (n = 5 LV-EGFP-Cre, n = 5 LV-EGFP-Empty). B: IKKβ mRNA expression C: TNF-α mRNA expression. D: IL-6 mRNA expression. All values shown relative to LV-EGFP-Empty treated mice. IKKβ protein levels were analyzed using immunohistochemistry. IKKβ mRNA levels at the target site in the NAc and CeA were assessed by quantitative RT-PCR and normalized relative to GADPH. **p<0.01, ***p<0.001 determined by Student t test. All data are shown as the mean ± SEM.

IKKβ Cell Type-Specificity NAc and CeA

To further investigate IKKβ's role in the brain, we determined the cell type localization of IKKβ in the NAc and CeA. Brain slices were co-stained using antibodies against IKKβ and three common cell type markers in the brain (neurons: anti-NeuN; astrocytes: anti-GFAP; microglia: anti-Iba1) from 3 adult male alcohol-naive C57Bl/6J mice. Using fluorescent light microcopy to visualize IKKβ signal colocalization, we observed that in both the NAc and CeA IKKβ was expressed in all three cell types to some degree, but was primarily in neurons (Fig. 3.9).

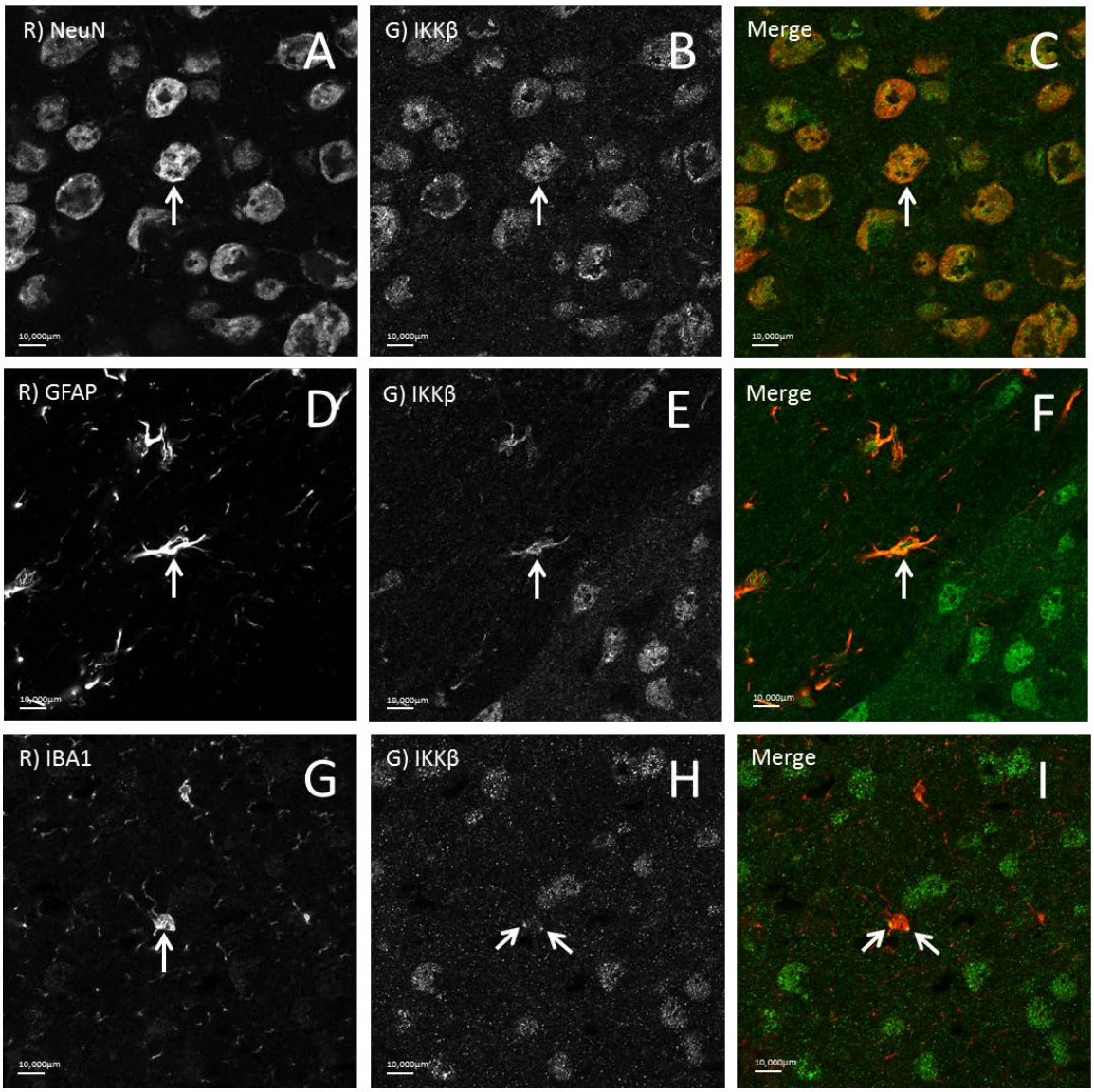

Figure 3.9. Cell Type-Specific Localization of IKKβ in the NAc and CeA. Representative fluorescent light microscope images illustrating cell-type specific antibodies in the first column (A: anti-NeuN for neurons; D: anti-GFAP for astrocytes; G: anti-Iba1 for microglia), anti-IKKβ stains in the second column (B, E, H), and overlay of the first two in the third column (C, F, I). Arrows illustrate co-localization cells between anti-IKKβ and cell type-specific stains.

Subsequently, we examined the trophism of the viral vector delivery system by co-staining brain slices from LV-EGFP-Cre treated animals in the NAc and CeA (n =2 NAc LV-EGFP-Cre, n=2 CeA LV-EGFP-Cre) using an antibody to target EGFP and the same three cell-specific described above. EGFP under the control of a CMV promoter in the VSV-G pseudotyped lentiviral vectors was expressed primarily in neurons (74.6% ± 1.3%), slightly in astrocytes (10.8% ± 2.2%), and only marginally in microglia (1.8% ± 0.5%) (Fig. 3.10). Thus, the brain-region specific knockdown of IKKβ observed in these studies was predominately neuronal.

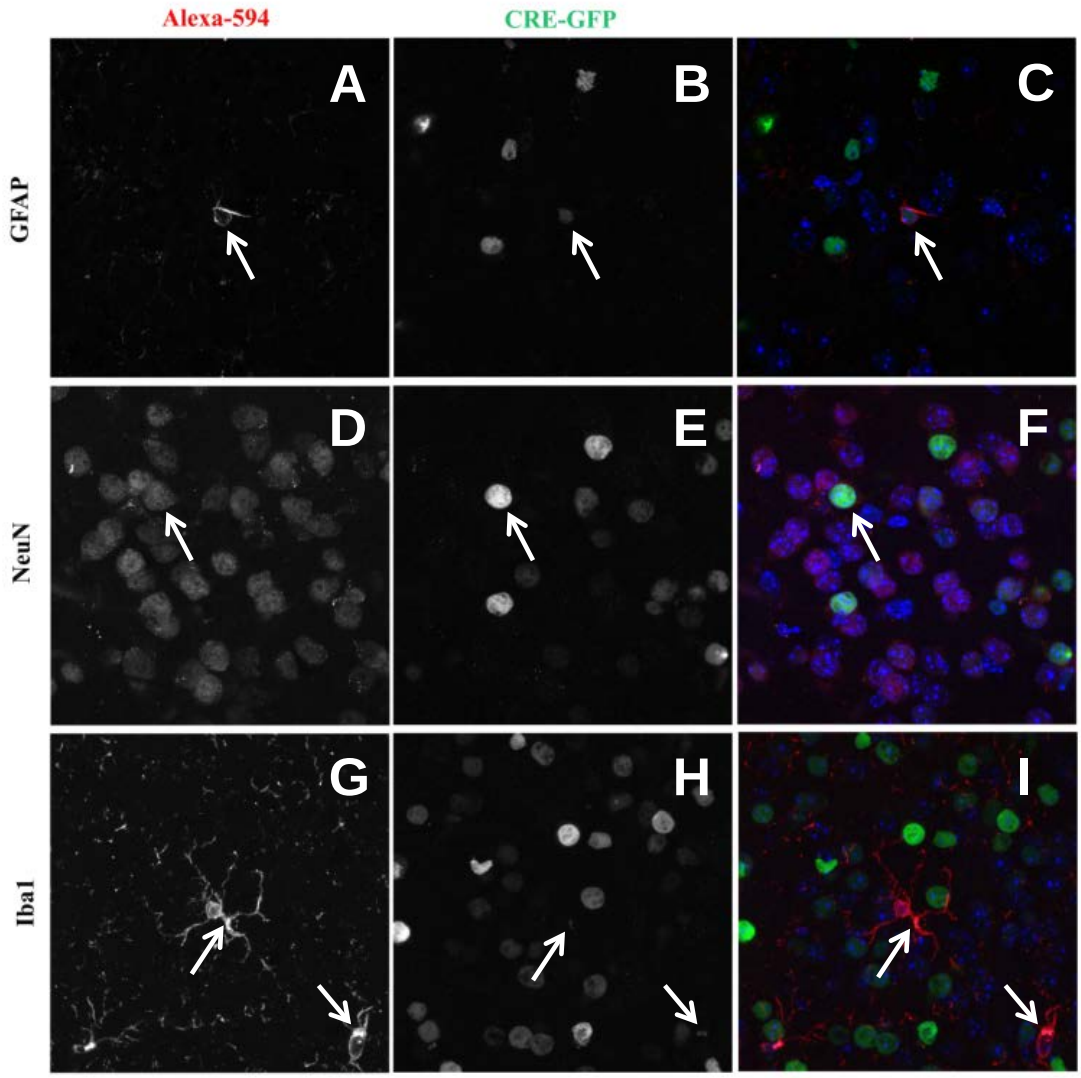

Figure 3.10. Cell Type Trophism of Lentiviral Vectors in the NAc and CeA. Representative fluorescent light microscope image illustrating cell-type specific stains in the first column (A: anti-GFAP for astrocytes; D: anti-NeuN for neurons; G: anti-Iba1 for microglia), anti-GFP stains in the second column (B, E, H), and overlay of the first two in the third column (C, F, I). Arrows illustrate cells in which co-localization can be seen between anti-GFP and cell type-specific stains.

DISCUSSION

We investigated the role of IKKβ in modulating drinking based upon previous findings showing that alcohol-dependent behaviors are mediated in part by pro-inflammatory genes (Blednov *et al.* 2011; Blednov *et al.* 2012). Inhibiting/knocking down IKKβ either peripherally, or in brain regions associated with addictive behaviors decreased ethanol consumption and preference. These effects were observed using two the IKKβ inhibitors, TPCA-1 and sulfasalazine, in two separate drinking models (2BC and 2BC-DID). Neither sulfasalazine nor TPCA-1 can penetrate the BBB, so their anti-inflammatory effects would be confined to the periphery (Liu *et al.* 2012a). This is consistent with other anti-inflammatory agents, such as minocycline which have also reduced drinking in adult mice (Agrawal *et al.* 2014).

Knockdown of IKKβ in the NAc or CeA was sufficient to disrupt the pro-inflammatory cascade and decrease voluntary 2BC ethanol drinking, showing that drinking behavior can also be selectively regulated by central actions. The NAc is part of the mesolimbic dopamine reward system, which has a well-documented role in substance abuse. The central amygdala is involved in fear-motivated behaviors associated with drug and alcohol abuse and has been shown to mediate the behavioral effects of acute and chronic ethanol consumption in rodents (Lam *et al.* 2008; Roberto *et al.* 2004b; Roberto *et al.* 2005; Roberto *et al.* 2004a). Lesions of the central, but not basolateral, amygdala decrease voluntary ethanol consumption (Möller et al., 1997), and a review of the neurocircuitry of drug addiction discussed plasticity in both frontal cortical and subregions of the amygdala as important for craving, withdrawal, negative affect, and loss of control (Koob and Volkow 2010). Thus, the brain regions targeted here are important in alcohol-mediated behaviors.

Evidence for disruption of the pro-inflammatory cascade in the NAc and CeA was verified by reduction of IKKβ protein and mRNA, as well as a decrease in expression of

downstream products of the NF-κB canonical pathway (TNF-α and IL-6) in these regions. In contrast, increases in cytokines following alcohol intake have been hypothesized to promote excessive alcohol consumption, which may in turn exacerbate pro-inflammatory responses (Blednov *et al.* 2011), in part via activation of NF-κB. In fact, NF-κB DNA binding in the brain has been shown to increase with ethanol treatments (Crews *et al.* 2006) and the human NFKB1 gene is linked to alcoholism (Edenberg *et al.* 2007).

In addition to brain regions, different cell types play unique roles in the neuroimmune response (Szabo and Lippai 2014). In our study, the selective knockdown of IKKβ did not affect all cell types equally. For example, IKKβ was expressed primarily in neurons in the NAc and CeA with lessor amounts found in glial cells (astrocytes and microglia). The cell-type specificity of the viral vector system delivering Cre favored the transduction in neurons, and to a lesser degree in astrocytes, and only marginally in microglia. It has been documented that VSV-G lentiviral vectors under the control of a CMV promoter predominately express their transgene in neurons compared to glia cells, and the in vivo activity of the CMV promoter in glia cells is low (Jakobsson and Lundberg 2006). Even though IKKβ was knocked down to some extent in all three cell types (neurons, astrocytes, microglia), neurons were the primary target, suggesting that the majority of central IKKβ knockdown was neuronal.

The IKK complex (IKKα, IKKβ, and IKKγ) is a key mediator for several pro-inflammatory pathways that ultimately result in the activation of the NF-κB canonical pathway. Specifically, IKKβ primarily regulates the NF-κB canonical pathway (transcription of pro-inflammatory genes/anti-apoptosis), IKKα regulates the NF-κB non-canonical pathway (cell cycle regulation/proliferation), while IKKγ participates in both pathways (Gamble *et al.* 2012; Perkins 2007). Thus, knockdown of IKKβ in the NAc and

CeA likely prevented activation of the canonical pathway in neurons, interrupting pro-inflammatory signaling and feedback loops (Fig. 1.1).

The central effects of IKKβ are not well studied, and its potential role in alcohol drinking had not been investigated. Our results provide novel evidence that peripheral or central inhibition of IKKβ decreases ethanol drinking. Ethanol could induce peripheral pro-inflammatory cytokines that ultimately activate expression of immune-related genes in the brain or it could directly stimulate central neuroimmune responses. Inhibiting IKKβ-mediated signaling could limit the peripheral and central inflammatory effects of ethanol. Our results are consistent with previous studies showing that null mutant mice lacking genes associated with pro-inflammatory signaling pathways displayed reduced levels of chemokines and cytokines and reduced ethanol consumption in voluntary 2BC drinking tests (Ponomarev *et al.* 2012; Blednov *et al.* 2005).

In summary, voluntary ethanol drinking can be decreased by inhibiting IKKβ peripherally using pharmacological inhibitors or centrally using genetic deletions in the CeA and NAc, regions known to be important in the neurobiology of alcohol abuse (Koob and Volkow 2010). Although the effects of neuroimmune signaling are thought to be predominately glial (astrocytes and microglia), this study highlights an important neuronal role in reducing alcohol drinking. Our results also provide evidence that the use of peripheral acting IKKβ inhibitors with anti-inflammatory properties is a potential treatment strategy for regulating drinking. In particular, drugs like sulfasalazine that are already FDA approved, may advance treatment options for AUD or other disorders linked with neuroimmune activation.

CHAPTER IV: Ethanol-Responsive MicroRNAs Associated with the IKKβ/NF-κB Pathway

INTRODUCTION

MicroRNAs have emerged as important regulators of gene expression. MicroRNAs are small (18-22 nucleotides) non-coding RNA molecules that post-transcriptionally regulate gene expression by binding to complementary sequences on the 3' UTR of mRNAs which results in either translational repression or cleavage of the message (Miranda *et al.* 2010) (Fig 1.3). They are highly abundant in the brain and mediate most biological processes, including neuroimmune signaling (Robinson *et al.* 2014; Soreq and Wolf 2011). For example, let-7 family members regulate responsiveness to LPS by targeting TLR4 (Chen *et al.* 2007) and modulate NF-κB expression by targeting IL-6 (Iliopoulos *et al.* 2009), while mir-9 has been implicated in the regulation of NF-κB (p50/p105) (O'Neill, Sheedy, & McCoy, 2011b). MicroRNAs have been implicated in adaptations resulting from ethanol exposure (Lewohl *et al.* 2011). A comprehensive study examined changes in gene and microRNA expression in the PFC of human alcoholics found 35 differentially expressed microRNAs targeted the 60% of the differentially expressed genes (Lewohl *et al.* 2011; Liu *et al.* 2005). Even with this supporting evidence, the role neuroimmune signaling plays in the development of AUD remains elusive. The goal of this study is to identify ethanol-responsive microRNAs associated with the IKKβ/NF-κB pathway, and then modulate those candidates the areas of the brain that are associated with the development of AUD

MATERIAL AND METHODS

Animals

Brain region-specific determination of ethanol-responsive microRNAs was conducted in adult female hybrid F1 FVBxB6 mice from reciprocal intercrosses

C57BL/6J x FVB/NJ F1 and FVB/NJ x C57BL/6J F1 (maternal strain x paternal strain). Brain region-specific modulation of microRNAs was conducted in adult male C57BL/6J mice. All mice were taken from a colony maintained at The University of Texas at Austin (original breeders were purchased from Jackson Laboratories, Bar Harbor, ME). Both mouse strains was chosen because of their propensity to drink large amounts of ethanol and to achieve behaviorally significant blood ethanol concentrations (Belknap *et al.* 1997; Blednov *et al.* 2005). Mice were group-housed 4 or 5 per cage on a 12h light/12h dark cycle (lights on at 7:00 a.m.) with ad libitum access to water and rodent chow (Prolab RMH 180 5LL2 chow, TestDiet, Richmond, IN). The temperature and humidity of the room were kept constant. Behavioral testing began when the mice were at least 2 months of age. Experiments were conducted in isolated behavioral testing rooms in the Animal Resources Center at The University of Texas at Austin. All experiments were approved by the university's Institute for Animal Care and Use Committee and conducted in accordance with NIH guidelines with regard to the use of animals in research.

Brain Region-Specific MicroRNA Modulation

For microRNA overexpression, C57BL/6J mice were injected bilaterally into the NAc with either a VSV-G pseudotyped lentivirus expressing the pri-mmu-let-7g and an EGFP both under the control of a CMV promoter (Let-7g-miRNA), or an equivalent vector expressing a scrambled shRNA sequence (Control) (Courtesy of Dr. Amy Lasek at the University of Illinois at Chicago). For the microRNA inhibition experiments, C57BL/6J mice were injected bilaterally into the NAc with either an Exiqon in vivo LNA™ microRNA inhibitor labeled with Tye 568 for mmu-let-7g-5p in PBS or an equivalent oligonucleotide expressing a scrambled shRNA sequence (Control) (Exiqon, Vedbaek, Denmark). Mice were anesthetized by isoflurane inhalation, placed in a model

1900 stereotaxic apparatus (David Kopf, Tujunga, CA), and administered preoperative analgesic (Rimadyl, 5 mg/kg). The skull was exposed, and bregma and lambda visualized with a dissecting microscope. A digitizer attached to the micromanipulator of the stereotaxic apparatus was used to locate coordinates relative to bregma. Burr holes were drilled bilaterally above the injection sites in the skull using a drill equipped with a #75 carbide bit (David Kopf, Tujunga, CA). The injection sites targeted the NAc using the following coordinates relative to bregma: anteroposterior (AP) +1.49 mm, mediolateral (ML) ±0.9 mm, dorsoventral (DV) -4.8 mm. Injections were performed using a Hamilton 10-µL microsyringe (model #1701) and a 30-gauge needle. The syringe was lowered to the DV coordinate and retracted 0.2 mm. Viral solutions (1.0 µL with titer of 1.8×10^8 vp/mL in PBS) or antagomirs (1.0 µL, 0.125 nmol) were injected into each site at a rate of 200 nL/min. After each injection, the syringe was left in place for 5 min before being retracted over a period of 3 minutes. Incisions were closed with tissue adhesive (Vetbond, 3 M; St. Paul, MN). Mice were individually housed after surgery and given a 1-week (let-7g mimic) or 4 days (anti-let-7g) recovery before starting the ethanol drinking tests.

Behavioral Testing

Brain region-specific determination of ethanol-responsive microRNAs. The mice were given access to alcohol according to a 2BC-DID protocol previously described (Blednov *et al.* 2014) In this drinking paradigm, mice were allowed to voluntarily drink either water or 20% ethanol from two separate bottles during the first 3h of their dark cycle. Ethanol consumption (g/kg/3h), preference, and total fluid intake (g/kg/day) were measured once at the end of the 3h drinking period over a course of 20 days. Food was available ad libitum, and mice were weighed every 4 days.

Brain region-specific modulation of microRNAs. The mice were given access to alcohol according to continuous access and intermittent access 2BC drinking protocols previously described (Blednov 2003; Melendez 2011). In the continuous access 2BC drinking model, mice were allowed to voluntarily drink either water or ascending concentrations of ethanol solutions (3%, 6%, 8%, 10%, 12%, 14%, 16% v/v) from two separate bottle. Concentrations were changed every two days. In the intermittent access 2BC drinking model, mice were allowed to voluntarily drink either water every day or 15% ethanol solution every other day. For both drinking tests, ethanol consumption (g/kg/day), preference, and total fluid intake (g/kg/day) were measured daily over a period of 14 days for the continuous access and 16 days for intermittent access drinking paradigms. Food was available ad libitum, and mice were weighed every 4 days. Data was analyzed using analysis of variance (ANOVA) with repeated measures followed by Bonferroni post hoc tests (GraphPad Software, Inc., La Jolla, CA). Calculated p-values of less than 0.05 were considered statistically significant.

RNA Isolation

Within one day of completing the behavioral experiments, mice were sacrificed by cervical dislocation followed by decapitation. The brains were quickly removed, flash frozen in liquid nitrogen, and later embedded in Optimal Cutting Temperature (OCT) media in isopentane on dry ice. Brains were then stored at −80° C for future processing. Brains were transferred to a cryostat set at −6° C for at least 1 h before sectioning. Sections (300 μm) were collected from the PFC +3.20 mm to 1.80 mm, NAc +1.80 to +0.60 mm, and AMY -0.60 to -1.80 mm (AP) relative to bregma, and transferred to pre-cooled glass slides on dry ice. Micropunch sampling was performed on a frozen stage (−25° C) using Dual Fluorescent Protein Flashlight (Nightsea, Bedford, MA), and a mouse stereotaxic atlas to identify the EGFP expression and anatomical location of the

injection site. Microdissection punches (Stoelting Co., Wood Dale, IL) with an inner diameter of 1.25 mm was used to obtain samples of the PFC, NAc and AMY. This inner diameter fit within the brain region of interest and minimized contamination from other tissue. Punches were taken bilaterally from the 300 μm sections and stored at −80°C until RNA extraction. Micropunches were washed with 100% ETOH and RNasZap (Life Technologies) between each animal. All equipment used to obtain tissue was treated with RNAseZap (Life Technologies) to prevent RNA degradation. Total RNA was extracted using the MagMAX™-96 for Microarrays Total RNA Isolation Kit (Life Technologies, Carlsbad, CA) according to the manufacturer's instructions. RNA yields and purity were assessed using a NanoDrop 8000 (Thermo Fisher Scientific, Waltham, MA) with both the 260/230 and 260/280 ratios >2.00. RNA quality was determined using the Agilent 2100 Bioanalyzer (Agilent, Santa Clara, CA) with RNA integrity numbers (RIN) averaging above 8.0.

Microarray Expression Profiling

To evaluate brain region-specific ethanol-responsive microRNAs, biotin-labeled cRNA was prepared using Illumina TotalPrep RNA Amplification kit (Ambion, Austin, TX) and then hybridized to Illumina MouseRef-8 v2.0 Expression BeadChips (Illumina, San Diego, CA). The Bioconductor packages Lumi and arrayQualityMetrics were used to assess the quality of the Illumina bead summary data. The Lumi package was used for data preprocessing and included variance stabilization and quantile normalization. Statistical analysis comparing ethanol-treated and control groups were performed using the Bioconductor package limma. Exiqon miRCURY LNA microRNA Arrays 5th generation (Exiqon) was used for hybridization and scanning at the Moffitt Cancer Center Microarray Facility (Tampa, FL). The limma package was used for data analysis preprocessing, which included minimum background correction and scale normalization

between arrays. Within-array replication was assessed using the limma duplicate correlation function since each probe was spotted as replicated of four on the arrays, False discovery rate (FDR) was assessed using the Benjamini-Hochberg method (Benjamini *et al.* 2001). We compared our list of differentially expressed microRNAs in the PFC with those found in a previously reported human alcoholics study (Lewohl *et al.* 2011). The statistical significance of the matches was empirically evaluated using Monte Carlo simulations in the R environment (R Foundation for Statistical Computing, Vienna, Austria).

Quantitative PCR

Quantitative PCR was used to both validate the brain region-specific expression of ethanol-responsive microRNAs, and to confirm microRNA/gene manipulations involved with the brain region-specific modulation of microRNAs. Following reverse transcription, qPCR was performed in triplicate, using TaqMan® MiRNA Assays together with the TaqMan® Universal PCR Master Mix (Life Technologies), as per manufacturer's instructions. TaqMan® miRNA assays used were: mmu-let-7g-5p (ID: 002282), mmu-miR-140-5p (ID: 001187), mmu-miR-152-3p (ID: 000475), mmu-miR-7a-5p (ID: 000268), mmu-let-7f-5p (ID: 000382), mmu-miR-15b-5p (ID: 000390), mmu-miR-101a-3p (ID: 002253), mmu-miR-301a-5p (ID: 006346), mmu-let-144-5p (ID: 000379), mmu-miR-34c-5p (ID: 000428). Assays used for endogenous control were: snoRNA234 (ID: 001234) and snoRNA142 (ID: 001231), which were chosen out of five endogenous control assays tested in our samples. For mRNA validation, single-stranded cDNA was synthesized from total RNA using the TaqMan® High Capacity cDNA Reverse Transcription Kit (Life Technologies). Following reverse transcription, qPCR was performed in triplicate, using TaqMan® Gene Expression Assays together with the TaqMan® Universal PCR Master Mix (Life Technologies), as per manufacturer's

instructions. TaqMan® Gene expression assays used were Igf2bp1 (Mm00501602_m1), Hmga2 (Mm04183367_g1), and pri-let-7g (Mm03306155_pri). Gapdh (Mm99999915_g1) gene was used as a reference gene, and relative mRNA levels were determined using the $2^{-\Delta\Delta CT}$ method (Schmittgen and Livak 2008). Gapdh was used as the endogenous control because it's low variability between samples. Reactions for the brain region-specific expression of ethanol-responsive micoRNAs were carried out in a 7900HT Fast Real-Time PCR System and data collected using SDS software (Life Technologies). Reactions for the brain region-specific modulations of microRNAs were carried out in a CFX384™ Real-Time PCR Detection System (Bio-Rad) and data collected using Bio-Rad CFX Manger. All genes were normalized to the endogenous housekeeping genes and expressed relative to their respective control treatment.

RESULTS

Brain Region-Specific Expression of Ethanol-Responsive MicroRNAs

To explore the impact that alcohol consumption has on microRNA expression in brain areas associated with AUD (PFC, NAc, AMY), we conducted a microRNA profiling study on 20 ethanol-treated mice and 12 matched controls. The analysis of the microarray data revealed numerous changes in microRNAs in alcohol-drinking mice relative.to the non-drinking controls in all three brain regions. For example, the PFC had 77 differentially expressed microRNAs (FDR <10%) (Table 4.1). We then compared our list with the 35 differentially expressed microRNAs found in the PFC of a previously reported human alcoholics study and noticed some interesting similarities (Lewohl *et al.* 2011). The microRNAs were predominately up regulated in both studies and had 14 microRNAs common between the mouse and the human ($p<1.8 \times 10^{-5}$ as determined after 10,000 Monte Carlo simulations) (Lewohl *et al.* 2011) (Fig. 4.1). The microRNAs

that changed expression in both mouse and human were: miR-7a let-7g, let-7f, miR-101a, miR-152, miR-15b, and miR-140 all validated by qPCR ($p < 0.05$), but miR-301, miR-144 as, miR-34c did not. Quantitative PCR was not performed on remaining commonly expressed microRNAs: miR-17, miR-146b, miR-339, and miR-368. Moreover, the NAc had 49 differentially expressed microRNAs with 11 upregulated and 38 downregulated (FDR <20%) (Table 4.1). The AMY had 60 differentially expressed microRNAs with 41 upregulated and 19 downregulated (FDR <20%) (Table 4.1).

PFC		NAc		AMY	
Name	Adjusted p value	Name	Adjusted p value	Name	Adjusted p value
mmu-let-7g-5p	1.27E-04	mmu-miR-465b-5p	7.90E-03	mmu-miR-433-3p	1.35E-06
mmu-let-7d-5p	1.27E-04	mmu-miR-187-3p	7.90E-03	mmu-miR-106b-5p	1.44E-05
mmu-miR-26a-5p	1.27E-04	mmu-miR-377-3p	4.34E-02	mmu-miR-145-5p	7.78E-05
mmu-let-7c-5p	1.49E-04	mmu-miR-7a-5p	4.41E-02	mmu-miR-669m-3p	1.12E-04
mmu-let-7b-5p	1.49E-04	mmu-miR-5097	4.41E-02	mmu-miR-541-5p	1.56E-04
mmu-miR-30d-5p	3.79E-04	mmu-miR-411-3p	4.51E-02	mmu-miR-183-3p	4.27E-04
mmu-let-7a-5p	6.88E-04	mmu-miR-708-5p	4.51E-02	mmu-miR-27b-3p	4.26E-03
mmu-let-7i-5p	6.88E-04	mmu-miR-148b-3p	4.51E-02	mmu-miR-187-5p	6.50E-03
mmu-miR-320-3p	6.88E-04	mmu-miR-153-3p	4.51E-02	mmu-miR-24-1-5p	1.25E-02
mmu-miR-34c-5p	6.88E-04	mmu-miR-30c-5p	5.83E-02	mmu-miR-214-5p	2.11E-02
mmu-miR-7a-5p	7.91E-04	mmu-miR-26a-5p	5.96E-02	mmu-miR-325-3p	2.11E-02
mmu-miR-101b-3p	9.11E-04	mmu-miR-34a-5p	5.96E-02	mmu-miR-7b-5p	2.11E-02
mmu-miR-24-2-5p	9.26E-04	mmu-let-7a-5p	7.50E-02	mmu-miR-328-3p	2.11E-02
mmu-miR-16-5p	1.25E-03	mmu-let-7i-5p	8.41E-02	mmu-miR-882-5p	2.11E-02
mmu-miR-29a-5p	1.34E-03	mmu-miR-1983	8.41E-02	mmu-miR-30a-5p	2.32E-02
mmu-miR-15a-5p	2.24E-03	mmu-miR-335-5p	8.41E-02	mmu-miR-1952-5p	3.09E-02
mmu-miR-361-5p	2.90E-03	mmu-miR-491-3p	8.41E-02	mmu-miR-1954-5p	3.25E-02
mmu-miR-138-5p	3.20E-03	mmu-miR-691	8.72E-02	mmu-miR-664-3p	3.25E-02
mmu-miR-376b-3p	3.50E-03	mmu-miR-218-5p	1.04E-01	mmu-miR-466d-3p	3.25E-02
mmu-miR-195-5p	4.01E-03	mmu-miR-212-3p	1.17E-01	mmu-miR-693-5p	3.25E-02
mmu-miR-181d-5p	4.59E-03	mmu-miR-503-3p	1.20E-01	mmu-miR-490-3p	3.25E-02
mmu-let-7f-5p	4.83E-03	mmu-let-7b-5p	1.20E-01	mmu-miR-184-3p	3.25E-02
mmu-miR-434-3p	4.88E-03	mmu-miR-190-5p	1.20E-01	mmu-miR-382-5p	3.25E-02
mmu-miR-24-3p	5.27E-03	mmu-miR-126-3p	1.20E-01	mmu-miR-1958-5p	3.25E-02
mmu-miR-152-3p	5.65E-03	mmu-let-7g-5p	1.20E-01	mmu-let-7d-3p	3.25E-02
mmu-miR-222-3p	5.81E-03	mmu-miR-299-5p	1.20E-01	mmu-miR-203-3p	3.25E-02
mmu-miR-451-5p	6.57E-03	mmu-miR-409-5p	1.20E-01	mmu-miR-883b-5p	3.25E-02
mmu-miR-193-3p	8.12E-03	mmu-miR-767	1.20E-01	mmu-miR-298-5p	3.25E-02
mmu-miR-1952-5p	8.12E-03	mmu-miR-1902	1.23E-01	mmu-miR-140-3p	3.25E-02
mmu-miR-335-5p	8.50E-03	mmu-miR-129-1-3p	1.33E-01	mmu-miR-34c-3p	3.25E-02
mmu-miR-149-5p	8.75E-03	mmu-miR-883a-5p	1.48E-01	mmu-miR-494-3p	3.25E-02
mmu-miR-9-3p	1.28E-02	mmu-miR-301a-3p	1.48E-01	mmu-miR-124-3p	3.25E-02
mmu-miR-301a-3p	1.29E-02	mmu-miR-1957	1.52E-01	mmu-miR-200b-3p	3.25E-02
mmu-miR-204-5p	1.29E-02	mmu-miR-541-5p	1.69E-01	mmu-miR-1839-3p	3.25E-02
mmu-miR-221-3p	1.54E-02	mmu-miR-30e-3p	1.69E-01	mmu-miR-320-3p	3.25E-02
mmu-miR-708-5p	1.61E-02	mmu-miR-382-3p	1.81E-01	mmu-miR-297b-3p	3.25E-02
mmu-miR-101a-3p	1.92E-02	mmu-miR-32-5p	1.81E-01	mmu-miR-466a-3p	3.25E-02
mmu-miR-23a-3p	1.92E-02	mmu-miR-674-3p	1.81E-01	mmu-miR-150-5p	3.25E-02
mmu-miR-30e-5p	1.92E-02	mmu-miR-329-3p	1.81E-01	mmu-miR-1903-5p	3.25E-02
mmu-miR-140-3p	1.94E-02	mmu-miR-146b-5p	1.81E-01	mmu-miR-7a-5p	3.25E-02
mmu-miR-191-5p	1.94E-02	mmu-miR-103-3p	1.81E-01	mmu-miR-741-3p	3.25E-02
mmu-miR-125a-5p	2.26E-02	mmu-miR-30b-5p	1.81E-01	mmu-miR-300-3p	3.25E-02
mmu-miR-30e-3p	2.38E-02	mmu-miR-139-5p	1.81E-01	mmu-let-7a-2-3p	3.25E-02
mmu-miR-93-5p	2.45E-02	mmu-miR-379-5p	1.84E-01	mmu-miR-503-5p	3.25E-02
mmu-miR-340-5p	2.45E-02	mmu-miR-434-3p	1.84E-01	mmu-miR-381-3p	3.25E-02
mmu-miR-144-3p	3.30E-02	mmu-miR-302a-3p	1.84E-01	mmu-miR-1249-3p	3.25E-02
mmu-miR-26b-5p	3.35E-02	mmu-miR-99b-5p	1.84E-01	mmu-miR-467e-5p	3.25E-02
mmu-miR-146b-5p	3.38E-02	mmu-miR-132-5p	1.84E-01	mmu-miR-34a-5p	3.25E-02
mmu-miR-185-5p	3.38E-02	mmu-miR-298-5p	1.98E-01	mmu-miR-467b-3p	3.25E-02
mmu-miR-107-3p	4.12E-02			mmu-miR-337-3p	3.25E-02
mmu-miR-23b-3p	4.63E-02			mmu-miR-467d-3p	3.25E-02
mmu-miR-135b-5p	4.99E-02			mmu-miR-483-3p	3.25E-02
mmu-miR-15b-5p	4.99E-02			mmu-miR-361-3p	3.25E-02
mmu-miR-676-3p	5.28E-02			mmu-miR-195-5p	3.25E-02
mmu-miR-485-3p	6.39E-02			mmu-miR-881-5p	3.25E-02
mmu-miR-376a-3p	6.40E-02			mmu-miR-151-5p	3.25E-02
mmu-miR-130a-3p	6.44E-02			mmu-miR-877-5p	3.25E-02
mmu-miR-181a-5p	6.44E-02			mmu-miR-706-5p	3.25E-02
mmu-miR-24-1-5p	6.44E-02			mmu-miR-346-5p	3.25E-02
mmu-miR-674-5p	6.45E-02			mmu-miR-713-5p	3.25E-02
mmu-miR-183-5p	6.99E-02				
mmu-miR-221-5p	6.99E-02				
mmu-miR-9-5p	6.99E-02				
mmu-miR-124-5p	7.09E-02				
mmu-miR-669n-5p	7.31E-02				
mmu-miR-669c-5p	7.41E-02				
mmu-miR-339-5p	7.53E-02				
mmu-miR-145-5p	7.73E-02				
mmu-miR-182-5p	8.21E-02				
mmu-miR-429-3p	8.68E-02				
mmu-miR-330-5p	8.70E-02				
mmu-miR-1961-5p	9.11E-02				
mmu-miR-96-5p	9.22E-02				
mmu-miR-136-5p	9.39E-02				
mmu-miR-30b-5p	9.39E-02				
mmu-miR-34a-5p	9.66E-02				

Table 4.1. Ethanol-Responsive MicroRNAs. Differentially expressed microRNAs in the PFC, NAc, and AMY after exposure to a 2BC-DID test. Yellow highlights indicate mouse microRNAs commonly expressed with human alcoholics.

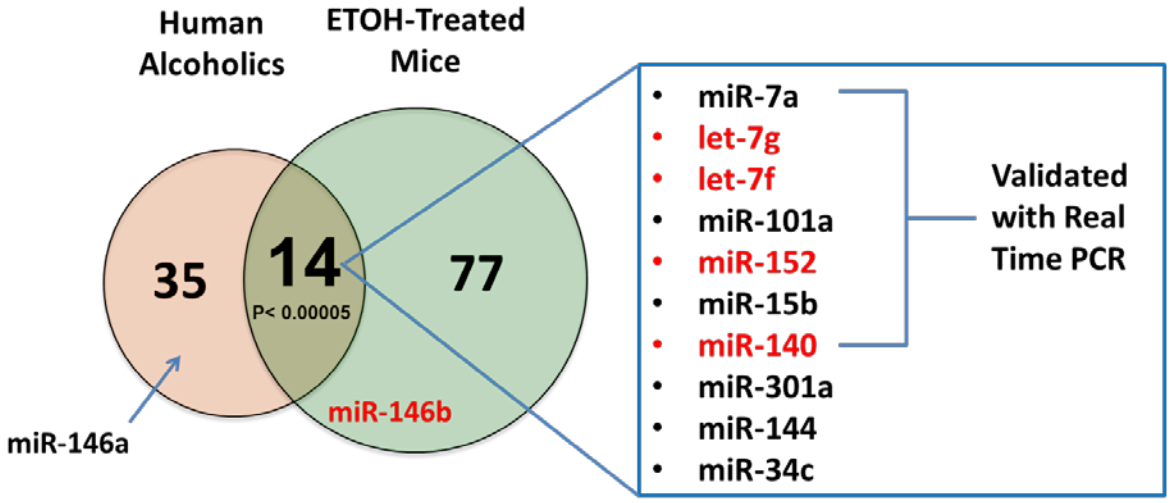

Figure 4.1. Ethanol-Responsive MicroRNAs in the PFC of Humans and Mice. Venn diagram highlighting a common set of 14 upregulated microRNAs in prefrontal cortex of human alcoholics (Lewohl *et al.* 2011) and ethanol-treated mice (current study). MicroRNAs associated with the IKKβ pathway are in red. (p value empirically assessed after 100,000 Monte Carlo simulations).

Differentially expressed MicroRNAs across the three brain regions were subsequently screened to find validated/predicted targets associated with the IKKβ/NF-κB pathway and five candidates were identified: let-7g, let-7f, miR-152, miR-140, and miR-146b. Each of the candidates shared differential expression in PFC with the human alcoholic, but some were changed in other brain regions, such as let-7g (NAc), miR-140 (AMY), and miR-146b (NAc) (Table 4.1). The let-7 family has been shown to target TLR4 and IL-6 and regulate responsiveness to LPS (Chen *et al.* 2007; Iliopoulos *et al.* 2009). Let-7g is predicted to target TRAF3 and IKKβ. miR-140 is upregulated after LPS treatment in mice (Moschos *et al.* 2007). miR152 inhibits TLR-triggered major histocompatibility complex (MHC) II expression (Liu *et al.* 2010) and is predicted to target IKKβ, IKKγ, and TRAF3. Lastly, miR-146 fine tunes many pro-inflammatory genes that utilize the IKKβ/NF-κB pathway (TLR4, IRAK1, TRAF6 and cytokine signaling) (Sonkoly *et al.* 2007; Virtue *et al.* 2012).

In Vivo Validation of Brain Region-Specific MicroRNA Modulation

Let-7g was selected as the best candidate to manipulate *in vivo* since it was differentially expressed in both mouse and humans in the PFC, was changed in other brain regions (NAc), and has many validated/predicted targets associated with the IKKβ/NF-κB pathway (TLR4, IL-6, IKKβ). The NAc was selected since manipulations of the IKKβ/NF-κB pathway were successful in altering ethanol drinking phenotypes in dissertation chapter 3. Trial experiments for both the let-7g mimic (1 µL of 1 x 10^8 vp/mL) vs. control and anti-let-7g antagomir (1 µL of 0.125 nmols) vs. control were conducted at 1 wk and 4 wk time points (n=6/group/time point). We measured mRNA levels for both precursor and mature let-7g, and its validated targets (HMGA2, and IGF2B1) to evaluate overexpression, and other unrelated micoRNAs (miR-140) to evaluate off-target effects. For the let-7g mimic at 1 week we observed a 70% increase

in mature let-7g and no changes in unrelated microRNAs (mir-140). We also saw a substantial increase in the precursor let-7g (53%) that the virus was actually expressing, and respectable decreases of 30 to 35% in the validated targets (HMGA2 and IGF2B1) (Fig. 4.2 A and B). We observed essentially the same results for the 4-week time point (Fig 4.2 C and D). For the let-7g antagomir at 1 week, we observed a 60% decrease in mature let-7g and no changes in unrelated microRNAs (mir-140), or in the precursor let-7g. The validated targets (HMGA2 and IGF2B1) decreased 20 to 25% (Fig. 4.3 A and B). We observed essentially the same results for the 4-week time point except that the decrease in mature let-7g was blunted being 44 %, instead of 60% (Figure 4.3 C and D). Thus, it was determined that we had a stable modulating effect over a month and there was an absence of nonspecific binding at the administered doses.

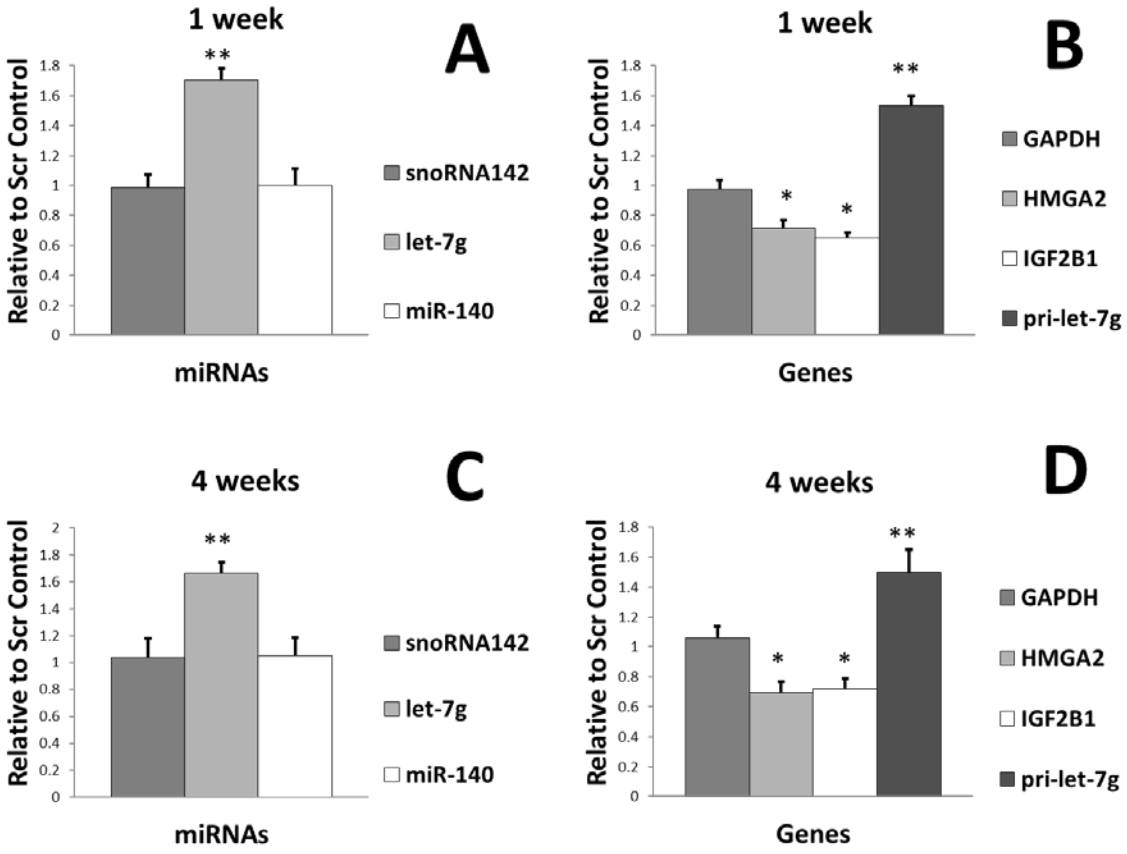

Figure 4.2. *In Vivo* Validation of Let-7g Mimic. Mice were bilaterally injected into the NAc with a let-7g mimic and incubated for 1 and 4 weeks, respectively (N=6/group/time point). A) microRNA expresion 1 wk post injection. B) gene expression 1 wk post injection. C) microRNA expression 4 wks post injection. D) gene expression 4 wks post injection. Students T-test, ***** $p < .0.05$, ** $p < 0.01$.

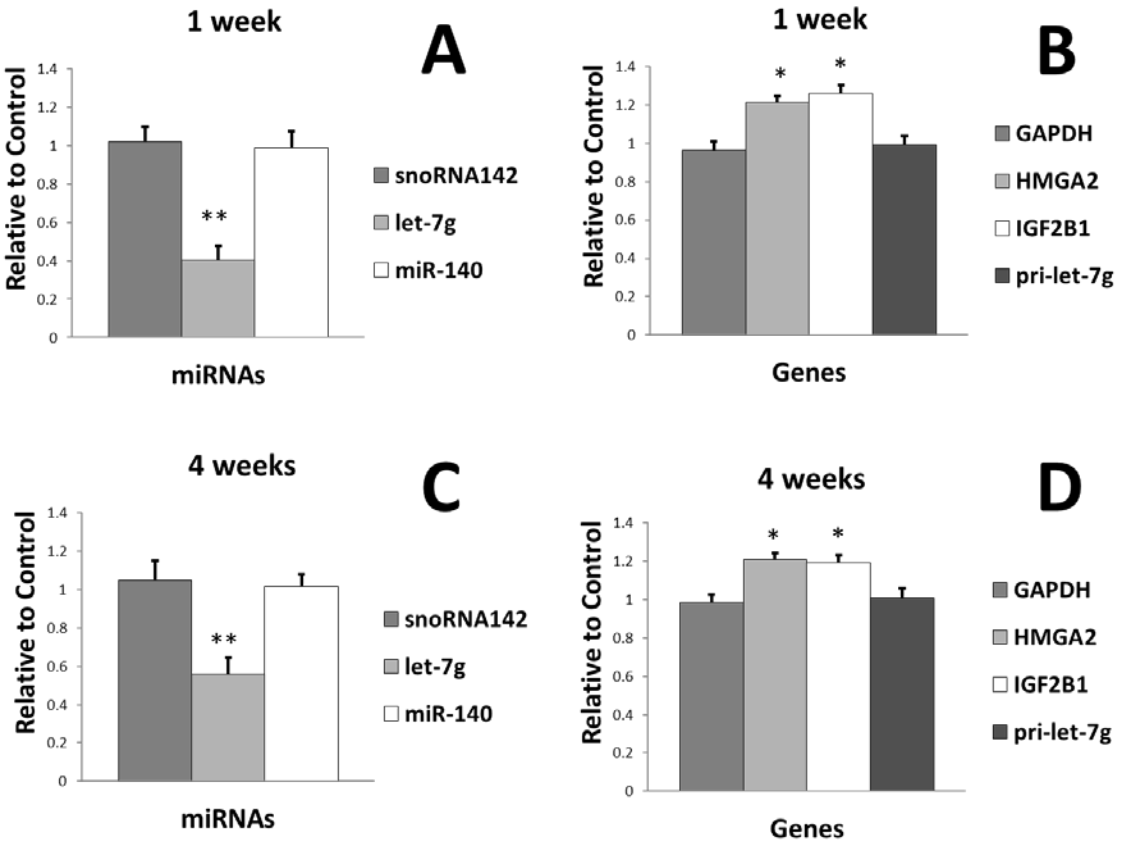

Figure 4.2. *In Vivo* Validation of Let-7g Antagomir. Mice were bilaterally injected into the NAc with a let-7g antagomir and incubated for 1 and 4 weeks, respectively (N=6/gorup/time point). A) microRNA expresion 1 wk post injection. B) gene expression 1 wk post injection. C) microRNA expression 4 wks posti injection. D) gene expression 4 wks post injection. Students T-test, ***** $p < .0.05$, ** $p < 0.01$.

Brain Region-Specific Modulation of MicroRNAs associated with the IKKβ/NF-κB Pathway

Let-7g was modulated in the NAc by either overexpression or inhibition. For let-7g overexpression, we injected 15 mice with a lentiviral vector containing a precursor let-7g shRNA and 15 mice with an equivalent scrambled shRNA. Mice were left to recover for a week and a continuous access 2BC drinking model was started. However, we did not see any significant changes in ethanol consumption, preference or total fluid intake (Fig 4.4). We subsequently exposed the same treated mice to a more stringent intermittent access 2BC paradigm, but again observed no phenotypic changes in ethanol intake, preference or total fluid intake (Fig 4.5). For let-7g inhibition, we injected 15 mice with a lentiviral vector containing a let-7g antagomir and 15 mice with an equivalent scrambled shRNA oligonucleotide. Mice were left to recover for 4 days and a continuous access 2BC drinking model was started. However, similar to the overexpression we did not see any significant changes in ethanol consumption, preference or total fluid intake (Fig 4.6). Upon completion of these experiments, mice brains were harvested and a subset (n=6/group) were micropunched at the injection site, and processed for qPCR to validate modulation of microRNAs/target genes. Results were closely matched to the previous week 4 results for the respective treatments (data not shown).

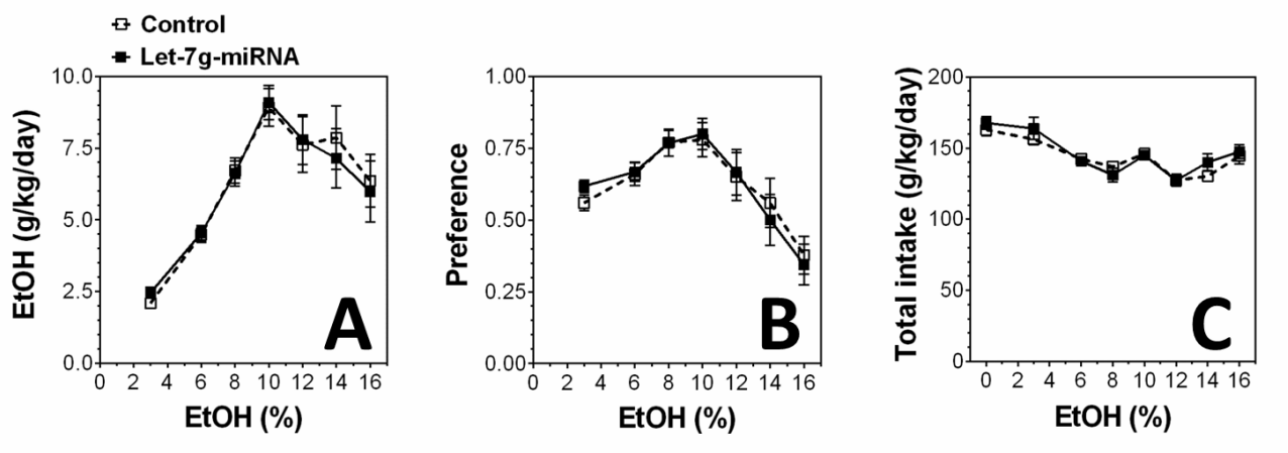

Figure 4.4. Overexpression of Let-7g in the NAc had No Effect on Ethanol Drinking Behaviors in a Continuous Access 2BC model. A lentiviral vector expressing either the precursor let-7g shRNA (let-7g-miRNA) (N =15) or an equivalent scrambled control was injected bilaterally into the NAc. Mice were then exposed to a continuous access 2BC drinking model. A) Ethanol consumption (g/kg/day), B) Preference, C) Total fluid intake (g/kg/day). Each point is the average of 2 days of drinking ± SEM. Analyzed with a two-way ANOVA with repeated measures. Statistical significance of let-7g-miRNA treatment compared with Bonferroni post-hoc test for multiple comparisons.

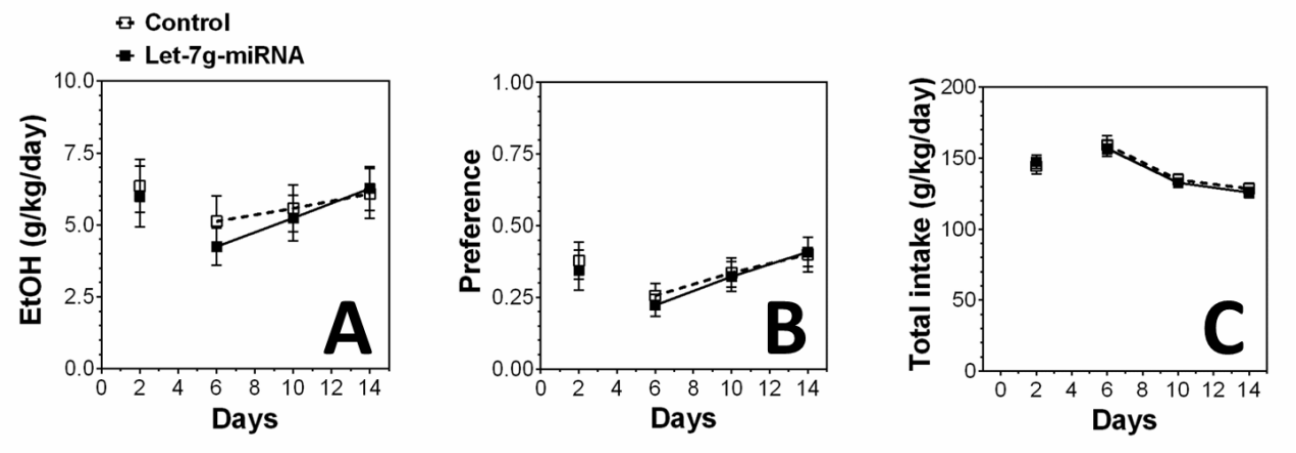

Figure 4.5. Overexpression of Let-7g in the NAc had No Effect on Ethanol Drinking Behaviors in an Intermittent Access 2BC Model. A lentiviral vector expressing either the precursor let-7g shRNA (let-7g-miRNA) (N =15) or an equivalent scrambled control was injected bilaterally into the NAc. Mice were then exposed to an intermitted access 2BC drinking model. A) Ethanol consumption (g/kg/day), B) Preference, C) Total fluid intake (g/kg/day). Each point is the average of 2 days of drinking ± SEM. Analyzed with a two-way ANOVA with repeated measures. Statistical significance of let-7g-miRNA treatment compared with Bonferroni post-hoc test for multiple comparisons.

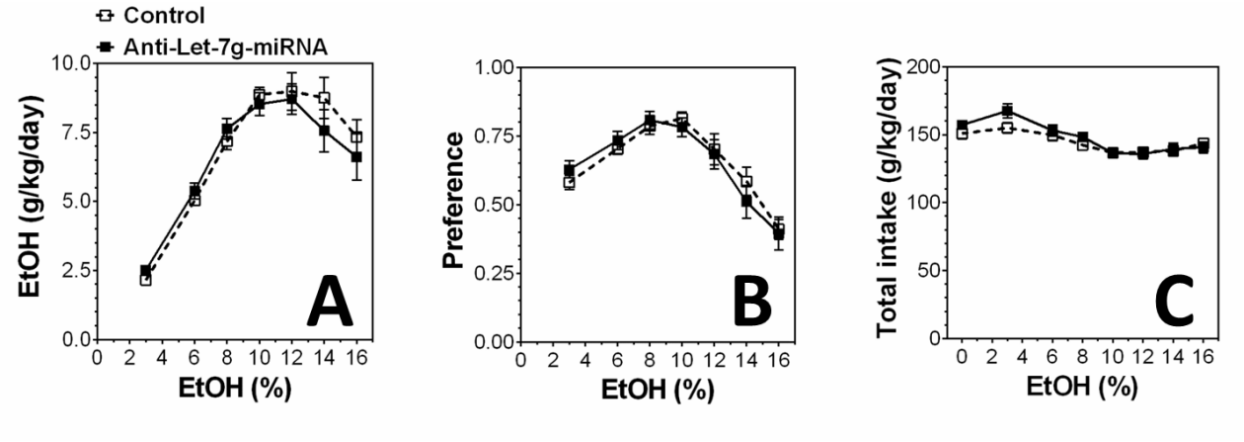

Figure 4.6. Inhibition of Let-7g in the NAc had No Effect on Ethanol Drinking Behaviors in an Continuous Access 2BC model. Either a let-7g antagomir (N =15) or an equivalent scrambled control oligonucleotide was injected bilaterally into the NAc. Mice were then exposed to a continuous access 2BC drinking model. A) Ethanol consumption (g/kg/day), B) Preference, C) Total fluid intake (g/kg/day). Each point is the average of 2 days of drinking ± SEM. Analyzed with a two-way ANOVA with repeated measures. Statistical significance of let-7g-miRNA treatment compared with Bonferroni post-hoc test for multiple comparisons.

DISCUSSION

The fact that we discovered numerous microRNAs differentially expressed in the brain regions important for AUD underscores the relevance of gene regulation by miRNAs in response to alcohol consumption. Likewise, the observation that the many of the differentially expressed microRNAs in the PFC were common between mouse and human, and even changed in the same direction, suggests there is conservation of alcohol-responsive microRNA regulatory pathways. However there are caveats when trying to make this comparison, our analysis represents mice drinking for a relatively short time (20 days) and were probably undergoing withdrawal since they were harvested 24 hours post drinking experiments. Conversely, the post-mortem human brain samples originated from lifelong human alcoholics that were heavy drinkers until the time of death, and thus would not be in acute withdrawal. For mouse studies, it would be beneficial to conduct longer drinking studies and harvest them immediately after drinking to better replicate what is happening in the human samples.

The connection between microRNAs and neuroimmune in AUD is becoming increasingly evident. It has been shown that neuroimmune signaling pathways, such as those mediated by TLRs and chemokines, are up regulated by alcohol and over-targeted by up-regulated microRNAs (Nunez *et al.* 2013; Lewohl *et al.* 2011; Nunez and Mayfield 2012). This was evident in our study where we found many up regulated ethanol-responsive microRNAs associated with the IKKβ/NF-κB Pathway (let-7g, let-7f, miR-152, miR-146b, and miR-140). In particular, let-7g stood out as an attractive modulation target in the NAc because it appears to be a central regulator in alcohol-responsive gene modules preferentially targeted by alcohol-induced miRNAs. (Nunez *et al.* 2013). Also, a previous study manipulated a let-7 family member in the NAc and was able to alter cocaine-induced conditioned place preference behavior in rats

(Chandrasekar and Dreyer 2011). Even though we demonstrated successful modulation of let-7g in the NAc as evident by changes in gene expression of both precursor and mature let-7g, and those of known targeted genes (HMGA2 and IGF2B1), our manipulation produced no changes in ethanol drinking phenotypes in 2BC tests. There are many possible explanations for this outcome. For example, our microRNA expression profiles came from adult female hybrid F1 FVBxB6 mice that may or may not be relevant in adult male C567BL/6J mice since they are a different sex and a slightly different mouse strain. Moreover the F1 FVBxB6 mice have a higher propensity to drink more alcohol that the C57BL/6J (Blednov *et al.* 2005) and were exposed to a 2BC-DID drinking paradigm that leads to higher blood ethanol concentrations than our drinking studies (Blednov *et al.* 2014). This could mean that our microRNA expression profile might only exist or be important when higher amounts of ethanol are present. Lastly, let-7g is known to be related/target TLR4 responsive neuroimmune signaling (Iliopoulos *et al.* 2009), so it is possible that the TLR4 pathway may not be important for regulating ethanol drinking behaviors in the NAc. Regardless of our in *vivo* results, miRNAs are still promising therapeutic candidates for the treatment of alcoholism and other substance abuse disorders.

CHAPTER V: Discussions and Implications

AUD is a devastating disease that affects over 17 million people in the US and is responsible for exacting an immeasurable toll on the individual's lives, families, and society (SAMHSA 2015). It is characterized as a chronic, relapsing condition that has very few treatment options (Jonas *et al.* 2014). Although the exact etiology of alcoholism is unknown, it is thought that it arises from cortical executive dysfunction, cognitive inflexibility, and increased limbic anxiety, and impulsivity (Vetreno and Crews 2014). These neurobiological changes are thought to be, in part, mediated by increased pro-inflammatory neuroimmune signaling in areas of the brain such as the PFC, NAc, AMY and VTA (Crews and Vetreno 2014; Koob 2014; Koob and Volkow 2010; Vetreno and Crews 2014).

Current theory suggests that increases in cytokines following alcohol intake promotes excessive alcohol consumption, producing a positive feedback loop promoting additional inflammatory responses and leads to persistent neurobiological changes in the brain (Blednov *et al.* 2011; Crews and Vetreno 2015; Vetreno and Crews 2014). This is consistent with previous studies showing that null mutant mice lacking genes necessary for pro-inflammatory signaling pathways displayed both decreased levels of cytokines and reduced voluntary ethanol consumption (Ponomarev *et al.* 2012; Blednov *et al.* 2005). Likewise, LPS-treated mice had prolonged increases in voluntary ethanol consumption (Blednov *et al.* 2011). However, genes do not solely regulate the neuroimmune response to alcohol. MicroRNAs have been implicated in neuroadaptations resulting from long-term ethanol exposure in humans (Lewohl *et al.* 2011), and participate in positive pro-inflammatory feedback loops including entities such as NF-κB, let-7, and IL-6 in cell culture (Iliopoulos *et al.* 2009) .

Activation of NF-κB is an important part of the neuroimmune response because of its role in transcribing numerous pro-inflammatory chemokines and cytokines (Perkins 2007). In fact, NF-κB DNA binding in the brain has been shown to increase with ethanol treatments (Crews *et al.* 2006) and the human NF-κB1 gene, which codes for the precursor of the p50, is genetically linked to alcoholism (Edenberg *et al.* 2007). However, NF-κB is also crucial for normal physiological functions such as regulating immunity, cell proliferation and cell death. In this regard, non-selective inhibition of NF-κB could be detrimental to both normal development and susceptibility to infection (Gamble *et al.* 2012; Perkins 2007). The IKK complex (IKKα, IKKβ and IKKγ) includes key mediators for numerous pro-inflammatory pathways that ultimately result in the activation of the NF-κB canonical pathway, or alternatively called the IKKβ/NF-κB pathway. However, not all IKK isoforms are specific to a particular NF-κB pathway. For example, IKKβ primarily regulates the NF-κB canonical pathway (transcription of pro-inflammatory genes/anti-apoptosis), IKKα regulates the NF-κB non-canonical pathway (cell cycle regulation/proliferation), and IKKγ participates in both pathways (Gamble *et al.* 2012; Perkins 2007). We investigated the role of IKKβ and the IKKβ/NF-κB pathway in modulating drinking behaviors based upon previous finding alcohol-dependent behaviors are mediated in part by pro-inflammatory genes.

Our understanding of how neuroimmune systems affect ethanol-drinking behavior is constantly expanding; however, very little is known about the IKKβ/NF-κB pathway's role. There are many questions that this study addressed. For example, does the IKKβ/NF-κB pathway even regulate ethanol-drinking behaviors? There are no published studies that have directly manipulated IKKβ either *in vitro* or *in vivo* to specifically investigate alcohol or any other substance abuse disorder. Even though it is generally accepted that NF-κB is ubiquitously expressed throughout the body (Perkins

and Gilmore 2006), it is still a matter of debate whether peripheral and/or central mediation by neuroimmune pathways are important in the development of AUD (Crews 2012; Szabo and Lippai 2014; Vetreno and Crews 2014). What brain regions play a role the IKKβ/NF-κB pathway's effect on ethanol drinking behaviors? There is extensive evidence supporting the PFC, NAC, AMY, and VTA in the neurobiology of AUD (Koob and Volkow 2010). However, little is known where the IKKβ/NF-κB pathway is expressed and its involvement in modulating ethanol-drinking behavior in these brain areas. In what central nervous system cell types does the IKKβ/NF-κB pathway exist, and which are critical for IKKβ/NF-κB pathway-mediated changes in ethanol drinking phenotypes? It is currently thought that astrocytes and microglia are the predominate cell types involved in neuroimmune-mediated changes in ethanol drinking (Crews and Vetreno 2015; Szabo and Lippai 2014). What upstream pro-inflammatory signaling cascades are responsible for mediating the IKKβ/NF-κB pathway's effect on ethanol drinking? The IKK complex represents a point of convergence for many pro-inflammatory extracellular signals, including endotoxins (LPS), pro-inflammatory cytokines (IL-1 and TNF-α), lymphokines, growth factors, double stranded RNA, certain bacterial antigens, and B or T-Cell activation, etc. (Fig.1.1.). It is unclear which one of these stimuli is important in mediating the IKKβ/NF-κB pathway's effect on ethanol drinking. What ethanol-responsive microRNAs are differentially expressed in these brain regions? Even though the field of investigating ethanol-responsive microRNAs is ever increasing, there is limited knowledge about brain region-specific changes in microRNAs in response to ethanol exposure. Can microRNAs associated with the IKKβ/NF-κB pathway modulate ethanol drinking? There are only a few studies that have looked at which micoRNAs are important for regulating the IKKβ/NF-κB pathway, but

none have investigated how modulating these specific microRNAs would affect ethanol drinking behaviors (Bazzoni *et al.* 2009; Virtue *et al.* 2012).

The goal of this dissertation was to help elucidate the IKKβ/NF-κB pathway's role in AUD by answering the questions presented above through two specific aims. Specific Aim I assessed how neuroimmune signaling genes in the IKKβ/NF-κB pathway regulate voluntary ethanol drinking by determining brain region and cell type-specific expression and modulation of genes associated with the IKKβ/NF-κB pathway. Specific Aim II assessed how ethanol-responsive microRNAs associated with the IKKβ/NF-κB pathway regulate voluntary ethanol drinking by determining brain region-specific expression and modulation of microRNAs associated with the IKKβ/NF-κB pathway. We hypothesized that inhibiting IKKβ would limit/decrease voluntary ethanol consumption based on previous findings that over-activation of pro-inflammatory neuroimmune signaling promotes alcohol drinking (Blednov *et al.* 2011), and inhibiting this signaling reduces alcohol drinking (Ponomarev *et al.* 2012),.

To explore genes associated with the IKKβ/NF-κB pathway, we determined brain region and cell-type expression characteristics of IKKα, IKKβ, IKKγ, and IKKε. These genes were selected since they make up the IKK complex (IKKα, IKKβ, IKKγ) that is responsible for disinhibiting NF-κB and so that it can translocate from the cytosol to the nucleus to transcribe numerous pro-inflammatory cytokines and chemokines (Perkins 2007). While IKKε was chosen since it has been implicated to interact with NF-κB, but through a poorly understood mechanism (Chau *et al.* 2008; Sankar *et al.* 2006; Takeda and Akira 2004). We discovered that all the IKK isoforms were found primarily in neurons (>80% of neurons), ubiquitously expressed (>60% of cells in the PFC, NAc and AMY), and that the brain regions studied (PFC, NAc, AMY, and VTA) were predominantly neuronal in composition. All the isoforms share a nuclear and cytosolic localization in the neurons and astrocytes, and at distinct areas at the beginning of

major processes in microglia, with the notable exception of IKKγ that is only found in the nucleus of astrocytes and neurons. The abundant expression throughout brain regions and cell types is likely due to the essential involvement of the IKK isoforms in many critical physiological pathways, such as immunity, inflammation, and cell-cycle regulation (Chau *et al.* 2008; Hacker and Karin 2006). However, the predominate neuronal expression of the IKK isoforms and neuronal composition of the individual brain regions were unexpected since glia cells (astrocytes and microglia) are commonly thought to be the preeminent cell type for neuroimmune signaling (Bailey *et al.* 2006; Tian *et al.* 2012; Tian *et al.* 2009), and to make up the vast majority of cells in the brain (Allen and Barres 2009; Bear *et al.* 2007; Kandel *et al.* 2000). The cytosolic location agrees with the notion that IKK isoforms are functionally active in the cytosol (Gamble *et al.* 2012; Perkins 2007). IKKγ's nuclear localization in neurons and astrocytes may be a regulatory mechanism to prevent the IKK complexes from becoming active until pro-inflammatory stimuli translocates them into the nucleus. Interestingly, all the members of the IKK complex (IKKα, IKKβ, IKKγ) share an almost identical expression profile with brain region-specific expression highest in the NAc, followed by the AMY and PFC, and least in the VTA, and cell type-specific expression in almost all neurons, about half of microglia, and a third of astrocytes. A notable exception is that IKKγ is found in a slightly higher percentage of cells than IKKα and IKKβ, but then again, IKKγ is a non-catalytic protein for many IKK-dependent pathways (Hacker and Karin 2006; Perkins 2007). These findings help answer the question regarding the brain region and cell type-specificity of genes associated with the IKKβ/NF-κB pathway, and provides guidance to selectively target this pathway *in vivo*.

We manipulated IKKβ both peripherally and centrally to examine the role of the IKKβ/NF-κB pathway in voluntary 2BC ethanol drinking paradigms. To evaluate peripheral effects, the pharmacological IKKβ antagonists, TPCA-1 and sulfasalazine, were systemically administered and drinking behaviors assessed with a 2BC and 2BC-

DID tests. Both antagonists act only peripherally and do not cross the BBB (Liu *et al.* 2012b). TPCA-1 is a selective small molecule inhibitor of IKKβ (Podolin *et al.* 2005), while sulfasalazine possess strong IKKβ inhibitory activity (Lappas *et al.* 2005). TPCA-1 reduced ethanol consumption and preference with no changes in total fluid intake in both the 2BC and the 2BC-DID tests. Sulfasalazine reduced ethanol consumption in the 2BC test, but only reduced ethanol preference in the 2BC-DID with no changes in total fluid intake in either test. One possible explanation for this slight discrepancy in the 2BC-DID results is that TPCA-1 specifically inhibits IKKβ, while sulfasalazine, even though it possess strong activity towards IKKβ, is not as specific as TPCA-1 for IKKβ. To evaluate central effects, we performed a virally-mediated IKKβ genetic knockdown in brain-specific regions (NAc and CeA) and drinking behaviors were assessed with a 2BC test. We selected the NAc and CeA because of their previously stated roles in AUD development (Koob and Volkow 2010). We observed that knockdown of IKKβ in both the NAc and CeA decreased ethanol intake and preference without affecting total fluid intake or sweet tastes preferences. Furthermore, the genetic knockdown of IKKβ decreased pro-inflammatory cytokines (TNF-α and IL-6) that are commonly associated with the IKKβ/NF-κB pathway (Perkins 2007). We then investigated the tropism of our viral vector and discovered that it primarily transduced neurons. These results provide insight into the central vs peripheral question by suggesting that both are important for modulating ethanol-drinking phenotypes, but that certain brain regions, such as the NAc and CeA can mediate ethanol-drinking on their own. This new data also supports our previous IKK characterization study, and reiterates the importance of the IKKβ/NF-κB pathway in neurons.

Lastly, we explored the role of ethanol-responsive microRNAs associated with the IKKβ/NF-κB pathway. We first determined which microRNAs were differentially expressed in the PFC, NAc, and AMY. Female F1 FVBxB6 hybrid mice were exposed to a 20-day 2BC-DID paradigm. The sex, strain, and drinking test were selected to facilitate the highest possible drinking in order to maximize differences in microRNA expression. For example, females generally drink more than males, the F1 FVBxB6 strain drink more than C57BL/6J mice, and the 2BC-DID test generates higher ethanol consumption than the continuous 2BC test (Blednov et al. 2005; Thiele and Navarro 2014). Upon completion of drinking, RNA was extracted, microarray expression analysis was performed, and the results were validated with qPCR. We discovered numerous microRNAs that were changed in each brain region (77 in the PFC, 49 in the NAc, and 60 in the AMY). Interestingly, all the microRNAs in the PFC were upregulated, while those in the NAc and AMY had mixed levels of regulation with the NAc being primarily downregulated and the AMY primarily upregulated. There were numerous microRNAs that were common between the brains regions, but changed in different directions. For example let-7g was upregulated in the PFC and downregulated in the NAc. This suggests that some microRNAs might play a unique role depending on the brain region. Moreover, the expression pattern in the PFC was similar to that seen in a study that examined the PFC of human alcoholics that reported 35 differentially expressed microRNAs that were all up regulated with 14 of these common with our mouse results (Lewohl et al. 2011). Interestingly, 5 of these 14 microRNAs were associated with the IKKβ/NF-κB pathway. This suggests there may be conserved ethanol responsive-microRNA-mediated pathways between the two species.

We selected let-7g for *in vivo* modulation in NAc to explore the effects of a microRNA that is associated with the IKKβ/NF-κB pathway on ethanol drinking. Let-7g

was selected for a number of reasons. It was differentially expressed in the human and mouse PFC, as well as other brain regions including the NAc. Moreover, the let-7 family is responsible for mediating the effects of LPS by targeting TLR4 (Chen *et al.* 2007), regulating NF-κB and IL-6 (Iliopoulos *et al.* 2009), and let-7g is predicted to specifically target IKKβ. The NAc was selected since we previously demonstrated that knocking down IKKβ in this area decreases ethanol consumption and preference, and since let-7g is predicted to target IKKβ, we expected to see a similar change. Moreover, the let-7 family has been shown to alter behavioral phenotypes in other substance abuse rodent models in the NAc (Chandrasekar and Dreyer 2011). We observed successful overexpression of let-7g in the NAc. Both the precursor and mature let-7g mRNA levels were increased by over 50% and 70%, respectively, over the period of the behavioral experiments (4 weeks). There were no negative effects on the microRNA processing machinery as indicated by an absence of changes in unrelated microRNAs. The ability of let-7g to modulate the known validated target genes of HMGA2 and IGF2B1 were verified when we observed approximately 30% reductions in both of their mRNA expression levels. Likewise, we observed similar results, but in opposite direction, when we inhibited let-7g. Unfortunately, we did not see any ethanol drinking phenotypic changes in either the overexpression or inhibition let-7g in the NAc using either continuous access or limited access 2BC drinking tests. There are many possible explanations for this outcome. For example, the microRNA expression profiles may be different in the naturally higher drinking female F1 FVBxB6 hybrid strain then in the male C57CL/6J mice used in the behavioral experiments (Blednov *et al.* 2005). Another possibility is let-7g is known to be target TLR4 responsive neuroimmune signaling (Iliopoulos *et al.* 2009), so it is possible that the TLR4 pathway may not be important for regulating ethanol drinking behaviors in the NAc. This ideas is supported by previous

work in which we specifically manipulated TLR4 and the TLR/IL-R adaptor protein, MYD88, in the NAc and observed no changes in ethanol drinking behavior during 2BC tests (Fig 5.1 and 5.2). Similarly, we observed relatively modest changes (20 to 30%) in the validated targets of let-7g, which could possibly indicate that this microRNA only fine tunes expression of its targets that may not produce a noticeable phenotypic change, or that we simply did not inject a high enough dose of (lentivirus/antagomir) to elicit a significant effect. Alternatively, IKKβ is only a predicted target of let-7g, and thus let-7g may not actually target this molecule. However, we still found many other ethanol-responsive-microRNAs associated with the IKKβ/NF-κB pathway in the PFC, NAc, and AMY, which could be promising therapeutic candidates for the treatment of AUD.

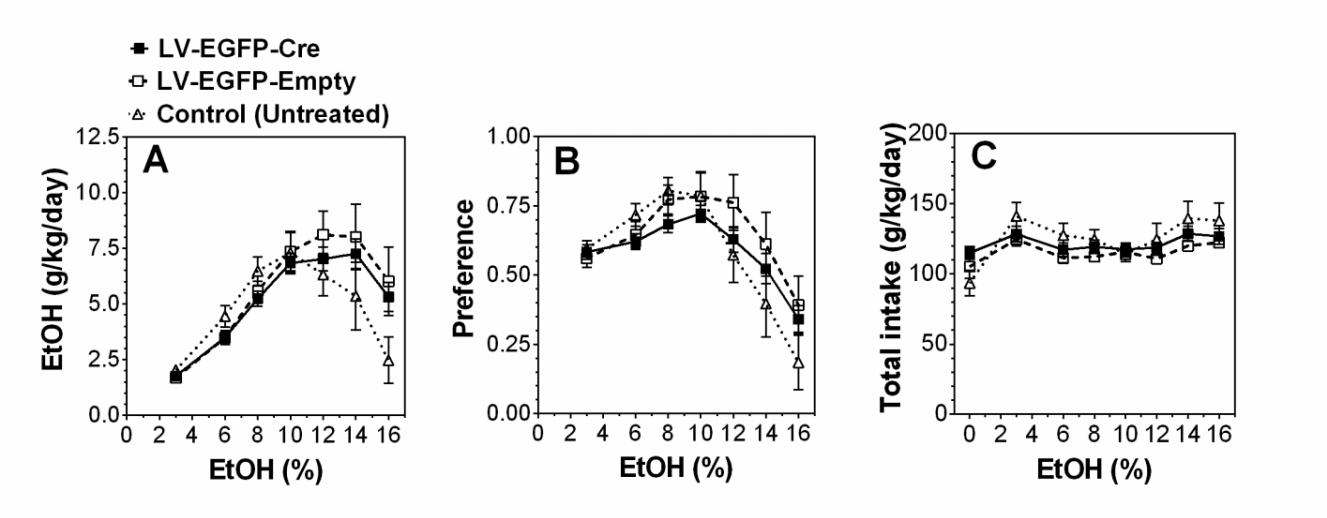

Figure 5.1. TLR4 Knockdown in NAc had no Effect on Ethanol Intake during 2BC test *Tlr4*$^{F/F}$ Mice. A) Ethanol consumption (g/kg/24h). B) Preference C) Total fluid intake (g/kg/24h). Each point is the average of 2 days of drinking ± SEM. Main effects were determined using a two-way ANOVA with repeated measures. Statistical significance of LV-EGFP-Cre treatment compared with corresponding LV-EGFP-Empty was determined using a Bonferroni post-hoc test for multiple comparisons. (N = 20 LV-Cre-EGFP, N = 10 LV-Cre-Empty, and N= 10 Untreated Control).

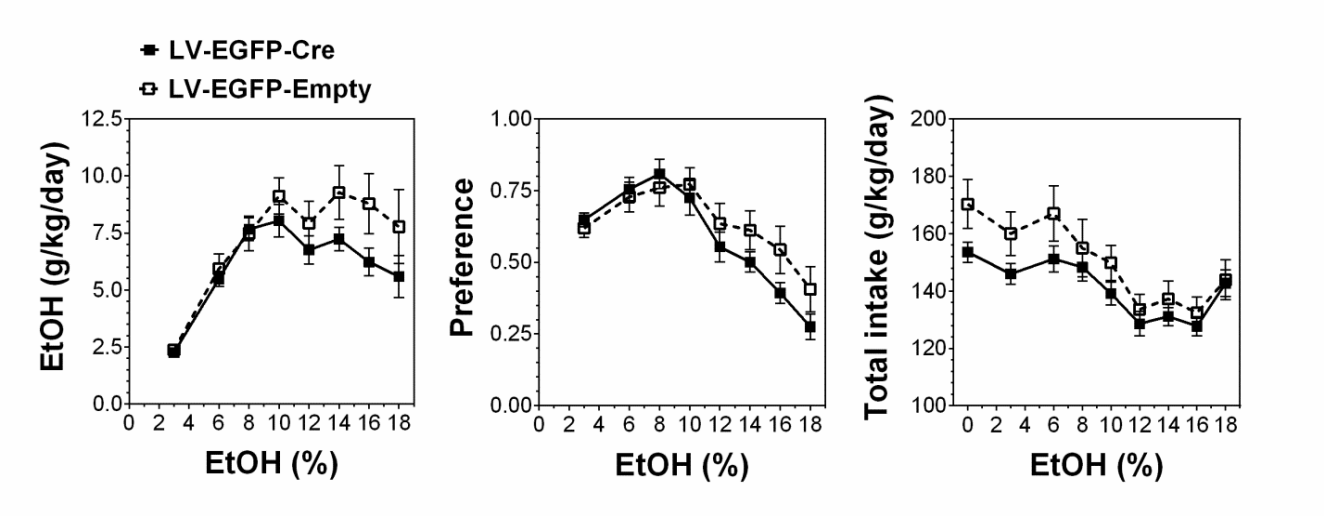

Figure 5.2. MYD88 Knockdown in NAc had no Effect on Ethanol Intake during 2BC test *Myd88*$^{F/F}$ Mice. A) Ethanol consumption (g/kg/24h). B) Preference C) Total fluid intake (g/kg/24h). Each point is the average of 2 days of drinking ± SEM. Main effects were determined using a two-way ANOVA with repeated measures. Statistical significance of LV-EGFP-Cre treatment compared with corresponding LV-EGFP-Empty was determined using a Bonferroni post-hoc test for multiple comparisons. (N = 10 LV-Cre-EGFP, N = 10 LV-Cre-Empty).

Our results provide novel evidence that peripheral or central inhibition of IKKβ decreases ethanol drinking. Ethanol could induce peripheral pro-inflammatory cytokines that ultimately activate expression of immune-related genes in the brain or it could directly stimulate central neuroimmune responses. Inhibiting IKKβ-mediated signaling could limit the peripheral and central inflammatory effects of ethanol. Pharmacological data demonstrate that neither sulfasalazine nor TPCA-1 can penetrate the blood brain barrier, so their anti-inflammatory effect would be peripheral (Liu *et al.* 2012a). One possible mechanism is that high doses of ethanol (causing the gut to become permeable by disrupting tight junctions and allowing the gut biome to enter the portal circulation and subsequently the liver (Ferrier *et al.* 2006; Sims *et al.* 2010). Biome leakage contain endotoxins, such as LPS, which can induce Kupffer cell activation in the liver resulting in secretion of TNF-α and other pro-inflammatory cytokines into the blood (Qin *et al.* 2008). In fact, LPS levels are elevated in the serum of alcoholics (Szabo and Lippai 2014). Ethanol and pro-inflammatory cytokines, such as TNF-α, are then transported across the blood brain barrier (BBB) (Qin *et al.* 2008; Banks and Erickson 2010; Vetreno and Crews 2014). Even though the exact mechanism for the movement of cytokines across the BBB has yet to be fully elucidated, it is thought that they are either directly transported across by receptors (e.g., TNF-α by TNF-α receptor) or indirectly activate the release of cytokines through endothelial cells (Watkins *et al.* 1995; Mayfield *et al.* 2012; Banks and Erickson 2010). The former method is supported by a study that demonstrated radiolabeled TNF-α does directly cross BBB (Pan and Kastin 2002). However, it is unlikely that LPS itself can directly cross the BBB (Singh

and Jiang 2004). Once ethanol and the peripheral cytokines (TNF-α) enter the brain they activate positive loops of pro-inflammatory neuroimmune signaling in neurons and glial cells that all converge upon nuclear translocation of NF-κB. Consequently, NF-κB transcribes numerous pro-inflammatory mediators that amplify through autocrine and paracrine positive loops (Vetreno and Crews 2014). Unfortunately, It is unknown if the levels of ethanol in our voluntary drinking models would produce high enough concentrations for this to happen as this effect has only been demonstrated when ethanol is administered in concentrated doses over a short period of time using gastric gavage. However, if the gut did become leaky, the IKKβ inhibition from the pharmacological inhibitors would probably be near the beginning of this pro-inflammatory cascade in the liver. It is here that LPS, which is a ligand for Toll-like 4 receptors (TLR4), would induce the expression of TNF-α and other pro-inflammatory cytokines through IKKβ and NF-κB (Fig. 5.3) (Vetreno and Crews 2014).

Conversely, it is possible that the reduced ethanol drinking observed from the local knockdown of IKKβ in the NAc and CeA prevented the activation of NF-κB pathway in neurons, effectively reducing the amplification of pro-inflammatory mediators through autocrine and paracrine positive loops. More specifically, it is known that ethanol can induce the high-mobility group box 1 (HMGB1) protein, which is a nuclear protein that is ligand for TLR4 and has endogenous cytokine-like activity. This activation occurs primarily in neurons and is responsible for activating microglia and neuronal TLR4 mediated by IKKβ resulting in expression of pro-inflammatory cytokines (Zou and Crews 2014; Crews and Vetreno 2015). Moreover, peripheral cytokines such as TNF-α

can activate TNF receptor pathways in neurons, astrocytes, or microglia that are also mediated by IKKβ through NF-κB that produce additional pro-inflammatory cytokines (Vetreno and Crews 2014; Crews and Vetreno 2015). Initiation of these pro-inflammatory mediators ultimately reinforces positive feedback loops (Vetreno and Crews 2014; Crews and Vetreno 2015). However, if there is no IKKβ in the neurons, than this could possibly interrupt these pro-inflammatory feedback loops (Fig. 1) (Zou and Crews 2014) (Fig. 5.3).

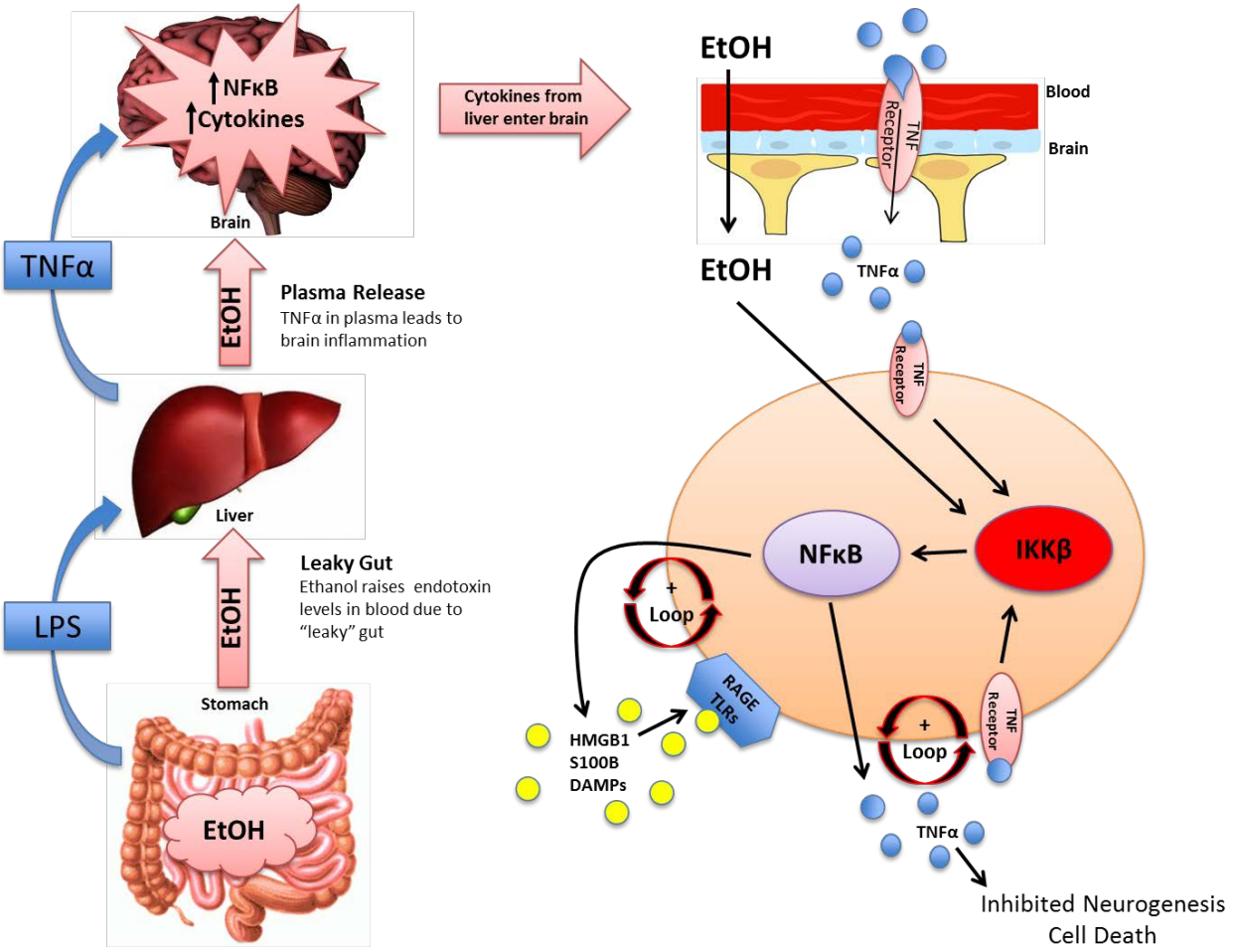

Figure 5.3. Possible Mechanism of the IKKβ/NF-κB Pathway can Affect Drinking Both Peripherally and in Brain Specific Regions. For peripheral activation: Ethanol in gut may cause leakage of bacterial products (LPS), which in turn activates TLR4 receptors in liver, and subsequently TNF-α, which can cross the barrier through a transporter and activate the IKKβ/NF-κB pathway and induce reinforcing pro-inflammatory positive feed forward loops that cause long term neurobiological changes in the brain. For central activation: Ethanol enters the brain directly and activates the IKKβ/NF-κB pathway to induce the same pro-inflammatory positive feed forward loops.

In summary, we found that all the members of the IKK complex (IKKα, IKKβ, IKKγ), which are the key mediators of the IKKβ/NF-κB pathway, are located primarily in neurons. The IKK complex is ubiquitously found throughout brain regions associated with alcohol reward and dependence (PFC, NAc, AMY, and VTA), which are primarily neuronal in cell-type composition. Knockdown of IKKβ both peripherally or in the brain-specific regions of the NAc and CeA decreased/limited voluntary ethanol drinking in 2BC tests. The central knockdown of IKKβ down was primarily in neurons and reduced production of pro-inflammatory cytokines (TNF-α and IL-6) in both the NAc and CeA. There were numerous differentially expressed ethanol-responsive microRNAs in the PFC, NAc and AMY. Many of the ethanol-responsive microRNAs in the PFC of mice were conserved in human alcoholics suggesting there may be conserved microRNA-mediated pathways between the two species. Interestingly, 5 out the 14 conserved microRNAs in the PFC were associated with the IKKβ/NF-κB pathway. Of these, let-7g was the most prominent member. Let-7g was successfully modulated in the NAc, but produced no changes in ethanol drinking behaviors. However, this result does that exclude the possible significance of microRNAs associated with the IKKβ/NF-κB pathway regulating ethanol drinking, but rather justifies additional research. Thus, the work contained in this dissertation, when taken in its totality, strongly supports the hypothesis that inhibiting the IKKβ/NF-κB pathway decreases voluntary ethanol drinking. However, future studies are needed to better elucidate the exact mechanism, such as exploring which of the upstream stimuli are essential for IKKβ/NF-κB pathway's effect on ethanol drinking behaviors and to determine how microRNAs play a role.

REFERENCES

Agrawal R. G., Owen J. A., Levin P. S., Hewetson A., Berman A. E., Franklin S. R., Hogue R. J., et al. (2014) Bioinformatics analyses reveal age-specific neuroimmune modulation as a target for treatment of high ethanol drinking. *Alcohol Clin Exp Res* **38**, 428–437.

Ahmed B. Y., Chakravarthy S., Eggers R. (2004) Efficient delivery of Cre-recombinase to neurons in vivo and stable transduction of neurons using adeno-associated and lentiviral vectors. *BMC Neurosci.* **5**, 4.

Ahmed S., Blumberg J. (2011) Dietary guidelines for Americans 2010. *Nutr Rev*. **69**, 754-756.

Allen N. J., Barres B. A. (2009) Neuroscience: Glia — more than just brain glue. *Nature* **457**, 675.

American Psychiatric Association (2013) *Diagnostic and Statistical Manual of Mental Disorders (DSM-5®)*. American Psychiatric Pub.

Androulidaki A., Arranz A., Doxaki C., Schworer S., Zacharioudaki V., Margioris A. N., Tsichlis P. N., Tsatsanis C., Iliopoulos D. (2009) The Kinase Akt1 Controls Macrophage Response to Lipopolysaccharide by Regulating MicroRNAs. *Immunity* **31**, 220–231.

Azevedo F. A. C., Carvalho L. R. B., Grinberg L. T., Farfel J. M., Ferretti R. E. L., Leite R. E. P., Filho W. J., Lent R., Herculano-Houzel S. (2009) Equal numbers of neuronal and nonneuronal cells make the human brain an isometrically scaled-up primate brain. *Journal of Comparative Neurology* **513**, 532–541.

Bachmanov A. A., Kiefer S. W., Molina J. C., Tordoff M. G., Duffy V. B., Bartoshuk L. M., Mennella J. A. (2003) Chemosensory factors influencing alcohol perception, preferences, and consumption. *Alcohol. Clin. Exp. Res.* **27**, 220–31–231.

Bahi A. (2012) Viral-Mediated Knockdown of mGluR7 in the Nucleus Accumbens Mediates Excessive Alcohol Drinking and Increased Ethanol-Elicited Conditioned Place Preference in Rats. *Neuropsychopharmacology* **38**, 2109.

Bahi A., Dreyer J.-L. (2012) Involvement of nucleus accumbens dopamine D1 receptors in ethanol drinking, ethanol-induced conditioned place preference, and ethanol-induced psychomotor sensitization in mice. *Psychopharmacology (Berl.)* **222**, 141–53–153.

Bailey S. L., Carpentier P. A., McMahon E. J., Begolka W. S., Miller S. D. (2006) Innate

and Adaptive Immune Responses of the Central Nervous System. *Critical Reviews™ in Immunology* **26**, 149.

Banks W. A., Erickson M. A. (2010) The blood–brain barrier and immune function and dysfunction. *Neurobiology of Disease* **37**, 26.

Bazzoni F., Rossato M., Fabbri M., Gaudiosi D., Mirolo M., Mori L., Tamassia N., Mantovani A., Cassatella M. A., Locati M. (2009) Induction and regulatory function of miR-9 in human monocytes and neutrophils exposed to proinflammatory signals. *Proc. Natl. Acad. Sci. U.S.A.* **106**, 5282–5287.

Bear M. F., Connors B. W., Paradiso M. A. (2007) *Neuroscience: Exploring the brain (3rd ed)*. Philadelphia: Lippincott William Wilkins.

Belknap J. K., Richards S. P., O'Toole L. A., Helms M. L., Phillips T. J. (1997) Short-term selective breeding as a tool for QTL mapping: ethanol preference drinking in mice. *Behavior genetics* **27**, 55–66.

Benjamini Y., Drai D., Elmer G., Kafkafi N., Golani I. (2001) Controlling the false discovery rate in behavior genetics research. *Behavioural Brain Research* **125**, 279–284.

Blednov Y. A. (2003) GABAA Receptor alpha1 and beta2 Subunit Null Mutant Mice: Behavioral Responses to Ethanol. *Journal of Pharmacology and Experimental Therapeutics* **305**, 854–863.

Blednov Y. A., Benavidez J. M., Black M., Harris R. A. (2014) Inhibition of phosphodiesterase 4 reduces ethanol intake and preference in C57BL/6J mice. *Front Neurosci* **8**, 129.

Blednov Y. A., Benavidez J. M., Geil C., Perra S., Morikawa H., Harris R. A. (2011) Activation of inflammatory signaling by lipopolysaccharide produces a prolonged increase of voluntary alcohol intake in mice. *Brain Behav. Immun.* **25**, S92.

Blednov Y. A., Mayfield R. D., Belknap J., Harris R. A. (2012) Behavioral actions of alcohol: phenotypic relations from multivariate analysis of mutant mouse data. *Genes Brain Behav.* **11**, 424–435.

Blednov Y., BERGESON S., Walker D., FERREIRA V., KUZIEL W., HARRIS R. (2005) Perturbation of chemokine networks by gene deletion alters the reinforcing actions of ethanol. *Behavioural Brain Research* **165**, 110.

Blomqvist O., Ericson M., Engel J. A., Söderpalm B. (1997) Accumbal dopamine overflow after ethanol: Localization of the antagonizing effect of mecamylamine.

European Journal of Pharmacology **334**, 149.

Boileau I., Assaad J.-M., Pihl R. O., Benkelfat C., Leyton M., Diksic M., Tremblay R. E., Dagher A. (2003) Alcohol promotes dopamine release in the human nucleus accumbens. *Synapse* **49**, 226-231.

Bouchery E. E., Harwood H. J., Sacks J. J., Simon C. J. (2011) Economic costs of excessive alcohol consumption in the US, 2006. *American Journal of Preventive Medicine.* **41**, 516-524.

Carr G. D. (2011) Alcoholism: a modern look at an ancient illness. *Primary Care: Clinics in Office Practice.* **38**, 9-21.

Chandrasekar V., Dreyer J.-L. (2011) Regulation of MiR-124, Let-7d, and MiR-181a in the Accumbens Affects the Expression, Extinction, and Reinstatement of Cocaine-Induced Conditioned Place Preference. *Neuropsychopharmacology* **36**, 1149.

Chau T.-L., Gioia R., Gatot J.-S., Patrascu F., Carpentier I., Chapelle J.-P., O'Neill L., Beyaert R., Piette J., Chariot A. (2008) Are the IKKs and IKK-related kinases TBK1 and IKK-ε similarly activated? *Trends in Biochemical Sciences* **33**, 171–180.

Chen X.-M., Splinter P. L., O'Hara S. P., LaRusso N. F. (2007) A Cellular Micro-RNA, let-7i , Regulates Toll-like Receptor 4 Expression and Contributes to Cholangiocyte Immune Responses against Cryptosporidium parvum Infection. *J. Biol. Chem.* **282**, 28929–28938.

Coller J. K., Hutchinson M. R. (2012) Implications of central immune signaling caused by drugs of abuse: Mechanisms, mediators and new therapeutic approaches for prediction and treatment of drug dependence. *Pharmacol. Ther.* **134**, 219.

Crews F. T. (2012) Immune function genes, genetics, and the neurobiology of addiction. *Alcohol Res* **34**, 355–361.

Crews F. T., Boettiger C. A. (2009) Impulsivity, frontal lobes and risk for addiction. *Pharmacol. Biochem. Behav.* **93**, 237.

Crews F. T., Vetreno R. P. (2014) *Neuroimmune Basis of Alcoholic Brain Damage*. **118**, 315-357.

Crews F. T., Vetreno R. P. (2015) Mechanisms of neuroimmune gene induction in alcoholism. *Psychopharmacology (Berl.)*, 1–15.

Crews F. T., Zou J., Qin L. (2011) Induction of innate immune genes in brain create the neurobiology of addiction. *Brain*. **25**, S4-S12.

Crews F., Nixon K., Kim D., Joseph J., Shukitt-Hale B., Qin L., Zou J. (2006) BHT Blocks NF-κB activation and Ethanol-Induced Brain Damage. *Alcohol Clin Exp Res* **30**, 1938–1949.

Dombrowski S. M., Hilgetag C. C., Barbas H. (2001) Quantitative architecture distinguishes prefrontal cortical systems in the rhesus monkey. *Cerebral Cortex* **11**, 975–88–988.

Edenberg H. J., Xuei X., Wetherill L. F., Bierut L., Bucholz K., Dick D. M., Hesselbrock V., et al. (2007) Association of NFKB1, which encodes a subunit of the transcription factor NF- B, with alcohol dependence. *Human Molecular Genetics* **17**, 963–970.

Engel J. A., Jerlhag E. (2014) Alcohol: mechanisms along the mesolimbic dopamine system. *Progress in brain research* **211**, 201–233.

Ethridge R. T., Hashimoto K., Chung D. H., Ehlers R. A., Rajaraman S., Evers B. M. (2002) Selective inhibition of NF-κB attenuates the severity of cerulein-induced acute pancreatitis. *Journal of the American College of Surgeons* **195**, 497–505.

Ferrier L., Bérard F., Debrauwer L., Chabo C., Langella P., Buéno L., Fioramonti J. (2006) Impairment of the Intestinal Barrier by Ethanol Involves Enteric Microflora and Mast Cell Activation in Rodents. *The American Journal of Pathology* **168**, 1148–1154.

Gamble C., McIntosh K., Scott R., Ho K. H., Plevin R., Paul A. (2012) Inhibitory kappa B kinases as targets for pharmacological regulation. *Br. J. Pharmacol.* **165**, 802–819.

Gessa G. L., Muntoni F., Collu M., Vargiu L., Mereu G. (1985) Low doses of ethanol activate dopaminergic neurons in the ventral tegmental area. *Brain Res.* **348**, 201–203.

Gilpin N.W., Koob G.F. (2008) Neurobiology of alcohol dependence: focus on motivational mechanisms. *Alcohol Res Health*. **31**, 185-195.

Gorini G., Nunez Y. O., Mayfield R. D. (2013a) Integration of miRNA and protein profiling reveals coordinated neuroadaptations in the alcohol-dependent mouse brain. *PLoS ONE* **8**, e82565.

Gorini G., Roberts A. J., Mayfield R. D. (2013b) Neurobiological signatures of alcohol dependence revealed by protein profiling. *PLoS ONE* **8**, e82656.

Grivennikov S. I., Greten F. R., Karin M. (2010) Immunity, inflammation, and cancer. *Cell* **140**, 883–899.

Hacker H., Karin M. (2006) Regulation and Function of IKK and IKK-Related Kinases. *Science Signaling* **2006**, re13–re13.

Harris R. A., Blednov Y. A. (2012) *Neuroimmune Genes and Alcohol Drinking Behavior*. Springer US.

Hayden M. S., Ghosh S. (2004) Signaling to NF-κB. *Genes & development*. **18**, 2195-2224.

Huang X., Li X., Ma Q., Xu Q., Duan W., Lei J., Zhang L., Wu Z. (2014) Chronic alcohol exposure exacerbates inflammation and triggers pancreatic acinar-to-ductal metaplasia through PI3K/Akt/IKK. *International Journal of Molecular Medicine* **35**, 653–63–663.

Iliopoulos D., Hirsch H. A., Struhl K. (2009) An epigenetic switch involving NF-kappaB, Lin28, Let-7 MicroRNA, and IL6 links inflammation to cell transformation. *Cell* **139**, 693-706.

Jakobsson J., Lundberg C. (2006) Lentiviral Vectors for Use in the Central Nervous System. *Molecular Therapy* **13**, 484.

Jimi E., Aoki K., Saito H., D'Acquisto F., May M. J., Nakamura I., Sudo T., et al. (2004) Selective inhibition of NF-κB blocks osteoclastogenesis and prevents inflammatory bone destruction in vivo. *Nature Medicine* **10**, 617.

Jonas D. E., Amick H. R., Feltner C., Bobashev G., Thomas K., Wines R., Kim M. M., et al. (2014) Pharmacotherapy for Adults With Alcohol Use Disorders in Outpatient Settings: A systematic Review and Meta-analysis. *JAMA* **311**, 1889–1900.

Kandel E. R., Schwartz J. H., Jessell T. M. (2000) *Principles of neural science*. New York: McGraw Hill.

Koob G. F. (2014) Neurocircuitry of alcohol addiction: synthesis from animal models. *Handb Clin Neurol* **125**, 33–54.

Koob G. F., Le Moal M. (2008) Neurobiological mechanisms for opponent motivational processes in addiction. *Philos. Trans. R. Soc. Lond., B, Biol. Sci.* **363**, 3113–23–3123.

Koob G. F., Volkow N. D. (2010) Neurocircuitry of Addiction. *Neuropsychopharmacology* **35**, 217.

Lam M. P., Marinelli P. W., Bai L., Gianoulakis C. (2008) Effects of acute ethanol on

opioid peptide release in the central amygdala: an in vivo microdialysis study. *Psychopharmacology (Berl.)* **201**, 261–71–271.

Lappas M., Yee K., Permezel M., Rice G. E. (2005) Sulfasalazine and BAY 11-7082 interfere with the nuclear factor-κB and IκB kinase pathway to regulate the release of proinflammatory cytokines from human adipose tissue and skeletal muscle in vitro. *Endocrinology* **146**, 1491-1497.

Larsson A., Edström L., Svensson L., Söderpalm B., Engel J. A. (2005) Voluntary ethanol intake increases extracellular acetylcholine levels in the ventral tegmental area in the rat. *Alcohol and Alcoholism* **40**, 349-358.

Larsson A., Svensson L., Söderpalm B., Engel J. A. (2003) Role of different nicotinic acetylcholine receptors in mediating behavioral and neurochemical effects of ethanol in mice. *Alcohol* **28**, 157-167.

Lewohl J. M., Nunez Y. O., Dodd P. R., Tiwari G. R., Harris R. A., Mayfield R. D. (2011) Up-regulation of microRNAs in brain of human alcoholics. *Alcohol. Clin. Exp. Res.* **35**, 1928–1937.

Lidow M. S., Song Z.-M. (2001) Primates exposed to cocaine in utero display reduced density and number of cerebral cortical neurons. *J Comp Neurol* **435**, 263–275.

Liu J., Lewohl J. M., Harris R. A., Iyer V. R., Dodd P. R., Randall P. K., Mayfield R. D. (2006) Patterns of Gene Expression in the Frontal Cortex Discriminate Alcoholic from Nonalcoholic Individuals. *Neuropsychopharmacology* **31**, 1574.

Liu J., Yang A. R., Kelly T., Puche A., Esoga C., June H. L., Elnabawi A., et al. (2011) Binge alcohol drinking is associated with GABAA 2-regulated Toll-like receptor 4 (TLR4) expression in the central amygdala. *Proc. Natl. Acad. Sci. U.S.A.* **108**, 4465–4470.

Liu X., Ding X., Deshmukh G., Liederer B. M., Hop C. E. C. A. (2012a) Use of the Cassette-Dosing Approach to Assess Brain Penetration in Drug Discovery. *Drug Metabolism and Disposition* **40**, 963–969.

Liu X., Ding X., Deshmukh G., Liederer B. M., Hop C. E. C. A. (2012b) Use of the cassette-dosing approach to assess brain penetration in drug discovery. *Drug Metabolism and Disposition* **40**, 963–9–969.

Liu X., Zhan Z., Xu L., Ma F., Li D., Guo Z., Li N., Cao X. (2010) MicroRNA-148/152 Impair Innate Response and Antigen Presentation of TLR-Triggered Dendritic Cells by Targeting CaMKII. *The Journal of Immunology* **185**, 7244–7251.

Long Y.-M., Chen K., Liu X.-J., Xie W.-R., Wang H. (2009) Cell-permeable Tat-NBD peptide attenuates rat pancreatitis and acinus cell inflammation response. *World journal of gastroenterology : WJG* **15**, 561–569.

Manit J. M., Walsh M. L., Lowrey S. A. (2009) *SAMHSA: National Survey on Drug Use and Health*.

Maqbool A., Lattke M., Wirth T., Baumann B. (2013) Sustained, neuron-specific IKK/NF-κB activation generates a selective neuroinflammatory response promoting local neurodegeneration with aging. *Molecular Neurodegeneration* **8**, 40.

Mayfield J., Ferguson L., Harris R. A. (2013) Neuroimmune signaling: a key component of alcohol abuse. *Curr. Opin. Neurobiol.* **23**, 513.

Mayfield R. D., Belknap J., Harris R. A., Blednov Y. A. (2012) Behavioral actions of alcohol: phenotypic relations from multivariate analysis of mutant mouse data. *Genes Brain Behav.* **11**, 424–435.

McGovern P. E., Zhang J., Tang J., Zhang Z., Hall G. R., Moreau R. A., Nunez A., et al. (2004) Fermented beverages of pre- and proto-historic China. *Proc. Natl. Acad. Sci. U.S.A.* **101**, 17593–17598.

Melendez R. I. (2011) Intermittent (Every-Other-Day) Drinking Induces Rapid Escalation of Ethanol Intake and Preference in Adolescent and Adult C57BL/6J Mice. *Alcohol Clin Exp Res* **35**, 652–658.

Miranda R. C., Pietrzykowski A. Z., Tang Y., Sathyan P., Mayfield D., Keshavarzian A., Sampson W., Hereld D. (2010) MicroRNAs: master regulators of ethanol abuse and toxicity? *Alcohol Clin Exp Res* **34**, 575–87–587.

Mokdad A. H. (2004) Actual Causes of Death in the United States, 2000. *JAMA* **291**, 1238–1245.

Moschos S. A., Williams A. E., Perry M. M., Birrell M. A., Belvisi M. G., Lindsay M. A. (2007) Expression profiling in vivo demonstrates rapid changes in lung microRNA levels following lipopolysaccharide-induced inflammation but not in the anti-inflammatory action of glucocorticoids. *BMC Genomics* **8**, 240.

Mulligan M. K., Ponomarev I., Hitzemann R. J., Belknap J. K., Tabakoff B., Harris R. A., Crabbe J. C., et al. (2006) Toward understanding the genetics of alcohol drinking through transcriptome meta-analysis. *Proc. Natl. Acad. Sci. U.S.A.* **103**, 6368–73–6373.

Nunez Y. O., Mayfield R. D. (2012) Understanding Alcoholism Through microRNA

Signatures in Brains of Human Alcoholics. *Front Genet* **3**, 43.

Nunez Y. O., Truitt J. M., Gorini G., Ponomareva O. N., Harris R. A., Mayfield R. D. (2013) Positively correlated miRNA-mRNA regulatory networks in mouse frontal cortex during early stages of alcohol dependence. *BMC Genomics* **14**, 725.

Oeckinghaus A., Ghosh S. (2009) The NF-κB family of transcription factors and its regulation. *Cold Spring Harbor Perspectives in Biology*. **4**, 1-10.

Okvist A., Johansson S., Kuzmin A., Bazov I. (2007) Neuroadaptations in human chronic alcoholics: dysregulation of the NF-kappaB system. *PLoS ONE*. **2**, e930.

Osterndorff E. (2013) Gene expression in brain and liver produced by three different regimens of alcohol consumption in mice: comparison with immune activation. *PLoS ONE*. **8**, e59870.

Pan W., Kastin A. J. (2002) TNFα Transport across the Blood–Brain Barrier Is Abolished in Receptor Knockout Mice. *Exp. Neurol.* **174**, 193.

Pastor I. J., Laso F. J., Avila J. J., Rodríguez R. E., González-Sarmiento R. (2000) Polymorphism in the interleukin-1 receptor antagonist gene is associated with alcoholism in Spanish men. *Alcohol. Clin. Exp. Res.* **24**, 1479–1482.

Pastor I. J., Laso F. J., Romero A., González-Sarmiento R. (2005) Interleukin-1 gene cluster polymorphisms and alcoholism in Spanish men. *Alcohol and Alcoholism* **40**, 181–186.

Perkins N. D. (2007) Integrating cell-signalling pathways with NF-κB and IKK function. *Nat. Rev. Mol. Cell Biol.* **8**, 49.

Perkins N. D., Gilmore T. D. (2006) Good cop, bad cop: the different faces of NF-κB. *Cell Death & Differentiation* **13**, 759.

Peters J., Kalivas P. W., Quirk G. J. (2009) Extinction circuits for fear and addiction overlap in prefrontal cortex. *Learning & Memory* **16**, 279–288.

Podolin P. L., Callahan J. F., Bolognese B. J., Li Y. H., Carlson K., Davis T. G., Mellor G. W., Evans C., Roshak A. K. (2005) Attenuation of murine collagen-induced arthritis by a novel, potent, selective small molecule inhibitor of IkappaB Kinase 2, TPCA-1 (2-[(aminocarbonyl)amino]-5-(4-fluorophenyl)-3-thiophenecarboxamide), occurs via reduction of proinflammatory cytokines and antigen-induced T cell Proliferation. *J. Pharmacol. Exp. Ther.* **312**, 373–381.

Ponomarev I., Geil C., Bergeson S., Harris R. A. (2012) Neuroimmune regulation of alcohol consumption: behavioral validation of genes obtained from genomic studies. *Addict Biol* **17**, 108–120.

Qin L., He J., Hanes R. N., Pluzarev O., Hong J.-S., Crews F. T. (2008) Increased systemic and brain cytokine production and neuroinflammation by endotoxin following ethanol treatment. *J Neuroinflammation* **5**, 10.

Qin L., Wu X., Block M. L., Liu Y., Breese G. R., Hong J.-S., Knapp D. J., Crews F. T. (2007) Systemic LPS causes chronic neuroinflammation and progressive neurodegeneration. *Glia* **55**, 453–462.

Roberto M., Bajo M., Crawford E., Madamba S. G., Siggins G. R. (2005) Chronic Ethanol Exposure and Protracted Abstinence Alter NMDA Receptors in Central Amygdala. *Neuropsychopharmacology* **31**, 988.

Roberto M., Madamba S. G., Stouffer D. G., Parsons L. H., Siggins G. R. (2004a) Increased GABA release in the central amygdala of ethanol-dependent rats. *Journal of Neuroscience* **24**, 10159–10166.

Roberto M., Schweitzer P., Madamba S. G., Stouffer D. G., Parsons L. H., Siggins G. R. (2004b) Acute and chronic ethanol alter glutamatergic transmission in rat central amygdala: an in vitro and in vivo analysis. *Journal of Neuroscience* **24**, 1594–1603.

Robinson G., Most D., Ferguson L. B., Mayfield J., Harris R. A., Blednov Y. A. (2014) Neuroimmune pathways in alcohol consumption: evidence from behavioral and genetic studies in rodents and humans. *Int. Rev. Neurobiol.* **118**, 13–39.

Ross S., Peselow E. (2009) The Neurobiology of Addictive Disorders. *Clinical Neuropharmacology* **32**, 269–276.

Saiz P. A., Garcia-Portilla M. P., Florez G., Corcoran P., Arango C., Morales B., Leza J. C., et al. (2009) Polymorphisms of the IL-1 gene complex are associated with alcohol dependence in Spanish Caucasians: data from an association study. *Alcohol Clin Exp Res* **33**, 2147–2153.

SAMHSA (2015) *2013 National Survey on Drug Use and Health (NSDUH).*

Sankar S., Chan H., Romanow W. J., Li J., Bates R. J. (2006) IKK-i signals through IRF3 and NFκB to mediate the production of inflammatory cytokines. *Cellular Signalling* **18**, 982.

Scheidereit C. (2006) IκB kinase complexes: gateways to NF-κB activation and transcription. *Oncogene* **25**, 6685.

Schmid J. A., Birbach A. (2008) IκB kinase β (IKKβ/IKK2/IKBKB)—A key molecule in signaling to the transcription factor NF-κB. *Cytokine and Growth Factor Reviews* **19**, 157–165.

Schmittgen T. D., Livak K. J. (2008) Analyzing real-time PCR data by the comparative CT method. *Nat Protoc* **3**, 1101.

Shimada T. (1999) IKK-i, a novel lipopolysaccharide-inducible kinase that is related to IkappaB kinases. *International Immunology* **11**, 1357–1362.

Sims G. P., Rowe D. C., Rietdijk S. T., Herbst R., Coyle A. J. (2010) HMGB1 and RAGE in Inflammation and Cancer. *Annual Review of Immunology* **28**, 367.

Singh A. K., Jiang Y. (2004) How does peripheral lipopolysaccharide induce gene expression in the brain of rats? *Toxicology* **201**, 197.

Sonkoly E., Wei T., Janson P. C. J., Sääf A., Lundeberg L., Tengvall-Linder M., Norstedt G., et al. (2007) MicroRNAs: novel regulators involved in the pathogenesis of psoriasis? *PLoS ONE* **2**, e610.

Soreq H., Wolf Y. (2011) NeurimmiRs: microRNAs in the neuroimmune interface. *Trends in Molecular Medicine* **17**, 548–555.

Sunami Y., Leithäuser F., Gul S., Fiedler K., Güldiken N., Espenlaub S., Holzmann K.-H., et al. (2012) Hepatic activation of IKK/NFκB signaling induces liver fibrosis via macrophage-mediated chronic inflammation. *Hepatology* **56**, 1117–28–1128.

Suzumura A. (2013) Neuron-microglia interaction in neuroinflammation. *Current protein & peptide science* **14**, 16–20.

Szabo G., Lippai D. (2014) Converging actions of alcohol on liver and brain immune signaling. *Int. Rev. Neurobiol.* **118**, 359–380.

Takeda K., Akira S. (2004) TLR signaling pathways. *Seminars in Immunology* **16**, 3.

Tanaka M., Fuentes M. E., Yamaguchi K., Durnin M. H., Dalrymple S. A., Hardy K. L., Goeddel D. V. (1999) Embryonic lethality, liver degeneration, and impaired NF-kappa B activation in IKK-beta-deficient mice. *Immunity* **10**, 421–9–429.

Thiele T. E., Navarro M. (2014) “Drinking in the dark” (DID) procedures: A model of binge-like ethanol drinking in non-dependent mice. *Alcohol* **48**, 235–241.

Tian L., Ma L., Kaarela T., Li Z. (2012) Neuroimmune crosstalk in the central nervous

system and its significance for neurological diseases. *J Neuroinflammation* **9**, 155.

Tian L., Rauvala H., Gahmberg C. G. (2009) Neuronal regulation of immune responses in the central nervous system. *Trends in Immunology* **30**, 91–99.

Vetreno R. P., Crews F. T. (2014) Current hypotheses on the mechanisms of alcoholism. *Handb Clin Neurol* **125**, 477–497.

Virtue A., Wang H., Yang X.-F. (2012) MicroRNAs and Toll-like Receptor/Interleukin-1 Receptor Signaling. *Journal of Hematology & Oncology* **5**, 66.

Watkins L. R., Maier S. F., Goehler L. E. (1995) Cytokine-to-brain communication: A review & analysis of alternative mechanisms. *Life Sciences* **57**, 1011.

World Health Organization (2014) *Global status report on alcohol and health-2014*.

Zhang X., Zhang G., Zhang H., Karin M., Bai H., Cai D. (2008) Hypothalamic IKKβ/NF-κB and ER stress link overnutrition to energy imbalance and obesity. *Cell* **135**, 61–73.

Ziegelbauer K., Gantner F., Lukacs N. W., Berlin A., Fuchikami K., Niki T., Sakai K., et al. (2005) A selective novel low-molecular-weight inhibitor of IkappaB kinase-beta (IKK-beta) prevents pulmonary inflammation and shows broad anti-inflammatory activity. *Br. J. Pharmacol.* **145**, 178–192.

Zou J. Y., Crews F. T. (2014) Release of Neuronal HMGB1 by Ethanol through Decreased HDAC Activity Activates Brain Neuroimmune Signaling. *PLoS ONE* **9**, e87915.

Zou J., Crews F. (2010) Induction of innate immune gene expression cascades in brain slice cultures by ethanol: key role of NF-κB and proinflammatory cytokines. *Alcohol Clin Exp Res.* **4**, 777-789.